

## ASSESSMENT OF STRUVITE AND K-STRUVITE RECOVERY FROM DIGESTED MANURE

**Elena Tarragó Abella**

Per citar o enllaçar aquest document:

Para citar o enlazar este documento:

Use this url to cite or link to this publication:

<http://hdl.handle.net/10803/663399>

**ADVERTIMENT.** L'accés als continguts d'aquesta tesi doctoral i la seva utilització ha de respectar els drets de la persona autora. Pot ser utilitzada per a consulta o estudi personal, així com en activitats o materials d'investigació i docència en els termes establerts a l'art. 32 del Text Refós de la Llei de Propietat Intel·lectual (RDL 1/1996). Per altres utilitzacions es requereix l'autorització prèvia i expressa de la persona autora. En qualsevol cas, en la utilització dels seus continguts caldrà indicar de forma clara el nom i cognoms de la persona autora i el títol de la tesi doctoral. No s'autoritza la seva reproducció o altres formes d'explotació efectuades amb finalitats de lucre ni la seva comunicació pública des d'un lloc aliè al servei TDX. Tampoc s'autoritza la presentació del seu contingut en una finestra o marc aliè a TDX (framing). Aquesta reserva de drets afecta tant als continguts de la tesi com als seus resums i índexs.

**ADVERTENCIA.** El acceso a los contenidos de esta tesis doctoral y su utilización debe respetar los derechos de la persona autora. Puede ser utilizada para consulta o estudio personal, así como en actividades o materiales de investigación y docencia en los términos establecidos en el art. 32 del Texto Refundido de la Ley de Propiedad Intelectual (RDL 1/1996). Para otros usos se requiere la autorización previa y expresa de la persona autora. En cualquier caso, en la utilización de sus contenidos se deberá indicar de forma clara el nombre y apellidos de la persona autora y el título de la tesis doctoral. No se autoriza su reproducción u otras formas de explotación efectuadas con fines lucrativos ni su comunicación pública desde un sitio ajeno al servicio TDR. Tampoco se autoriza la presentación de su contenido en una ventana o marco ajeno a TDR (framing). Esta reserva de derechos afecta tanto al contenido de la tesis como a sus resúmenes e índices.

**WARNING.** Access to the contents of this doctoral thesis and its use must respect the rights of the author. It can be used for reference or private study, as well as research and learning activities or materials in the terms established by the 32nd article of the Spanish Consolidated Copyright Act (RDL 1/1996). Express and previous authorization of the author is required for any other uses. In any case, when using its content, full name of the author and title of the thesis must be clearly indicated. Reproduction or other forms of for profit use or public communication from outside TDX service is not allowed. Presentation of its content in a window or frame external to TDX (framing) is not authorized either. These rights affect both the content of the thesis and its abstracts and indexes.



DOCTORAL THESIS

**Assessment of struvite and K-struvite  
recovery from digested manure**

Elena Tarragó Abella

2017

DOCTORAL PROGRAMME IN WATER SCIENCE AND TECHNOLOGY

**Supervisors:** Dra. Maria Dolors Balaguer Condom, Dr. Sebastià Puig Broch,

Dr. Maël Rusalleda Beylier

**Tutor:** Dra. Maria Dolors Balaguer Condom

PhD thesis submitted to aim for PhD degree for the University of Girona



## List of publications

---

Peer reviewed paper publications presented as chapter of this PhD thesis, and the candidate PhD contribution is listed below:

1. **E. Tarragó**, S. Puig, M. Rusalleda, M.D. Balaguer, J. Colprim, 2016. Controlling struvite particles' size using the up-flow velocity. Chemical Engineering Journal 302, 818-827.

<https://doi.org/10.1016/j.cej.2016.06.036>

Impact factor: 6.216. 1<sup>st</sup> quartile.

**Author's contribution:** Experimental design and performance. Data monitoring and crystallizer operation. Writing the paper.

2. **E. Tarragó**, M. Rusalleda, J. Colprim, M. D. Balaguer, S. Puig, 2017. Towards a methodology for recovering K-struvite from manure. Journal of Chemical Technology & Biotechnology, Accepted article.

<https://doi.org/10.1002/jctb.5518>

Impact factor: 3.135. 1<sup>st</sup> quartile.

**Author's contribution:** Design and performance of the experimental set-up, data monitoring, use of Minteq software. Writing the paper.

The following chapter of this PhD thesis is ready to be submitted as journal article, and the PhD contribution is below:

3. Effect of solids and its role on struvite formation from digested manure.

**Author's contribution:** Experimental design and performance. Data monitoring and crystallizer operation. Writing the paper.



## List of abbreviations and symbols

---

<b>ACP</b>	Amorphous calcium phosphates
<b>AD</b>	Anaerobic digestion
<b>ADox</b>	Digested and centrifuged manure after a partial nitrification plus Anammox process
<b>ADP</b>	Adenosine diphosphate
<b><math>A_{\text{downcomer}}</math></b>	Area of the downcomer
<b><math>A_{\text{riser}}</math></b>	Area of the riser
<b>ATP</b>	Adenosine triphosphate
<b>CTSR</b>	Continuous stirred tank reactor
<b>Deq</b>	Equivalent diameter
<b>DNA</b>	Deoxyribonucleic acid
<b>ESPP</b>	European Sustainable Phosphorus Platform
<b>EU</b>	European Union
<b>FBR</b>	Fluidized bed reactor
<b>g</b>	Standard acceleration
<b>HAP</b>	Hydroxiapatite
<b>HRT</b>	Hydraulic retention time
<b><math>H_{\text{downcomer}}</math></b>	Downcomer height
<b>IAP</b>	Ion activity product
<b><math>J_G</math></b>	Superficial gas velocity
<b><math>K_b</math></b>	Hydraulic pressure loss coefficients in the bottom
<b><math>K_t</math></b>	Hydraulic pressure loss coefficients in the top

<b>K<sub>s</sub></b>	Solubility constant
<b>K<sub>sp</sub></b>	Solubility product
<b>MAP</b>	Struvite (MgNH <sub>4</sub> PO <sub>4</sub> ·6H <sub>2</sub> O)
<b>MEM</b>	ManureEcoMine
<b>MKP</b>	K-struvite (MgKPO <sub>4</sub> ·6H <sub>2</sub> O)
<b>MTD</b>	Minimum theoretical equivalent diameter
<b>OM</b>	Organic matter
<b>P<sub>cs</sub></b>	Conditional solubility product
<b>PLR</b>	Phosphate loading rate
<b>P-recovery</b>	Phosphorus recovery
<b>P<sub>so</sub></b>	Product of the analytical molar concentration
<b>Q<sub>inf</sub></b>	Influent flow
<b>Q<sub>rec</sub></b>	Recirculation flow
<b>Q<sub>t</sub></b>	Total flow
<b>RNA</b>	Ribonucleic acid
<b>S/L separation</b>	Solid / Liquid separation
<b>S<sub>c</sub></b>	Supersaturation ratio
<b>SI</b>	Saturation index
<b>S<sub>r</sub></b>	Relative supersaturation
<b>TS</b>	Total solids
<b>TSS</b>	Total suspended solids
<b>U<sub>Lr</sub></b>	Average superficial liquid velocity in the riser
<b>V</b>	Settling velocity
<b>VS</b>	Volatile solids
<b>VSS</b>	Volatile suspended solids

<b>WW</b>	Wastewater
<b>WWTP</b>	Wastewater treatment plant
<b>XRD</b>	X-ray diffraction
$\alpha_i$	Ionization fraction
$\gamma_i$	Activity coefficient
$\Phi_{\text{downcomer}}$	Downcomer gas holdup
$\Phi_{\text{riser}}$	Riser gas holdup
$\rho_{\text{air}}$	Density of the air
$\rho_L$	Density of the fluid
$\rho_p$	Density of the particle
$\mu$	Fluid viscosity





## List of figures

---

<b>Figure 1. 1</b> Key processes of the natural phosphorus' cycle. Adapted from Bergmans (2011). .....	<b>3</b>
<b>Figure 1. 2</b> Phosphate rock reserve in the world. Adapted from Liu et al., 2013. ....	<b>4</b>
<b>Figure 1. 3</b> Scheme of the crystallization process .....	<b>9</b>
<b>Figure 1. 4</b> Influence of supersaturation on crystallization process (Wiesmann et al., 2007). .....	<b>10</b>
<b>Figure 1. 5</b> Synergistic coherence of the ManureEcoMine recovery core technologies, with two options indicated for P-recovery and residual N-removal. ....	<b>30</b>
<b>Figure 3. 1</b> The designed crystallizer: (A) scheme with the three differentiated parts (clarifier in green, riser in red, and collector in yellow; (B) image of the crystallizer; and (C) hydraulics of the reactor, representing the aeration air and liquid flows ( $Q_t$ , $Q_{rec}$ and $Q_{inf}$ ). .....	<b>40</b>
<b>Figure 3. 2</b> General scheme of the crystallizer used as experimental set-up. ....	<b>41</b>
<b>Figure 3. 3</b> Visual Minteq's input interface. ....	<b>43</b>
<b>Figure 3. 4</b> Visual Minteq's output of the saturation indices for minerals. Oversaturation in red, undersaturation in blue, and apparent equilibrium in green.	<b>45</b>
<b>Figure 4. 1</b> Scheme of the crystallizer designed for struvite recovery. Crystallizer's parts: riser (1), clarifier (2) and collector (3). In the zoom, crystallizer's hydrodynamics in the riser: recirculation flow ( $Q_{rec}$ ), induced by the air-flow rate applied; influent flow ( $Q_{inf}$ ); and total flow ( $Q_t$ ) as the sum of $Q_{rec}$ and $Q_{inf}$ . ....	<b>57</b>

<b>Figure 4. 2</b> Minimum theoretical equivalent diameter (MTD), in $\mu\text{m}$ , that can be retained in the riser as a function of the up-flow velocity ( $\text{m h}^{-1}$ ). The total flow ( $\text{m}^3 \text{d}^{-1}$ ), as a sum of the recirculation ( $Q_{\text{rec}}$ ) and the influent flow ( $Q_{\text{inf}}$ ), is represented as $Q_{\text{total}}$ . .....	<b>61</b>
<b>Figure 4. 3</b> XRD diffractograms of the precipitates settled in the collector of the crystallizer at the up-flow velocity of $22.55 \text{ m h}^{-1}$ . (A) Test for struvite recovery at different up-flow velocities (1 h tests); (B) continuous mode tests. ....	<b>67</b>
<b>Figure 4. 4</b> Particle size recovered ( $D_{\text{eq}}$ ) as a function of the up-flow velocity. The curve fitted is showed in black, the 95% confidence band in blue, and the 95% prediction band in red. ....	<b>69</b>
<b>Figure 4. 5</b> Average phosphate's concentration during the tests of 138.6 h at the up-flow velocity of $22.6 \text{ m h}^{-1}$ . pH control (pH in the riser) is presented in green and pH in the clarifier zone in pink, for one of the replicates. ....	<b>73</b>
<b>Figure 4. 6</b> Particle size distribution results over time in 14 particle size ranges (from $0\text{-}50 \mu\text{m}$ to $900\text{-}1000 \mu\text{m}$ ), from the continuous mode experiments at the up-flow velocity of $22.6 \text{ m h}^{-1}$ . The results presented are the average of replicates. ....	<b>74</b>
<b>Figure S4. 1</b> Particle size distribution results, by the laser diffraction method, for each up-flow velocity studied. ....	<b>71</b>
<b>Figure 5. 1</b> P-recovery efficiencies and solids' load during the synthetic digestate tests (S1-S4), the 20% digestate tests (M1-M2) and the 50% digestate tests (M3)..	<b>84</b>
<b>Figure 5. 2</b> Average $D_{\text{eq}}$ over time during the control tests (S1-S4), with a representative optic microscope image of the crystals recovered in each test. The scale bar represents $250 \mu\text{m}$ . ....	<b>86</b>
<b>Figure 5. 3</b> XRD diffractogram of the product recovered during M3. ....	<b>87</b>

<b>Figure 5. 4</b> Composition of the product recovered, expressed as g in a Kg of product recovered, during the synthetic (S3-S4) and digestate (M1-M3) tests. NI means “Not Identified”.	89
<b>Figure 5. 5</b> Average Deq over time during the digestate tests (M1-M3), with a representative optic microscope image of the crystals recovered in each test. The scale bar represents 100 $\mu\text{m}$ .	91
<b>Figure 5. 6</b> Optic microscope images. A) Optic microscope image (20x) of a crystal formed around a solid particle (red) which acted as nuclei for heterogeneous nucleation, during M1 period. B) Optic microscope image (10x) of a crystal net observed during M1 period, in which solid particles acted as linking bonds for previously formed struvite crystals. The scale bar represents 100 $\mu\text{m}$ .	92
<b>Figure 6. 1</b> Saturation Index (SI) of K-struvite as a function of pH, for a range of temperatures from 20°C to 50°C.	103
<b>Figure 6. 2</b> Nutrient recoveries in mmols recovered per liter treated of the 10% ADox manure solution, obtained during the batch tests performed in a range of pH from 9 to 12 to determine the effect of pH on K-struvite formation. Dot line represents the maximum P-recovery, assuming 100% P-recovery.	105
<b>Figure 6. 3</b> Composition of the product recovered, for each manure level tested, expressed in percentage of mmols per liter of feed solution.	109
<b>Figure S6. 1</b> XRD diffractogram of the product recovered at pH 10, during the batch tests carried out to determine the effect of pH on K-struvite formation. K-struvite is identified in green, magnesium phosphate in blue, potassium chloride in red and the background noise indicates an amorphous substance, most likely magnesium hydroxide (typically found as amorphous).	106

**Figure S6. 2** XRD diffractogram of the product recovered using a 100% manure solution, during the tests to determine the influence of manure’s matrix on nutrient recovery performance. K-struvite is identified in purple, sodium chloride in red, potassium chloride in blue, and the background noise indicates an amorphous substance, most likely magnesium hydroxide (typically found as amorphous). ... **108**

**Figure S6. 3** Images of crystals’ morphology obtained through optic microscope observation (10x) for the test using 10% manure solution. .... **111**

**Figure S6. 4** Images of crystals’ morphology obtained through optic microscope observation (10x) for the test using 50% manure solution. .... **111**

**Figure S6. 5** Images of crystals’ morphology obtained through optic microscope observation (20x) for the test using 100% manure solution. .... **111**

## List of tables

---

<b>Table 1. 1</b> Summary of the state of the art on struvite recovery from manure. ....	<b>17</b>
<b>Table 1. 2</b> Operational and developing technologies for P-recovery by struvite and/or K-struvite crystallization. ....	<b>21</b>
<b>Table 4. 1</b> Physico-chemical characteristics of the influent. The results are presented as mean $\pm$ standard deviation. ....	<b>59</b>
<b>Table 4. 2</b> Relative supersaturation, induction time, struvite production and phosphate recovery efficiency for each up-flow velocity studied. Also, volatile suspended solids (VSS) in the effluent of each test are presented. ....	<b>63</b>
<b>Table 4. 3</b> Comparison between performances of the designed crystallizer and similar reactors available in the literature cited. Adapted from Tarragó et al., 2016. ....	<b>66</b>
<b>Table 4. 4</b> Comparison between the MTD and the experimental mean equivalent diameter recovered (Mean Deq) for each up-flow velocity studied. ....	<b>68</b>
<b>Table 5. 1</b> Physical-chemical characteristics of the influent. The results are presented as mean $\pm$ standard deviation. The range expresses the parameter at M1-M2, respectively (see section 5.2.3). ....	<b>80</b>
<b>Table 5. 2</b> Operational conditions for each influent used, and established periods: synthetic digestate (S) and digestate (M). ....	<b>82</b>
<b>Table 6. 1</b> Physico-chemical characteristics of the ADox solutions used (0-10-50-100%). The results are presented as mean $\pm$ standard deviation. ....	<b>101</b>

**Table 6. 2** SI of the three compounds that can be formed at 38°C, according to Visual Minteq software. .... **104**

**Table 7. 1** Comparison between performances of the designed crystallizer and similar reactors available in the literature cited. Adapted from Chapter 4 (Table 4.3) ..... **119**



### **Certificate of thesis direction**

La Dra. Maria Dolors Balaguer Condom, el Dr. Sebastià Puig Broch, i el Dr. Maël Rusalleda Beylier del Laboratori d'Enginyeria Química i Ambiental (LEQUIA) de la Universitat de Girona,

#### **DECLAREM:**

Que el treball titulat "Assessment of struvite and K-struvite recovery from digested manure", que presenta l'Elena Tarragó Abella per a l'obtenció del títol de doctor/a, ha estat realitzat sota la nostra direcció, i que compleix els requisits per poder optar a Menció Internacional.

I perquè així consti i tingui els efectes oportuns, signem aquest document.

Dra. Maria Dolors Balaguer Condom

Dr. Sebastià Puig Broch

Dr. Maël Rusalleda Beylier

Girona,

de 2017





**Nothing that's worthwhile is ever easy.**

**Remember that.**

**N. Sparks**

Per a tu, Enric, i per a vosaltres, papes.



## Agraïments / Acknowledgements

---

Heus aquí una de les parts de la tesi més difícils d'escriure, però suposo que tot és començar, i anar pensant una mica, i segur que em surten totes les persones que han estat importants durant el transcurs de tota aquesta tesi. Així doncs, som-hi!

En primer lloc, m'agradaria agrair als meus directors de tesi i en Jesús, pels esforços dedicats en mi, perquè sense ells no hagués estat possible fer aquest camí. Sebastià, tu vas ser qui em va iniciar en això de la recerca, i mira a on estem! Has estat un gran pilar al llarg de tot aquest procés, donant ànims en tot moment, i essent tu, moltes gràcies. Marilós, m'agradaria agrair-te tot el temps que m'has dedicat, ajudant-me a entendre bé tots els processos i càlculs, i intentant plasmar bé tots aquests resultats, a vegades tant dispers, moltes gràcies. Jesús, les teves pressions constants i visites sorpresa han fet que sàpiga estar al corrent de tots els processos, i sobretot, a voler millorar constantment, moltes gràcies. I per últim, també en incorporació al MEM, en Maël, a qui li agreixo els seus ànims constants sempre veient el millor de tot plegat (que en moltes ocasions no ha estat fàcil), fent xerrades ràpides que sempre s'allargaven, acompanyant-me al llarg de tot aquest procés que és fer un Doctorat, i sempre compartint bons moments en els Project Meetings, que ja ens feia falta! Així doncs, una vegada més, moltes gràcies als quatre.

Formar part del LEQUIA ha estat un plaer, i he tingut la oportunitat de conèixer a grans persones i grans professionals, entre ells a l'equip de piles, que m'ha acollit com una més tot i ser una mica infiltrada perquè de piles en tinc poc. Moltes gràcies Anna, per tots els moments viscuts a dins i fora del laboratori, Narcís, Pau, i l'última incorporació, el andorrano Ramiro. No em voldria deixar d'agradir a la resta de companys del LEQUIA, la Patri, la Sara J. (good luck in your thesis, you can do it!), l'Alba C., la Montse, la Sara G., en Serni (i el seu ordinador fantasma), l'Alba A.

(gràcies per ajudar-me i compartir la paciència amb els equips), l'Antonia, en Tico, l'Eric, l'Alba C., en Lluís, en Gaetan, l'Hèctor, en Ramon, i la Teresa (sempre present i ajudant en el que ha fet falta).

També voldria donar les gràcies a en Tommy, thanks to come and help me with the crystallizer, feeding the baby with manure, and spending many hours in the lab. I gràcies a tots els estudiants que m'han ajudat durant aquest temps, la Marta G., la Marta P., l'Ester, en Màrius, en Tomáš, en Marc, en Miquel, la Clara i l'Alba B.

Però voldria donar les gràcies als que ara anomeno amics, i que sense el LEQUIA no ens haguéssim conegut. Tiago, Stijn, Daniele and Julian (also Therese and Peter), you have been fundamental along this thesis. Not only have we shared good moments in the lab, but also outside. From visiting the whole Costa Brava to visit three countries in one weekend, sharing numerous meals and trips, and more important, being around each other and sharing really good moments. Knowing you it has been a plus, and now I can say you are my friends, and there are still many things to do together!

I would like to thank Prof. Arne Verliefde, for allowing me to do my research stage in PaInT (UGent, Belgium) and to improve my knowledge about K-struvite recovery. It has been a pleasure to be part of your group. In addition, special thanks to Sebastiaan to make me feel like home during my time in Gent, and involving me in everything. I have learned a lot during the stage, and it has been also thanks to you. So, thanks to all my colleagues in PaInT, and also thanks to Youri (BioMath, UGent), for the discussions about crystallization processes and models.

Moreover, this thesis wouldn't be possible without the ManureEcoMine project. Having the opportunity to be involved in this European project has allowed me to meet interesting and good professionals and grow professionally, but more important, to have a holistic approach of the manure treatment. Thus, I would like to say thank you to everyone involved in this project, especially Prof. Siegfried

Vlaeminck for making this project possible. Special thanks to CMET (Siegfried, Cristina, Delphine, Curro, Samuel, Lai, Giovanni, ...), Biogrup (Juan Lema, Marta, Chiara, Iván, Maite, ...), AgrEcon (Jeroen, Gwen, Andreas, ...), BOKU-IFA (Werner, Johannes, ...), BOKU-SIG (Norbert, ...), FZJ (Nicolai, Ana, ...), Colsen (Merijn, Sam, Bert, Joop, ...), Ahidra (Jimena, Oscar, Alejandro, ...), Balsa (Francesc, ...), LVA (Céline, Sabrina, Barbara, ...), Peltracom (Oliver, ...), and Van Alphen (Jan, ...).

Per últim, no podria deixar-me a la meua família: Gràcies mama i papa, els vostres ànims i consells han estat indispensables, i sobretot, gràcies per confiar en mi en tot moment, recolzar-me en totes les decisions, i donar-me la oportunitat de rebre aquesta formació, us estimo. Gràcies a l'Anna i la Pilar, pels ànims constants rebuts, perquè aquesta tesi també va per tu Pilar. També gràcies a les àvies i sogre, i als meus tius (i cosines i cosí), per estar al meu costat durant l'estada a Bèlgica, qui ho havia de dir que acabaria allà!

Tampoc em podria descuidar de donar les gràcies a l'Enric i a la Silvia, el meu marranot i la meua pitufa. Per vosaltres també va aquesta tesi, perquè pugueu indagar una mica més sobre el que he estat fent tot aquest temps, i saber perquè no us he pogut dedicar tot el temps que hagués volgut. Gràcies per confiar en mi, i donar-me ànims, també des de la distància. Us estimo, i us necessito!

I gràcies a l'Enric, el meu marit, millor amic, confident, i company de vida. No sabia per on començar, però gràcies per estar sempre al meu costat, recolzar-me i donar-me ànims quan més ho necessitava. Tot i no comprendre massa al principi de què anava tot això de fer la tesi, has estat amb mi durant tots els passos. Només dir-te que ara comença una altra etapa de la nostra vida, i que junts l'afrontarem. T'estimo.

Moltes gràcies a tots els que m'heu acompanyat al llarg d'aquest camí ☺



This thesis was financially supported by the Catalan Government (2014FI\_B 00264, pre-doctoral grant), the University of Girona (MOB16, mobility grant), the European Community's Framework Programme (FP7/2007-2013) under Grant Agreement nº603744, within the ManureEcoMine project. LEQUIA has been recognized as a consolidated research group by the Catalan Government with code 2014-SGR-1168. LEQUIA would like to thank the University of Girona (MPCUdG2016/137) for its financial support.





## Resum

---

Durant els últims segles, els humans han tingut un impacte en el cicle natural del fòsfor degut al creixement exponencial de la població, amb el consegüent augment en la demanda de menjar, i en la demanda del fòsfor com a fertilitzant. El fòsfor s'obté del guano (excrements d'aus) i de la roca fosfàtica (apatita), essent així un recurs limitat. Són vàries les prediccions sobre la possible extinció d'aquest en 100-250 anys, fet que fa augmentar el preu d'aquest cada any. Per tant, les accions a dur a terme durant els propers 10-25 anys haurien d'anar enfocades a la recuperació de fòsfor en comptes de l'eliminació, fet reforçat pel canvi en les polítiques europees. Així, es podria recuperar fòsfor a partir de fonts renovables, com podrien ser els purins.

En relació, els purins s'han estat aplicant directament al sòl com a fertilitzant, però l'impacte d'aquesta pràctica en el medi ambient, especialment en la qualitat de l'aigua, ha forçat el tractament dels purins abans de ser aplicats, normalment a través de l'eliminació de compostos orgànics i nutrients. No obstant, els purins tenen un alt contingut en nutrients, fet que permet la recuperació d'aquests a partir de fonts renovables. En aquesta tesi doctoral es planteja la recuperació de fòsfor en forma d'estruvita ( $\text{MgNH}_4\text{PO}_4 \cdot 6\text{H}_2\text{O}$ ) o K-estruvita ( $\text{MgKPO}_4 \cdot 6\text{H}_2\text{O}$ ). La recuperació de nutrients (nitrogen, N; fòsfor, P; i potassi, K) es considera un avanç important i essencial per assegurar el subministrament de fòsfor econòmicament a llarg termini, al mateix temps que s'obté un fertilitzant d'alliberació lenta.

Els primers dos capítols d'aquesta tesi doctoral estan relacionats amb les propietats del producte recuperat a partir dels purins, així com també en el tamany dels cristalls d'aquest. En el primer capítol, es desenvolupa una metodologia per al control del

tamany de partícula de l'estruvita, basada en el control de la velocitat ascensional. El cristal·litzador dissenyat (una combinació de reactor "air-lift" i sedimentador) permet estudiar la viabilitat de la velocitat ascensional com a paràmetre de control del tamany de partícula, tant en testos en discontinu com en continu, per a potenciar la fase de creixement dels cristalls. A més a més, es demostra que la velocitat ascensional determina el tamany mínim de partícula que es pot recuperar. Així doncs, la velocitat ascensional resulta una eina útil per al control del tamany de partícula als requeriments dels clients finals.

A continuació, s'estudia la recuperació d'estruvita a partir de purins prèviament digerits, així com també les propietats del producte recuperat. Es demostra que es pot recuperar estruvita a pH 8.5, tot i que també s'observa la co-precipitació d'altres productes (com per exemple,  $Mg_3(PO_4)_2$ ) sense afectar-ne les propietats com a fertilitzant. Malgrat això, els purins representen una matriu complexa per a la recuperació d'estruvita, i una tecnologia desafiant degut a l'elevada concentració de sòlids, que s'identifica com una de les principals limitacions. Es realitza un estudi per a determinar el paper dels sòlids durant la fase de nucleació i creixement de l'estruvita, i l'efecte dels sòlids en suspensió en les propietats del producte recuperat. S'estableix que la presència de sòlids en suspensió no limita la formació d'estruvita, sinó que aquests actuen com a nuclis potenciant la nucleació heterogènia, i afavorint l'agregació i/o aglomeració de cristalls d'estruvita.

Finalment, en l'últim capítol es pretén proporcionar una metodologia per a recuperar a partir dels purins un dels macronutrients més limitat en el sòl (el potassi) com a K-estruvita. Actualment, la recuperació de K-estruvita és incipient, i la seva cristal·lització a partir d'aigües residuals es troba en l'etapa de prova de concepte. Per tant, primer es realitza un enfoc teòric amb el programa Minteq, per a posteriorment modelar i ajustar experimentalment en testos en discontinu, i determinar l'efecte del pH i la temperatura. Així, es demostra la viabilitat de la

recuperació de K-estruvita a partir de purins digerits i després d'un procés de separació sòlid/líquid, i de l'eliminació de nitrogen per un procés Anammox.

Aquesta tesi doctoral pretén aportar innovacions i reflexions sobre la recuperació dels macronutrients essencials (potassi, fòsfor i nitrogen) pel creixement de les plantes, a partir d'aigües residuals. Més concretament, sobre la recuperació sostenible de fertilitzants (struvita i/o K-estruvita) a partir de purins.



## Resumen

---

Durante los últimos siglos, los humanos han tenido un impacto en el ciclo natural del fósforo debido al crecimiento exponencial de la población, con el consecuente incremento en la demanda de comida, y en la demanda de fósforo como fertilizante. El fósforo se obtiene del guano (excrementos de aves marinas) y de las rocas fosfáticas (apatita), siendo así un recurso limitado. Hay varias predicciones sobre la posible extinción de este recurso en 100-250 años, hecho que hace aumentar el precio de éste cada año. Por lo tanto, las acciones a llevar a cabo durante los siguientes 10-25 años deben enfocarse a la recuperación del fósforo en vez de a su eliminación, hecho reforzado por el cambio en las políticas europeas. Así, el fósforo se podría recuperar de fuentes renovables, como podrían ser los purines.

En relación, los purines llevan años aplicándose directamente como fertilizante en el suelo, pero el impacto de ésta práctica en el medio ambiente, especialmente en la calidad del agua, ha forzado el tratamiento de los purines antes de ser aplicados, normalmente mediante la eliminación de compuestos orgánicos y nutrientes. Sin embargo, los purines presentan un elevado contenido en nutrientes, los cuáles pueden ser recuperados así a partir de fuentes renovables. En ésta tesis doctoral se plantea la recuperación de fósforo en forma de estruvita ( $\text{MgNH}_4\text{PO}_4 \cdot 6\text{H}_2\text{O}$ ) o K-estruvita ( $\text{MgKPO}_4 \cdot 6\text{H}_2\text{O}$ ). La recuperación de nutrientes (nitrógeno, N; fósforo, P; y potasio, K) a partir de aguas residuales se considera un avance importante y esencial para asegurar el suministro de fósforo económicamente a largo plazo, al mismo tiempo que se obtiene un fertilizante de liberación lenta.

Los dos primeros capítulos de ésta tesis doctoral están relacionados con las propiedades del producto recuperado a partir de purines, así como también en el tamaño de los cristales de éste. En el primer capítulo, se desarrolla una metodología

para controlar el tamaño de partícula de la estruvita, basada en el control de la velocidad ascensional. El cristizador diseñado (una combinación de reactor “air-lift” y sedimentador) permite estudiar la viabilidad de la velocidad ascensional como parámetro de control del tamaño de partícula, en pruebas en discontinuo y continuo, para potenciar la fase de crecimiento de los cristales. Además, se demuestra que la velocidad ascensional determina el tamaño mínimo de partícula que se puede recuperar. Así pues, resulta ser una herramienta útil para el control del tamaño de partícula a los requerimientos de los clientes.

A continuación, se estudia la recuperación de estruvita a partir de purines previamente digeridos, así como también las propiedades del producto recuperado. Se demuestra que se puede recuperar estruvita a pH 8.5, aunque también se observa la co-precipitación de otros compuestos (como por ejemplo,  $Mg_3(PO_4)_2$ ), sin por ello afectar a sus propiedades como fertilizante. Sin embargo, los purines presentan una matriz compleja para la recuperación de estruvita, y una tecnología desafiante debido a la elevada concentración de sólidos, hecho que se identifica cómo una de las principales limitaciones de ésta tecnología. Se realiza un estudio para determinar el papel de los sólidos durante la fase de nucleación y crecimiento de la estruvita, y el efecto de los sólidos en suspensión en las propiedades del producto recuperado. Se establece que la presencia de sólidos en suspensión no limita la formación de estruvita, sino que actúan cómo núcleos potenciando la nucleación heterogénea, y favoreciendo la agregación y/o aglomeración de cristales de estruvita.

Finalmente, en el último capítulo de ésta tesis se pretende proporcionar una metodología para la recuperación a partir de purines de uno de los macronutrientes más limitados en el suelo (el potasio) cómo K-estruvita. Actualmente, la recuperación de K-estruvita es incipiente, y la cristalización a partir de aguas residuales se encuentra en fase de prueba de concepto. Por lo tanto, en primer lugar, se realiza un enfoque teórico con el programa Minteq, para posteriormente modelar

y ajustar experimentalmente en pruebas en discontinuo y continuo, y determinar el efecto del pH y la temperatura. Así, se demuestra la viabilidad de la recuperación de K-estruvita a partir de purines digeridos y después de un proceso de separación sólido/líquido, y de la eliminación de nitrógeno por un proceso Anammox.

Ésta tesis doctoral pretende aportar innovaciones y reflexiones sobre la recuperación de los macronutrientes esenciales (potasio, fósforo y nitrógeno) para el crecimiento de las plantas, a partir de aguas residuales. Más concretamente, sobre la recuperación sostenible de fertilizantes /estruvita y/o K-estruvita) a partir de purines.





## Summary

---

During the last few centuries, humans have had an impact on the natural phosphate cycle due to the exponential increase of population, with its consequent increase in food demand, and its demand as a fertilizer. Phosphorus is obtained from guano (bird droppings) and phosphate rock (apatite), being a non-renewable resource. Many predictions establish that the resource could be exhausted in 100-250 years, increasing its price every year. Therefore, the actions for the coming 10–25 years must focus on the recovery of phosphorus rather than its removal, reinforced by European policies. Thus, phosphorus could be recovered from renewable sources, such as manure.

In relation, manure has been applied directly to the soil as a fertilizer for many years, but its impact on the environment, especially on water quality, has forced to treat manure before its application, usually by removing the organics and nutrient content. However, manure has a high content of nutrients, which can be recovered, obtaining nutrients from renewable sources. In this PhD thesis, the recovery of phosphorus as struvite ( $\text{MgNH}_4\text{PO}_4 \cdot 6\text{H}_2\text{O}$ ) and/or K-struvite ( $\text{MgKPO}_4 \cdot 6\text{H}_2\text{O}$ ) from manure are proposed. The recovery of nutrients (nitrogen, N; phosphorus, P; and potassium, K) from waste streams is considered to be an essential and significant breakthrough for assuring long-term and economical phosphorus supply, while recovering a valuable slow-release fertilizer.

The first two chapters of this PhD thesis are related to the properties of the product recovered from manure, as well as the size of the crystals recovered. First, a methodology is developed to control the particle size of struvite, based on the control of the up-flow velocity. The designed crystallizer (a combined air-lift reactor

with a settler) allows to assess the viability of using the up-flow velocity as a control parameter for the growth of struvite particles, first in batch tests and following, in continuous mode to enhance the growth phase. Moreover, it is demonstrated that the up-flow velocity determines the minimum theoretical equivalent diameter that can be recovered. Thus, the up-flow velocity is proven a successful controlling parameter of particle size to the customers' requirements for fertilizer application. Following, struvite recovery from digested manure is studied, as well as the properties of the product recovered. It was demonstrated that struvite could be recovered at the optimal pH of 8.5, although co-precipitation of other products (i.e.  $Mg_3(PO_4)_2$ ) was observed, without affecting the fertilizer properties. However, manure is a complex stream for struvite recovery, and a challenging technology due to the high content of solids, which many authors identify as one of the main limitations. Therefore, a study to determine the role of solids in struvite nucleation and growth, as well as the effect of suspended solids in the properties of the product recovered, was developed. It was demonstrated that solid particles not only did not inhibit struvite formation, but they acted as nuclei enhancing heterogeneous nucleation, and favored the aggregation and/or agglomeration of struvite crystals.

Finally, the last chapter of this PhD thesis aims to provide a methodology to recover the most limited macronutrient in soils (potassium) as K-struvite from swine manure. At present, the recovery of potassium struvite is nascent, and its crystallization from waste streams is at the proof of concept stage. Therefore, a theoretical approach was first conducted with Minteq software, and later modelled and experimentally adjusted in batch tests, while determining the effect of pH and temperature. Thus, the viability of the process was proven recovering K-struvite directly from digested manure after a solid/liquid separation and a nitrogen removal through Anammox.

This PhD thesis aims to bring innovation and insights on the recovery of essential macronutrients (potassium, phosphorus and nitrogen) for plants' growth from waste streams. Specifically, the sustainable recovery of fertilizers (i.e. ammonium and/or potassium struvite) from swine manure.



## Table of contents

---

List of publications .....	III
List of abbreviations .....	V
List of figures .....	IX
List of tables .....	XIII
Certificate of thesis direction .....	XV
Agraïments / Acknowledgements .....	XIX
Resum.....	XXV
Resumen.....	XXIX
Summary. ....	XXXIII
Table of contents.....	XXXVII
Chapter One	
Introduction .....	1
1.1 Phosphorus, an essential nutrient and a limited resource .....	2
1.2 Nutrient recovery via struvite and K-struvite crystallization .....	6
1.2.1 Struvite crystallization.....	6
1.2.2 K-struvite crystallization.....	7
1.2.3 The crystallization process and its influencing factors .....	8
1.2.4 Operational conditions for struvite recovery: state-of-the-art .....	14
1.3 Applicability of struvite and K-struvite as fertilizers .....	23
1.4 Phosphorus recovery within circular economy and legislation .....	25
1.5 ManureEcoMine: a sustainable approach for nutrient recovery from manure ..	29

Chapter Two	
Objectives.....	33
Chapter Three	
Methodology.....	37
3.1 Design of the crystallizer .....	38
3.2 Visual Minteq software .....	42
3.3 Calculations .....	45
3.3.1 Chemical calculations.....	45
3.3.2 Minimum theoretical equivalent diameter.....	46
3.3.2 Up-flow velocity .....	47
3.4 Analytical methods.....	48
3.4.1 Physico-chemical analysis .....	48
3.4.2 Characterization of the product recovered .....	49
Chapter Four	
Controlling struvite particles' size using the up-flow velocity .....	53
4.1 Overview .....	54
4.2 Materials and methods .....	56
4.2.1 Experimental set-up .....	56
4.2.2 Experimental procedure .....	58
4.2.3 Influent wastewater .....	58
4.2.4 Calculations .....	59
4.2.5 Analytical methods.....	62
4.3 Results and discussion.....	62
4.3.1 MTD as a function of the up-flow velocity.....	62
4.3.2 Struvite recovery performance at different up-flow velocities .....	63
4.3.3 Experimental size of struvite particles .....	68

4.3.4 Promoting the growth of struvite particles by operating the crystallizer in continuous mode .....	71
4.4. Conclusions .....	75

## Chapter Five

Effect of suspended solids on struvite formation from digested manure supernatant.....	77
5.1. Overview .....	78
5.2. Materials and methods .....	79
5.2.1 Experimental set-up .....	79
5.2.2 Influent wastewater .....	80
5.2.3 Experimental procedure .....	81
5.2.4 Analytical methods.....	82
5.3. Results and discussion.....	83
5.3.1 Effect of the matrix on P-recovery .....	83
5.3.2 Characterization of the product recovered .....	87
5.3.3 The role of solids on struvite formation .....	90
5.3.3.1 Effect of solids on struvite crystallization .....	90
5.3.3.2 Effect of digestate matrix on particle size .....	93
5.4. Conclusions .....	95

## Chapter Six

Towards a methodology for recovering K-struvite from manure.....	97
6.1 Overview .....	98
6.2 Experimental .....	100
6.2.1 Visual Minteq software .....	100
6.2.2 Experimental procedure .....	100
6.2.3 Analytical methods.....	101



6.3 Results and Discussion .....	102
6.3.1 Theoretical approach .....	102
6.3.2 pH effect on K-struvite formation.....	104
6.3.3 Influence of manure matrix on K-struvite formation .....	107
6.3.3.1 Nutrient recovery efficiencies .....	107
6.3.3.2 Morphology of the crystals recovered .....	110
6.4 Conclusions.....	112
Chapter Seven	
General discussion .....	113
7.1 From waste to resource .....	114
7.2 The scope of this PhD thesis: ManureEcoMine project .....	114
7.3 The up-flow velocity as the parameter to control particle size .....	115
7.4 Influence of suspended solids present in the feedstock matrix on the quality of the product recovered .....	120
7.5 Potassium: the third essential macronutrient .....	122
Chapter Eight	
Conclusions .....	125
Chapter Nine	
References.....	129

# Chapter One

## Introduction

---

## 1.1 Phosphorus, an essential nutrient and a limited resource

Phosphorus is an essential element for the optimal growth of all living organisms. It plays an important role in intercellular energy transfer with the conversion of adenosine diphosphate (ADP) into adenosine triphosphate (ATP) (Bergmans, 2011), and is an essential element of deoxyribonucleic acid (DNA) and ribonucleic acid (RNA), phospholipids and for teeth and bones of humans and animals (Crutchik, 2015).

Figure 1. 1 presents a simplified phosphorus cycle scheme, with its key processes and without considering the effect of humans. Phosphorus is located in soils (land) and water (inland/coastal waters), from which plants, algae and animals uptake it and incorporate it into their cycle, and eventually, returns to soil/water, being available again. In parallel, phosphorus is continuously transported from land to inland/coastal waters by mechanical and chemical erosion of the Earth's crust, and ends up in sediments at the bottom of water bodies, which will appear at the Earth's surface as phosphate rock, thereby closing the geological cycle (Bergmans, 2011).

The exponential increase of population during the 20<sup>th</sup> century with its consequent increase in food demand, forced the addition of phosphorus in the soil to achieve the necessary concentrations to allow the growth of crops. The phosphorus demand was fulfilled with the addition of fertilizers (nitrogen-phosphorus-potassium fertilizers) in the soil, and in livestock areas with manure, replacing the widely use of guano during the 19<sup>th</sup> century (Cordell et al., 2009). However, phosphorus and potassium are limited resources in comparison to nitrogen, and the uncontrolled application of manure led to the degradation of water quality. In addition, urbanization and livestock intensification led to unbalanced phosphate transport towards urban areas, and deforestation and agriculture intensification accelerated

the natural transport of phosphate to the sea, depleting the phosphate reserves (Bergmans, 2011).

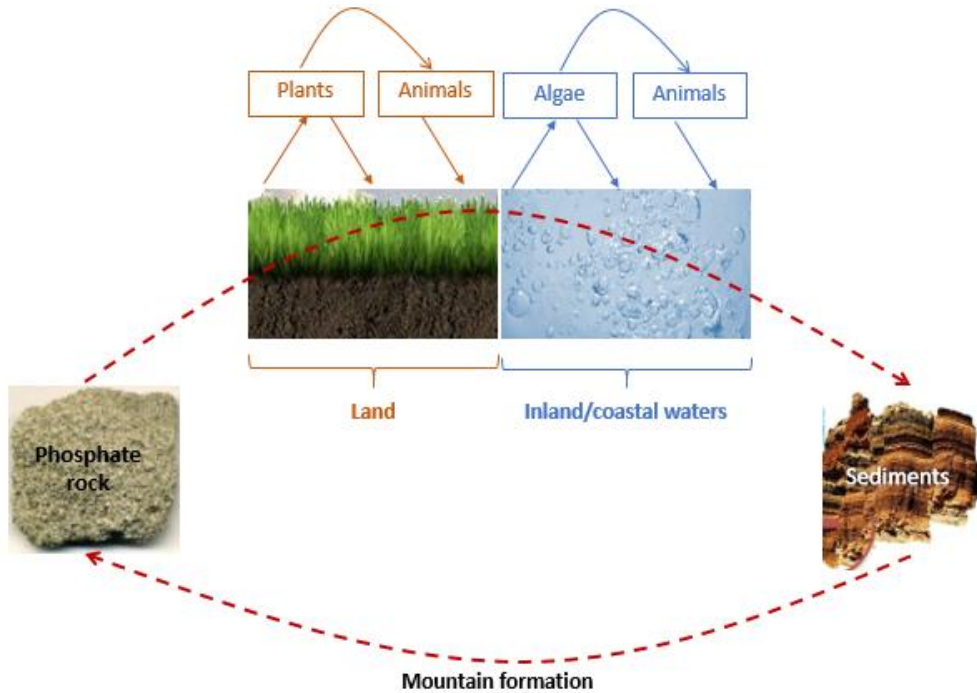


Figure 1. 1 Key processes of the natural phosphorus' cycle. Adapted from Bergmans (2011).

The two main sources for phosphate are guano (bird droppings) and mineral rocks containing concentration of the calcium phosphate mineral called Apatite ( $\text{Ca}_5(\text{PO}_4)_3(\text{F},\text{Cl},\text{OH})$ ). Phosphate rock (apatite) is a finite resource and is a non-detrital sedimentary rock which contains high amounts of phosphate minerals. According to Cordell et al., 2009, modern agriculture is totally dependent on regular inputs of phosphate fertilizers derived from mined apatite to replenish the phosphorus removed from the soil by the growing and harvesting of crops. However, deposits with high quantity and concentration of phosphate which can be mined as ore for their phosphate content are unevenly distributed throughout the world (Figure 1. 2). The largest deposits are found in Morocco, China, United States and South Africa. These countries contain over 80% of the world's phosphate resource.

Approximately 79% of phosphorus rock is used to make fertilizers (phosphate rock contains approximately 30 % of phosphorus as  $P_2O_5$ , 5% of calcium carbonate and less than 4% of combined iron and aluminium oxides), 11% for feed grade additives, and approximately 7% for detergents (Liu et al., 2013). The remaining is used in particular products, such as additives for human food or in metal surface treatments to delay corrosion.

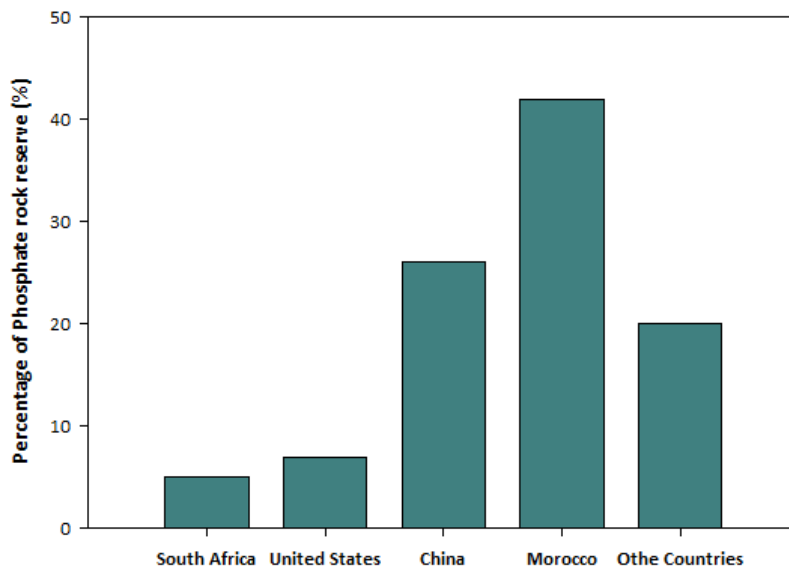


Figure 1. 2 Phosphate rock reserve in the world. Adapted from Liu et al., 2013.

Only 7000 million tons of phosphorus rock as  $P_2O_5$  are estimated to be remaining in reserves that could be economically mined. Furthermore, human population consumes 40 million tons of phosphorus as  $P_2O_5$  each year, and the predictions are that phosphorus demand will increase by 1.5% each year (Steen, 1998). According to these, the resource could be exhausted in 100-250 years, and the price will increase every year (Liu et al., 2013). It is estimated that the phosphate rock which can be economically exploited will last, at the best scenario, little more than 100 years and, in the worse scenario, it could be depleted in 50 years (Münch and Barr, 2001).

Thus, the reserves may be depleted if nothing is done to recover and recycle phosphate (Bergmans, 2011), and as a consequence, phosphate rock was added to the EU List of 20 Critical Raw Materials.

Therefore, the actions for the coming 10–25 years must focus on the recovery of phosphorus rather than its removal, a common practice until now.

Traditionally, phosphorus was removed either by chemical precipitation or by biological phosphorus removal processes. Chemical precipitation of phosphorus was widely used (still is) due to the simple operation and implementation. Despite this, one of the main disadvantage is the high cost of chemicals, and the high sludge production, which cannot be used in agriculture for its low bioavailability (Morse et al., 1998) and presence of metals (Shu et al., 2006). In contrast, sludge production and chemical costs are lower in biological phosphorus removal process. However, its low stability and flexibility, and its dependence on the wastewater characteristics are some of the disadvantages of this technology.

Nowadays, the use of mineral fertilizers is commonly widespread over the world, and every year its consumption increases due to the increasing food and feed production requests (Pintucci et al., 2016). These fertilizers have largely replaced animal manure, which is often considered as a waste product, in modern crop production. As a consequence, manure is generally disposed of by application to land within a narrow radius of where they are produced; a practice that has resulted in the buildup of phosphorus in soils surrounding livestock farms (Bateman et al., 2011). If manure is directly applied to the soil it can influence water quality, and represents an eutrophication threat in nitrate vulnerable zones (Menció et al., 2011).

Manure contains high concentrations of nutrients (nitrogen, N; phosphorus, P; potassium, K) (Riva et al., 2016). Traditionally, the removal of nutrients was applied

to diminish the environmental impact and prevent contamination of agricultural soils.

In addition, new European policies (European Commission, 2016, 2015) are reinforcing nutrient recovery instead of nutrient removal. Thus, if manure needs to be treated, and new ways for nutrient recovery must be investigated to assure the long-term and economical supply, manure represents a “mining” opportunity, as 1.27 billion ton of manure are produced each year in Europe (Tarragó et al., 2016). Nutrient recovery can be through struvite and K-struvite recovery from manure, as a valuable product can be obtained from a waste stream, which needs to be treated to diminish its environmental impact.

Phosphorus recovery (P-recovery) as struvite ( $\text{MgNH}_4\text{PO}_4 \cdot 6\text{H}_2\text{O}$ ) and/or K-struvite ( $\text{MgKPO}_4 \cdot 6\text{H}_2\text{O}$ ) from waste streams (e.g. manure) as a renewable source is considered to be an essential and significant breakthrough for assuring long-term and economical phosphorus supply. Struvite process allows the recycling of the limited resource phosphorus (Liu et al., 2013), while being a valuable slow-release fertilizer.

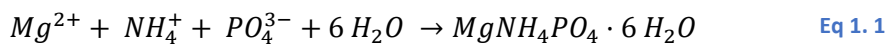
## 1.2 Nutrient recovery via struvite and K-struvite crystallization

### 1.2.1 Struvite crystallization

Magnesium Ammonium Phosphate, also known as MAP, ammonium struvite or struvite, is a white crystalline substance that consists of equimolar concentrations of magnesium ( $\text{Mg}^{2+}$ ), ammonium ( $\text{NH}_4^+$ ) and phosphate ( $\text{PO}_4^{3-}$ ), combined with six molecules of water. Struvite is considered a slow-release fertilizer, which offers many advantages versus conventional fertilizers: presents low leach rates and slowly release of nutrients (Münch and Barr, 2001); it is suitable in grasslands and forests

where fertilizers are applied once in several years (Rahman et al., 2014); it does not damage growing plants when a single high dose is applied (De-Bashan and Bashan, 2004); represents an alternative for those crops that require magnesium, such as sugar beets (Gaterell et al., 2000); and, phosphorus uptake is higher in ryegrass when struvite is used as a fertilizer (Johnston and Richards, 2003).

It is described as a soft mineral, with a molecular weight of 245.3 g mole<sup>-1</sup>, and a density of 1.7 Kg m<sup>-3</sup>. The structure is MgNH<sub>4</sub>PO<sub>4</sub> · 6 H<sub>2</sub>O, and typically precipitates as stable white orthorhombic crystals (Le Corre et al., 2005), according to Eq 1. 1.



Struvite crystallization has been widely investigated, and it occurs when the molar concentrations of magnesium, ammonium and phosphate exceed the solubility product ( $K_{sp}$ ) of struvite, which is 10<sup>-13.26</sup> at 25°C (Ohlinger et al., 1999). Struvite is produced under alkaline conditions due to phosphate speciation, and the solubility of struvite depends on the pH, as the speciation of the components is pH dependent (Ohlinger et al., 1998).

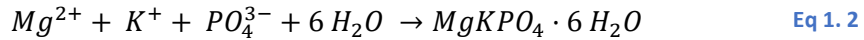
### 1.2.2 K-struvite crystallization

Magnesium Potassium Phosphate, known as MKP, potassium struvite or K-struvite is an inorganic phosphate mineral that contains equimolar concentrations of Mg<sup>2+</sup>, K<sup>+</sup> and PO<sub>4</sub><sup>3-</sup>. Its composition is similar to struvite (MgNH<sub>4</sub>PO<sub>4</sub>·6H<sub>2</sub>O), but it contains the most limited macronutrient in soils (potassium) instead of nitrogen, and is also considered an efficient fertilizer (Fernández-Lozano et al., 1999; Xu et al., 2015, 2011). The ion replacement is possible because the ion radius of K<sup>+</sup> and NH<sub>4</sub><sup>+</sup> are almost identical.

K-struvite contains equimolar concentrations of magnesium, potassium and phosphate, and it precipitates according to Eq 1. 2 (Wilsenach et al., 2007), under



alkaline conditions, due to phosphate speciation. It has a molecular weight of 266.47 g mole<sup>-1</sup>, a density of 1.86 Kg m<sup>-3</sup> and the K<sub>sp</sub> at 25°C is 2.4·10<sup>-11</sup> (Singh et al., 2006).



MKP has a higher solubility than MAP, which results in the preferable formation of MAP when ammonium is present in solution, even at low ammonium concentrations (10 mg NH<sub>4</sub><sup>+</sup> L<sup>-1</sup>).

### 1.2.3 The crystallization process and its influencing factors

In a crystallization processes, two phases can be distinguished during the crystallization process (Figure 1. 3): nucleation (crystal birth) and crystal growth.

Nucleation is the stage when the first new crystalline nuclei are formed and defined. It is characteristically divided into primary and secondary nucleation. Primary nucleation is further categorized into homogeneous and heterogeneous nucleation.

Homogeneous nucleation occurs in supersaturated solutions in the absence of crystals or other solid phases. Supersaturation is a measure of the deviation of a dissolved salt from its equilibrium value (Pastor et al., 2008), and is the driving force for crystallization. The time between the achievement of supersaturation conditions and the formation of first stable nuclei is called induction time (Crutchik, 2015). It can be affected by factors such as pH, mixing energy, supersaturation degree and the presence of foreign ions (Kabdaşlı et al., 2006).

Heterogeneous nucleation is induced by the influence of foreign particles, and is considered to be predominant over homogeneous nucleation. The existence of proper quantities of suspended particles can act as the nuclei for heterogeneous nucleation and increase the specific surface area of contact. Therefore, the existence of suspended solids (less than 1000 mg·L<sup>-1</sup>) could enhance the precipitation rate (Schuiling and Andrade, 1999).

The secondary nucleation occurs in the presence of primary crystals, and at a low supersaturation level. Parent crystals have a catalyzing effect on nucleation, and cause local fluctuations in supersaturation (Liu et al., 2013).

After the nucleation phase, the formed crystals continue to grow until the solid/liquid equilibrium is reached. Growth is the process of incorporating constituent ions into the crystal lattice of the embryos to form detectable crystals. To explain crystal growth, several theories have been proposed. Among these, only the theory of diffusion-reaction at a limited velocity can explain crystal growth effectively (Myerson, 1993). Diffusion is considered as the mass transport of ions from the supersaturated solution to the crystal surface, by diffusion, convection, or a combination of both mechanisms. And the ion integration (reaction) is the incorporation of ions into the crystal lattice. Thus, the overall rate of crystal growth can be controlled either by mass transport or by surface integration (Crutchik, 2015).

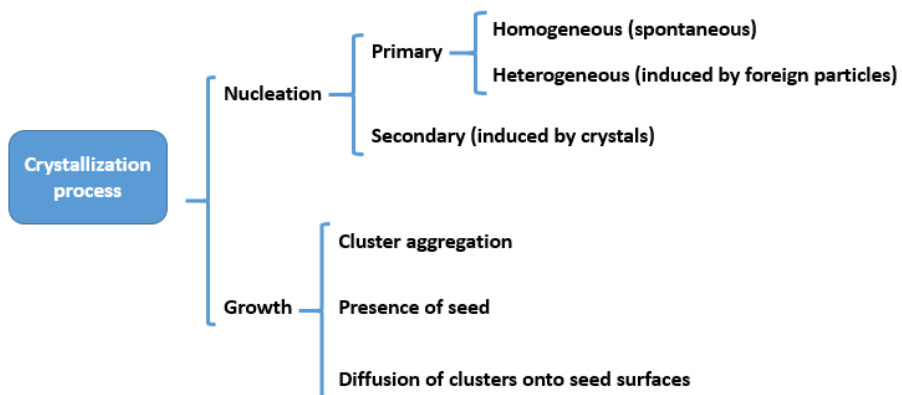


Figure 1. 3 Scheme of the crystallization process.

Nucleation and growth are strongly dependent on supersaturation. Whereas high supersaturation values enhance nucleation phase (predominant phase), low supersaturation values enhance growth over nucleation (Figure 1. 4). Metastable zone can be defined as the period of time in which crystal growth preferably takes

place over nucleation (Bergmans, 2011), and also, as the area between supersolubility and solubility curves (Bhuiyan et al., 2008). It is of high interest for processes where a certain minimum crystal size has to be reached (e.g. industrial crystallizers).

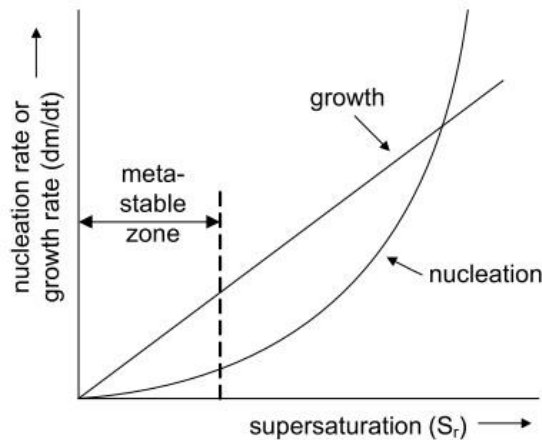


Figure 1. 4 Influence of supersaturation on crystallization process (Wiesmann et al., 2007).

The crystallization process is affected by several factors such as pH, molar ratios of  $Mg^{2+}$ ,  $NH_4^+$ ,  $K^+$  and  $PO_4^{3-}$ , degree of supersaturation, temperature of the solution, presence of other ions (Bouropoulos and Koutsoukos, 2000; Huchzermeier and Tao, 2012; Korchef et al., 2011), among other parameters.

#### ○ Operational pH

One of the main factors controlling the crystallization process of struvite and K-struvite is the pH, as the speciation of ions is highly pH dependent (Nelson et al., 2003). As an example, an increase in pH leads to the increase of the  $PO_4^{3-}$  concentration, whereas  $Mg^{2+}$  and  $NH_4^+$  concentration decreases, due to the formation of magnesium hydroxide and ammonia (not ionized specie), which can also be volatilized.

Struvite is highly soluble at acidic pHs and highly insoluble at alkaline pHs (Doyle and Parsons, 2002). Struvite solubility is conditioned by the pH of the solution, as the speciation of the components is pH dependent. The optimum pH for synthetic wastewater (WW) is between 8.5 and 10 (Stratful et al., 2001); for WW from urban wastewater treatment plants (WWTPs) is between 8.5 and 9.5 (El Diwani et al., 2007; Tünay et al., 1997); and for swine wastewater is between 8 and 10.5. There are few studies regarding K-struvite crystallization, in which a pH range from 9 to 11 (Wilsenach et al., 2007; Xu et al., 2011) is tested and evaluated in synthetic urine, and a pH range from 8 to 12 in swine wastewater (Bao et al., 2011) and digested manure after centrifugation (Zeng and Li, 2006).

### ○ Temperature

Solubility is affected by the temperature, and it increases with temperature, having the maximum at 30-35°C. Many studies have determined struvite's solubility at various temperatures. Hanhoun et al., 2011, modelled and validated the  $K_{sp}$  values of struvite in a temperature range from 15°C to 35°C, and the values varied from  $10^{-13.17 (\pm 0.01)}$  at 25°C to  $10^{-13.08 (\pm 0.06)}$  at 35°C; and Aage et al., 1997 established the solubility of struvite as  $10^{-12.52}$  at 40°C. Although lower solubility would increase precipitation, high temperatures difficult struvite formation and affect the size and shape of struvite crystals (Le Corre et al., 2009).

Regarding the effect of temperature on K-struvite formation, there are no studies.

The rate of crystal growth can be significantly affected by the temperature. Jones (2002) found that high temperatures were sufficient to produce diffusion-controlled growth, whereas low temperatures favored the surface integration step for crystal growth. In addition, the rate of precipitation increased at high temperatures.

### ○ **Mg<sup>2+</sup> dosage (and influence in molar ratios)**

Magnesium is usually the limiting component for struvite and K-struvite crystallization, as generally wastewaters contain low concentrations of this compound. Magnesium can be added as magnesium chloride (MgCl<sub>2</sub>·6H<sub>2</sub>O), magnesium sulphate (MgSO<sub>4</sub>·7H<sub>2</sub>O), magnesium oxide (MgO) or magnesium hydroxide (Mg(OH)<sub>2</sub>). Usually, the most common reagents used are MgO and Mg(OH)<sub>2</sub>, although their low solubility, instead of MgCl<sub>2</sub>·6H<sub>2</sub>O and MgSO<sub>4</sub>·7H<sub>2</sub>O because of their higher price.

An increase of the Mg<sup>2+</sup>:PO<sub>4</sub><sup>3-</sup> molar ratio would enhance the increase of P removal ratio at a fixed NH<sub>4</sub><sup>+</sup>:PO<sub>4</sub><sup>3-</sup> molar ratio and a given pH value (Münch and Barr, 2001). If magnesium is dosed under the theoretical value of the Mg<sup>2+</sup>:PO<sub>4</sub><sup>3-</sup> molar ratio of 1:1, the system is under-optimized for P-recovery, but if magnesium is dosed excessively, the system does not show a significant increase in P-recovery (Liu et al., 2013), as co-precipitation of other compounds can occur.

### ○ **Degree of supersaturation**

As previously stated (see Section 1.2.3), the achievement of supersaturation conditions is indispensable for the crystallization process.

Supersaturation is influenced by a change in pH and/or temperature, an increase of the compound concentrations, or because of the dissolution of solids. As stated by Crutchik (2015), the level of supersaturation at a fixed pH influences the crystallization of struvite, by affecting the induction time and crystal growth. The nucleation phase (homogeneous nucleation) takes place when supersaturation is achieved. Thus, the induction time is inversely proportional to the supersaturation degree (Kofina and Koutsoukos, 2005; Kabdaşlı et al., 2006).

On the contrary, crystal growth rate is proportional to the supersaturation degree. Bouropoulos and Koutsoukos (2000) studied the effect of supersaturation on both parameters: induction time and crystal growth rate. They established that an increase of the supersaturation degree caused a decrease

of the induction time (20 times) and an increase of the crystal growth rate (55 times). Therefore, they indicated that supersaturation is the key parameter to determine the extent and the rate of struvite crystallization.

### ○ Presence of other ions

Wastewater contains numerous compounds besides magnesium, ammonium, potassium and phosphate, which makes the thermodynamic system more complex as more chemical equilibriums can take place. Thus, the availability of  $Mg^{2+}$ ,  $NH_4^+$ ,  $K^+$  and  $PO_4^{3-}$  can be affected for struvite and K-struvite formation, leading to the co-precipitation of other compounds.

Calcium ( $Ca^{2+}$ ) is one of the most interfering ions. The precipitation of calcium phosphates has been observed in addition to or instead of struvite (Zeng and Li, 2006; Harris et al., 2008; Moerman et al., 2009). The precipitation of hydroxyapatite (HAP;  $Ca_5(PO_4)_3(OH)$ ) was reported at pH above 9.5 to 10 (Wang et al., 2006), and has a  $K_{sp}$  of  $4.7 \cdot 10^{-45}$  at 25°C (Martí et al., 2008). Other calcium phosphates can precipitate, such as  $CaHPO_4$  ( $K_{sp}$  of  $10^{-19.275}$  at 25°C according to Visual Minteq software),  $CaHPO_4 \cdot 2H_2O$ , also known as brushite ( $K_{sp}$  of  $10^{-18.995}$  at 25°C according to Visual Minteq software) and  $Ca_3(PO_4)_2 \cdot 2H_2O$  ( $K_{sp}$  of  $10^{-26}$  at 25°C; Yen, 2007) or amorphous calcium phosphates (ACP).

Some researchers stated that the presence of carbonate was reported to hinder calcium phosphate formation. Both carbonate and phosphate compete for calcium. De-Bashan and Bashan (2004) stated that high carbonate concentrations would enhance the preferential precipitation of calcium carbonate ( $K_{sp}$  of  $10^{-8.48}$  at 25°C according to Visual Minteq software) over calcium phosphates ( $K_{sp}$  range between  $10^{-18.995}$  and  $10^{-45}$  at 25°C) at pH 9-11, and avoid the precipitation of other phosphorus compounds (Huchzermeier and Tao, 2012), favoring the formation of struvite.

Other researchers established that struvite formation is enhanced by having a  $Ca^{2+}:Mg^{2+}$  molar ratio below 1 (Crutchik and Garrido, 2011; Hwang and Choi, 1998;

Le Corre et al., 2005) and/or a high ammonium concentration in a  $\text{NH}_4^+/\text{PO}_4^{3-}$  molar ratio of 9.4 (Stratful et al., 2004).

### ○ **Solid content**

There are many studies outstanding the hindrance to struvite formation due to the solids content (Barnes et al., 2007; Ping et al., 2016). It is quite common to establish a limit in the concentration of total suspended solids (TSS) for struvite recovery at  $1 \text{ g TSS L}^{-1}$  to assure the viability of the process.

Some studies have focused its interest on struvite recovery from swine wastewaters. Capdevielle et al., 2016 studied the influence of organic matter (OM) fractions (dissolved, colloidal and particulate) on struvite precipitation from biologically treated swine wastewater, and established that OM was negative on the struvite reaction kinetics, possibly because of repulsive force of colloids and the presence of particulate OM, but positive on the size of the struvite crystals due to the presence of colloidal particles. Ping et al., 2016 studied the effect of phosphate concentration and total suspended solids (TSS) on the morphology and composition of the formed struvite, and established that a high content of the last decreased struvite particle size and purity, and was strongly negative for pellet growth and for the operation of the fluidized bed reactor (FBR), as regular disposal of the excess sediment beyond pellets from the settling zone was needed to ensure the normal operation of the FBR.

### **1.2.4 Operational conditions for struvite recovery from manure: state-of-the-art review**

P-recovery from phosphate-rich wastewaters (municipal, animal manure, industrial) via struvite crystallization has been widely studied. However, P-recovery from dairy manure has posed challenges to researchers. These challenges include: a high suspended solids concentration, i.e. higher than  $1 \text{ g TSS}\cdot\text{L}^{-1}$  (Schuiling and Andrade, 1999; Barnes et al., 2007; Desmidt et al., 2013; Liu et al., 2013; Ping et al., 2016); the

ratio between particulate and dissolved phosphorus, as the dissolved phosphorus can be tied with the particulate phosphorus attached to the colloidal forms (Zeng and Li, 2006); the calcium to struvite ions molar ratio (Zhang et al., 2010); and, the high ionic strength, because it affects the precipitation potential (Zeng and Li, 2006).

Attempts to reinforce struvite recovery from dairy manure included  $Mg^{2+}$  amendment (Uludag-Demirer et al., 2005; Zeng and Li, 2006), pre-treatment of dairy manure using microwave-based heating and advanced oxidation (Jin et al., 2009), and pre-treatment by acidifying anaerobically digested manure adding a chelating agent (Zhang et al., 2010). Organic phosphorus and polyphosphate, commonly found in undigested dairy manure, were solubilised by microwave-based thermochemical treatment to increase struvite component ions for struvite formation. Although microwave-based thermochemical pre-treatment is effective at increasing struvite component ion concentrations, it is energy intensive and can require chemical inputs. Anaerobic digestion also has been found to enhance the ability to recover phosphorus as struvite, as it converts organic nitrogen and phosphorus to ammonium ( $NH_4^+$ ) and orthophosphate ( $PO_4^{3-}$ ).

K-struvite recovery has been hardly investigated, and most of the studies from synthetic urine (Wilsenach et al., 2007; Xu et al., 2011, 2012, 2015) or real urine (Sun et al., 2010). Only two studies observed the formation of K-struvite in manure. Bao et al., 2011 focused their study on determining the optimal pH to obtain a highly pure struvite crystal product from swine wastewater. They observed the co-precipitation of K-struvite, struvite, magnesium hydroxide and ACP when pH increased from 9 to 11. Zeng and Li (2006) investigated nutrient recovery efficiencies for simultaneous removal of P, N and K from digested cattle manure (thermophilic anaerobic digester) after a centrifugation process for solid separation. They concluded that K-struvite formation only occurred when the reactivity of K-struvite



formation surpasses that of struvite, thus, when the concentration of ammonium is low compared to the other ions.

Therefore, a combination of technologies is required to provide K-struvite viability: N would be recovered/removed first while K-struvite can be formed with the remaining P.

Table 1. 1 summarizes the state-of-the-art review for struvite and K-struvite recovery from manure at lab-scale, including a description of the source used, the precipitate obtained, molar ratios, pH, temperature, aeration rate and the type of reactor used, as well as some observations.

Table 1. 1 Summary of the state of the art on struvite recovery from manure.

REFERENCES	SOURCE	PRODUCT	pH	T (°C)	REACTOR	AERATION RATE	OBSERVATIONS
<b>Cerrillo et al., 2015.</b>	Synthetic solution for batch tests, and centrifuged digested pig slurry for continuous assays	Struvite and other elements (chloride, sodium and potassium)	Range from 7 to 10	25°C and 36°C	Batch experiments and continuous assays in a 20L lab-scale reactor (isotherm glass reactor with a settling zone)	A test was performed in continuous mode to reduce sodium hydroxide consumption, applying an aeration rate of 0.25 L L <sup>-1</sup> min <sup>-1</sup>	Optimum pH at 9, and no influence of temperature. High Ca <sup>2+</sup> reduces recovery of Mg <sup>2+</sup> and NH <sub>4</sub> <sup>+</sup> . The presence of organic matter resulted in the reduction of struvite crystal size.
<b>Huchzermeier and Tao (2012)</b>	Anaerobically digested dairy manure	Struvite and hydroxyapatite	pH = 9, adjusted with NaOH, 5M (or HCl, 1M)	-	Batch experiments	-	Ca <sup>2+</sup> was the interfering ion → HAP precipitated at pH>9.5-10. Carbonate inhibited calcium phosphates formation.
<b>Song et al., 2011.</b>	Aerobically digested swine WW	Struvite	pH = 8.5 - 9, increased by CO <sub>2</sub> stripping	From 0 °C to 29.5°C	Sequencing Batch Reactor (SBR) and Continuous-Flow Reactor	Aeration times 1-4h and HRT 6-15h.	Using computer models (PHREEQC and MINTEQA2) for understanding phosphate crystallisation. P-removal=36-74% NH <sub>4</sub> <sup>+</sup> -N-removal=40-90% through air stripping.
<b>Liu et al., 2011.</b>	Swine WW, screened by a sieve with 0.5 mm mesh to remove large solids.	Pure struvite (approximately 65% of total phosphorus and 67% of total nitrogen present in the sediment could	pH between 7.82 and 8.92 → average of 8.35 ± 0.23.	-	Plexiglass reactor with an aerator, with two zones: a reaction zone and a settling zone; operated in a continuous flow mode.	Five aeration rates were examined: 0-0.18-0.55-0.92-2.76 L·L <sup>-1</sup> ·min <sup>-1</sup> → struvite formation was enhanced (84-87-92-93-93%) by an increase in the	Struvite formation was stabilised at 0.73 L·L <sup>-1</sup> ·min <sup>-1</sup> of aeration rate as the optimum, due to CO <sub>2</sub> -air stripping by aeration. The optimum Mg:P molar ratio for enhancing the crystallization

		be recovered in pure struvite.				eration rates, so its formation is directly proportional to the aeration rate.	of struvite was found to be 0.8-1. The recovery of pure struvite from the sediment was by redissolving and recrystallizing using acid and alkali solutions.
<b>Bao et al., 2011.</b>	Swine WW	Struvite, K-struvite, calcium phosphate, Mg(OH) <sub>2</sub>	pH range from 8 to 11.	-	Batch experiments	-	They studied the optimal conditions for the recovery of pure struvite crystals, but observed co-precipitation: - Struvite dominant at pH=8-9. - K-struvite presence increased at pH=9-11. -Amorphous calcium phosphate and magnesium hydroxide dominant at pH>10.
<b>Zeng and Li (2006)</b>	Digested cattle manure after a centrifugation process	Struvite and K-struvite	pH range from 7 to 10	5-50°C	Batch experiments	-	They investigated nutrient recovery for simultaneous removal of P, N and K, and determined that K-struvite only occurs at low concentrations of ammonium.
<b>Suzuki et al., 2002.</b>	Swine WW, screened at 1.5mm	Mixture of struvite and hydroxyapatite	pH = 8 -8.5, increased by aeration	-	Continuous flow pilot scale reactor, with two functions: crystallisation by aeration and settling.	Optimum intensity of aeration at 13 m <sup>3</sup> ·h <sup>-1</sup> ·m <sup>-2</sup> .	Sedimentation speed of crystals was about 3 m·h <sup>-1</sup> , and over 90% of them settled after 1h.

<b>Suzuki et al., 2005.</b>	Swine WW, screened at 1.5mm	Pure (95%) struvite	pH = 8.1, increased by aeration	-	Continuous flow pilot scale reactor, with two functions: crystallisation by aeration and settling.	Optimum intensity of aeration=13 m <sup>3</sup> ·h <sup>-1</sup> ·m <sup>-2</sup> .	Tests with accumulation devices of stainless steel rods with coarse face (40 mg·cm <sup>-2</sup> ·d <sup>-1</sup> , 95% of pure struvite crystals), wood plates (7.1 mg·cm <sup>-2</sup> ·d <sup>-1</sup> ) and rubber plates (0.86 mg·cm <sup>-2</sup> ·d <sup>-1</sup> ) for the recovery of pure struvite crystals.
<b>Suzuki et al., 2007.</b>	Swine WW, screened at 1.5mm	Pure (95%) struvite, recovered after an air drying process before its application to farmland.	pH=7.5-8.5, increased by CO <sub>2</sub> stripping	-	Continuous flow pilot scale reactor, with two functions: crystallisation by aeration and settling.	Aeration rate between 12 and 16 m <sup>3</sup> ·h <sup>-1</sup> .	Large amounts of suspended solids settled in the reactor. The crystallisation reactor was integrated into the first stage of the swine wastewater treatment process, adding a primary settling tank before struvite crystallisation.
<b>Liu et al., 2011.</b>	Swine WW, screened by a sieve with 0.5 mm mesh to remove large solids.	Pure struvite (approximately 65% of total phosphorus and 67% of total nitrogen present in the sediment could be recovered in pure struvite.	pH between 7.82 and 8.92 → average of 8.35 ± 0.23.	-	Plexiglass reactor with an aerator, with two zones: a reaction zone and a settling zone; operated in a continuous flow mode.	Five aeration rates were examined: 0-0.18-0.55-0.92-2.76 L·L <sup>-1</sup> ·min <sup>-1</sup> → struvite formation was enhanced (84-87-92-93-93%) by an increase in the aeration rates, so its formation is directly proportional to the aeration rate.	Struvite formation was stabilised at 0.73 L·L <sup>-1</sup> ·min <sup>-1</sup> of aeration rate (optimum). The optimum Mg:P molar ratio for enhancing struvite crystallisation was found to be 0.8-1. The recovery of pure struvite from the sediment was by redissolving and recrystallizing using acid and alkali solutions.

Table 1. 2 gives an overview of the commercial technologies for P-recovery by struvite and/or K-struvite crystallization.

Not only struvite recovery has been performed at lab-scale, but also at industrial scale, and some of these technologies have been commercialized in Europe, North America and Asia (Crutchik, 2015).

Remarkably is the fact that K-struvite crystallization process is not yet optimized for its full-scale implementation and thus not applied in manure streams, even though high concentrations of potassium are found in manure. Therefore, K-struvite crystallization needs further investigations to determine the operational conditions for its recovery, specially from manure.

As stated by Crutchik (2015), several full-scale facilities have been developed in Europe (mainly Belgium, The Netherlands, Germany and United Kingdom) based on the technologies summarized in Table 1. 2. Depending on the technology implemented, the quality of the recovered product will vary, in terms of particle size for example, which can have an influence on the cost-effectiveness of the crystallization process.

**Table 1. 2** Operational and developing technologies for P-recovery by struvite and/or K-struvite crystallization.

Technology	Influent used	Product recovered	Characteristics
<b>PCS AirPrex®</b> <sup>1</sup>	Digested sludge	Struvite	Using an air-lift reactor because: i) air creates an internal recycle flow that allow crystals to grow until a critical size and settle, ii) air increases the pH by CO <sub>2</sub> stripping. Fully operational, and the company PCS obtained the license to market the AirPrex® technology. The AirPrex® process recovers 90-95% of the P in the returned liquor, reduces disposal costs by up to 20%, reduces maintenance costs by up to 50%, and has a hide increase revenue up to 10% from fertilizer.
<b>DHV Crystalactor</b> <sup>2</sup>	Dewatering reject streams; possibly digested sludge	Struvite, K-struvite, calcium and magnesium phosphates, and calcium carbonates	Fluidized Bed Reactor (FBR) using sand/small crushed pellets/minerals as seed material, as the crystals are formed into its surface to form pellets. Fully operational.
<b>Paques Phosphaq</b> <sup>3</sup>	Dewatering reject streams	Struvite	Continuous stirred tank reactor (CSTR) with aeration and magnesium oxide addition. It also removes biological degradable chemical oxygen demand due to the oxygen. Fully operational (removal efficiencies of 70-95%) and feasible if load > 100 kg P·d <sup>-1</sup> , 50 mg PO <sub>4</sub> -P·L <sup>-1</sup> and 200 mg NH <sub>4</sub> -N·L <sup>-1</sup> .

<sup>1</sup> <https://www.cnp-tec.com/><sup>2</sup> <https://www.royalhaskoningdhv.com/en-gb/markets/crystalactor><sup>3</sup> <http://en.paques.nl/products/other/phospaq>

<b>Ostara PEARL</b> <sup>4</sup>	Reject water (municipal WWTP in UK)	Struvite	FBR developed by the University of Columbia (Canada). The system is similar to DHV Crystalactor, using recycled struvite as seed material.  To improve its performance, phosphate is stripped from the activated sludge before digestion in an anaerobic zone, and added to the reject water (process called "WASSTRIP").  Fully operational, producing 150 tonnes of Crystal Green® fertilizer per year.
<b>NuReSys</b> <sup>5</sup>	Anaerobic effluent from potato and dairy processing industries	Struvite, calcium and magnesium phosphates	This process was developed by the University of Gent, using two completely stirred tanks: a stripping reactor and a stirred crystallization reactor, adding magnesium chloride and sodium hydroxide to promote struvite crystallization.  NuReSys technology is a mature fully developed technology (8 operational units in municipal/industrial WWTPs).  80-95% of the phosphate recovered as struvite pellets.
<b>Unitika Phosnix</b>	Sidestream sewage sludge	Struvite	FBR using recycled granulated struvite as seed material, and adding magnesium hydroxide and sodium hydroxide to promote struvite crystallization.  Treatment capacity of 1000 m <sup>3</sup> ·d <sup>-1</sup> , and 80-90% of PO <sub>4</sub> -P recovery rate.
<b>Multiform Harvest</b> <sup>6</sup>	Swine lagoon liquid	Struvite	Cone-shaped FBR, adding magnesium chloride and sodium hydroxide to produce struvite crystals.

<sup>4</sup> <http://ostara.com/nutrient-management-solutions/>

<sup>5</sup> <http://www.nuresys.be/>

<sup>6</sup> <http://www.multiformharvest.com/p-recovery>

### 1.3 Applicability of struvite and K-struvite as fertilizers

Struvite and K-struvite can be used as slow-release fertilizers. They present many advantages when compared to the conventional fertilizers:

- Low leach rates and slow release of nutrients (Münch and Barr, 2001),
- Suitable in grasslands and forests where fertilizers are applied once in several years, and ideal for coastal agriculture (Rahman et al., 2014),
- No damage in the growing plants when a single high dose is applied (De-Bashan and Bashan, 2004),
- Represent an alternative for those crops that require magnesium, such as sugar beets (Gaterell et al., 2000),

Many researchers have stated the excellent performance of struvite as a fertilizer (El Diwani et al., 2007; Rahman et al., 2011; Ryu et al., 2012; Uysal et al., 2010), and successfully used on turf grass, tree seedlings, ornamentals, vegetables, flower boards and garden grass as fertilizer (Münch and Barr, 2001; Nelson et al., 2003; Yetilmezsoy and Sapci-Zengin, 2009). Some concerns rely on the heavy metal content or trace contaminants presence in the product recovered, as they can be incorporated into the crystalline network during both nucleation and crystal growth. However, traces of heavy metals are maintained in the legal limits for fertilizers (Liu et al., 2011a, 2011c; Münch and Barr, 2001). For example, Münch and Barr (2001) used centrate from the sludge dewatering centrifuge of a urban WWTP for struvite recovery. The product obtained fulfilled with the legal requirements for selling it as a fertilizer in Queensland, as the concentrations of cadmium, lead and mercury were lower (mostly below the analytical detection limits and well below the legal limits) than the specified in the government regulations.

The presence of heavy metals in the struvite recovered is of special concern when using sludge from WWTPs, and less when using manure and/or digestate, as higher



concentrations of heavy metals can be found in the wastewater treated, finally ending into the sludge. In the last, the content of veterinary drugs should be determined, as not only they could be present in the manure due to accumulation and later be trapped into the product formed, but also they can degrade into other sub-products. This issue with the emerging contaminants has been further analyzed among the project ManureEcoMine<sup>7</sup>.

The value of the recovered products depends on its demand and its quality, having a highly variable market for recovered materials (ESPP, 2014). Some data can be found regarding the price of struvite sold to the fertilizer industry, which presents a wide range of prices as a function of its quality. As an example, from 40-60 € ton<sup>-1</sup> (Bergmans, 2011), to 276 US\$ ton<sup>-1</sup> (Unitika Ltd., Japan, from Unitika Phosnix technology), to 370 € ton<sup>-1</sup> (expressed as 41000 NR ton<sup>-1</sup> by Etter et al., 2011) and up to 500 \$ ton<sup>-1</sup> (Münch et al., 2001).

The market price of struvite can be lowered by minimizing the use of reagents. For example, some strategies could be: i) CO<sub>2</sub> stripping to increase pH (Suzuki et al., 2007; Morales et al., 2013), which not only would reduce the addition of NaOH, but also Mg<sup>2+</sup>; ii) use of cheaper magnesium reagents, such as MgO and Mg(OH)<sub>2</sub> (Ronteltap et al., 2007; Liu et al., 2008; Pastor et al., 2008; Moerman et al., 2009). These would contribute to the reduction of the operational costs associated with struvite crystallization.

Manure application has been overdosing the content of nitrogen (N) into the soil, due to the differences in the concentration of N and phosphorus (P), and their differences in the crop requirements. This has contributed to the balance of its global offtake, and as a result, some soils have an excess of nitrogen. In this cases, K-struvite

---

<sup>7</sup> ManureEcoMine project website: <http://www.manureecomine.ugent.be/>

could be applied as a fertilizer, as besides N, the essential nutrients for plants are P and K (Manning, 2015).

Other applications different as fertilizer can be found for K-struvite. A new published patent (Hauber et al., 2017) proposed a building material composed of K-struvite, syngenite ( $K_2Ca(SO_4)_2 \cdot H_2O$ ), magnesium oxide and stucco (calcium sulphate hemihydrate). They established that K-struvite offered good heat and abrasion resistance, properties that allowed the direct use of the composite material in building panel molds, it offers high structural integrity, low weight density than other materials, and high fire resistance. Moreover, the material is water resistant. The K-struvite – syngenite combination can also be used to coat inorganic fibers to provide a weather-proof, fire resistant and abrasion resistant material.

### **1.4 Phosphorus recovery within circular economy and legislation**

According to the European Environment Agency, circular economy minimizes the need for new inputs of materials and energy, while reducing environmental pressures linked to resource extraction, emissions and waste, requiring that natural resources are managed efficiently and sustainably throughout their life cycles. The scope of this PhD thesis is the sustainable recovery of fertilizers (i.e. ammonium and/or potassium struvite) from swine manure, fulfilling the premises of circular economy.

Nutrient recycling is featured in the European Commission's "Circular Economy Package" (COM(2015) 614 final; European Commission, 2015), as the EU Fertilizers Regulation revision included recycled nutrients, integrated resource efficiency into the Best Available Techniques, and developed secondary raw materials data systems.

The regulation followed an EU public consultation, in which 30% of the respondents identified bio-nutrients as “*secondary materials the EU should target first*”, and 54% cited bio-nutrients or phosphorus in their responses. They also indicated that bio-nutrients offer a huge potential for the Circular Economy, underlining the importance of nutrient cycles and the dependency of Europe on imported phosphates. Moreover, the key aspects to be addressed to develop bio-nutrient and materials recycling were also identified: improving quality, information, reliability and standards of recycled materials; increasing demand for recycled materials and addressing the cost differential with primary materials; regulatory obstacles and gaps at EU, national and regional levels; need for value chain cooperation and information and need for reliable data on secondary raw materials flows (ESPP, 2016).

Not only the EU targeted for recycling 65% and 75% of municipal and packaging waste, respectively, by 2030, but also revised the EU Fertilizer Regulation in order to “*facilitate the recognition of organic and waste-based fertilizers in the single market and support the role of bio-nutrients*”. This revision is needed as the Package from 2014 identified phosphorus as one of the five materials and wastes specially targeted for action. This PhD thesis agrees with the EU willingness to create a phosphorus framework including fertilizers, food, water and waste amongst the umbrella of circular economy: phosphorus is recovered from manure as a bio-waste that can be used as a fertilizer, instead of using direct manure as a fertilizer, as it can influence water quality.

Then, the revision of the EU Fertilizers Regulation noted the contribution of European Sustainable Phosphorus Platform (ESPP) to extend its scope to nutrients from secondary sources (e.g. recycled phosphates) and organic sources (ESPP, 2015). Moreover, it intended to include additional component material categories in the Annexes, to keep up with technological progress allowing the production of safe and

effective fertilizers from recovered, secondary raw materials, such as biochar, ashes and struvite<sup>8</sup>; and kept the requirements in the Annexes under constant review, and revise the, wherever necessary to provide an adequate protection of human, animal or plant health, safety or the environment.

Related, ESPP aims to address policies and tools (among other objectives), and has contributed actively to the regulation of public policies, specially the Fertilizer Regulation in order to create access to market for recycled P. Thus, many proposals have been published by ESPP regarding struvite and ashes (ESPP, 2017). This publication stated that struvite recovered from wastewater is authorized for use as a fertilizer for some producers in some EU Member States, but not in others, which represents an obstacle to roll-out of this P-recycling technology. A summary of the present situation is presented below:

- Certain recovered phosphates (struvite, magnesium phosphate, dicalcium phosphate) are authorized as fertilizers by national regulation in The Netherlands<sup>9</sup>
- Struvite is nationally authorized as a fertilizer in Denmark<sup>1</sup>
- Case-by-case authorizations have been accorded for recovered struvite by national/regional authorities. These are applicable only to the specific product from a specific waste stream/site/process.

For example, Agristo and Clarebout, both from potato processing (both NuReSys process) in Flanders<sup>1</sup>; slough sewage works (Ostara process) in the UK<sup>10</sup>; Berlin Wasser sewage works in Brandenburg, Germany<sup>2</sup>; as well as in a number of other

---

<sup>8</sup> Struvite cannot be considered as a “Phosphatic fertiliser” (A2) under EU 2003/2003 because this category specifies a limited list of 7 specific chemicals/materials.

<sup>9</sup> Documents available and published at <http://phosphorusplatform.eu/2016-11-29-03-29-00/regulatory-activities>

<sup>10</sup> Documents confidential.

states worldwide (e.g. Canada<sup>2</sup> – Ostara, 42 US states – Ostara, Japan<sup>1</sup> – Swing and others ...).

These case-by-case authorizations depend on the specific quality of the authorized product, thus, do not contribute a “blanket” authorization for struvite in the relevant country. However, they can provide a precedent for future authorization for other production sites, subject to their also proving quality and safety.

In addition, the EU’s “Expert Group for Technical Advice on Organic Production” established that struvite and calcined phosphates (from ash) should be authorized for use in organic farming (under EU Organic Farming Regulation 889/2008), subject to their authorization under the new EU Fertilizer Regulation.

However, ESPP (2017) also remarked some obstacles to the implementation of struvite recovery as a P-recycling solution, such as the fact that a technology successfully installed in one country cannot necessarily be sold in another, because the resulting product cannot be sold as a fertilizer due to the regulations and laws.

In conclusion, despite the changes in the legislation, a transition towards a sustainable use of phosphorus is also needed. Van Dijk et al., 2014 established that this transition should include the realign of P inputs, the reduction of P losses to water, the recycle of P in bioresources, the recovery of P in wastes, and the redefinitions of P in the food chain.

## 1.5 ManureEcoMine: a sustainable approach for nutrient recovery from manure

This thesis is part of the European project (FP7 2013-2016, Grant Agreement n° 603744) “**ManureEcoMine**<sup>11</sup>”, acronym of “Green fertilizer upcycling from manure: Technological, economic and environmental sustainability demonstration”. It is an ambitious European macro-project which aimed to propose an integrated approach to the treatment and reuse of animal husbandry waste in nitrate vulnerable and sensitive areas and beyond, by applying the eco-innovative principles of sustainability, resource recovery and energy efficiency (Figure 1. 5). Technologies of proven efficacy in the wastewater treatment field were combined in several process configurations to demonstrate their technological and environmental potential at pilot scale for cow (Spain) and pig manure (The Netherlands). Anaerobic digestion (mesophilic/thermophilic), ammonia stripping, struvite precipitation and partial nitrification/anammox were the key technologies. To render the cradle-to-cradle approach complete, the fertilizer and potential trace contaminants effects of recovered nutrients on plant growth and soil health and emissions were established, and safety was managed. Life cycle analyses determined the sustainability of the concept as such, and identified the most environmentally friendly technology and most effective and safe reuse strategy. Finally, the boundaries of economic viability were determined.

---

<sup>11</sup> <http://www.manureecomine.ugent.be/>

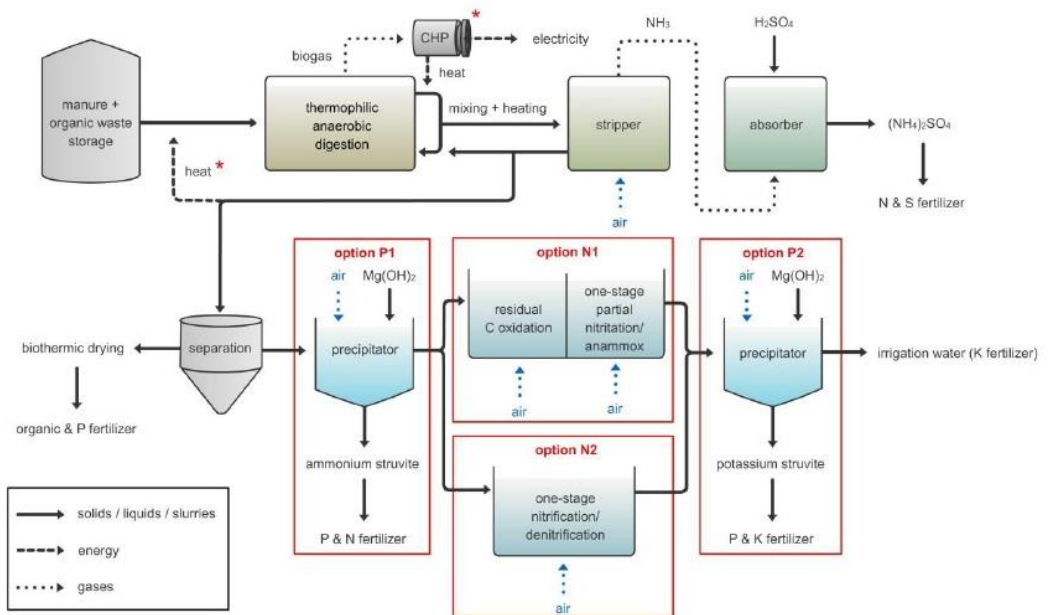


**Figure 1. 5** Synergistic coherence of the ManureEcoMine recovery core technologies, with two options indicated for P-recovery and residual N-removal.

As different technologies were tested during the ManureEcoMine (MEM) project, the project consortium was composed by research institutions and companies, which are detailed below:

- Van Alphen ([www.vanalphenaxel.com](http://www.vanalphenaxel.com)) and Balsa ([www.balsa-cvv.com](http://www.balsa-cvv.com)) were the manure processors in The Netherlands and Spain, respectively.
- Biogrup from the Universidade de Santiago de Compostela ([www.usc.es/biogrup](http://www.usc.es/biogrup)) was responsible for the thermophilic/mesophilic anaerobic digestion, the solid/liquid separation (S/L separation), and the LCA analysis along with the assessment in the environmental sustainability of the different alternatives for manure treatment.

- BOKU-IFA optimized the stage of ammonia removal in the stripping unit, and BOKU-SIG conducted the risk analysis and management, both groups belong to the University of Natural Resources and Life Sciences, BOKU ([www.boku.ac.at](http://www.boku.ac.at)).
- LEQUIA from the University of Girona ([www.lequia.udg.edu](http://www.lequia.udg.edu)) was responsible for nutrient recovery from manure via struvite and/or K-struvite crystallization, and measuring campaigns for greenhouse and acidifying gas emissions on the Spanish pilot plant.
- Ghent University (UGent) was involved in different tasks: CMET ([www.cmet.ugent.be](http://www.cmet.ugent.be)) was responsible for nutrient removal from manure (one-stage partial nitrification/anammox or one-stage nitrification/denitrification) and measuring campaigns for greenhouse and acidifying gas emissions on The Netherlands pilot plant; AgrEcon ([www.ugent.be/bw/agricultural-economics/en](http://www.ugent.be/bw/agricultural-economics/en)) demonstrated the economic feasibility of the ManureEcoMine systems through the evaluation of agro-economic parameters.
- LVA Gmbh (<http://lva.gmbh.at>) was responsible for the recovery of data concerning trace contaminants presence and behaviour in the fertilizers recovered, soil and water.
- Peltracom (now Greenyard Horticulture, [www.peltracom.be](http://www.peltracom.be)) developed a fertilizer blending for new sustainable growing media from the fertilizers obtained in the ManureEcoMine pilot plants in Spain and The Netherlands.
- Forschungszentrum Jülich (FZJ, [www.fz-juelich.de](http://www.fz-juelich.de)) evaluated the effect of manure derived fertilizer blends on plant growth and on soil health for energy and feed crops.
- Colsen ([www.colsen.nl](http://www.colsen.nl)) was the responsible for the design, engineering and construction of the pilot plant installation, and its start-up, operation and optimization in The Netherlands.
- Ahidra ([www.ahidra.com](http://www.ahidra.com)) collaborated for pilot plant design and engineering and controlled and optimized the pilot plant operation in Spain.



ManureEcoMine project started November 2013 and finished in October 2016. During the three years of the project, the consortium overcame many challenges, which allowed to acknowledge the problems associated with manure treatment, and provide a manure processing approach for nitrate vulnerable and sensitive areas such as The Netherlands and Spain, by recovering and upgrading nutrients from manure as agricultural fertilizers and crop enhancing products (Pintucci et al., 2016). Furthermore, it allowed the reduction of the environmental burden associated with nutrient leaching into surface water, induced by the direct application of manure in land, by recovering nutrients (N, P and K).

## Chapter Two

# Objectives

---

This PhD thesis aims to bring innovation and insights on the recovery of essential macronutrients (potassium, phosphorus and nitrogen) from waste streams. Specifically, the sustainable recovery of ammonium and/or potassium struvite fertilizers from swine manure.

While the crystallization of ammonium struvite has been widely studied, the present work has been mainly focused on establishing a methodology to control its particle size, and study the influence of high concentration of solids in the influent for its recovery. At present, the recovery of potassium struvite is an emerging technology, and its crystallization from waste streams is at the proof of concept stage. This PhD thesis aims to provide a methodology to recover the most limited macronutrient in soils (potassium) as K-struvite from swine manure.

This PhD thesis is outlined according to the objectives in various chapters, and are all connected to achieve the main goal of the sustainable recovery of struvite/K-struvite from swine manure.

The main objectives of the PhD are presented as follows:

- To develop a methodology to control the particle size of struvite by means of the up-flow velocity (Chapter 4). The methodologies used so far are reduced to the promotion of secondary nucleation or to the increase of the reaction time.
- To demonstrate that the up-flow velocity determines the minimum theoretical equivalent particles' diameter that can be recovered (Chapter 4).
- To understand the effect of suspended solids on struvite formation in a complex matrix as swine manure (Chapter 5). Specifically, to identify the role of solids in struvite nucleation and growth, and in the quality of the product recovered.

- To establish a methodology to determine the suitable operational conditions for the recovery of K-struvite from swine manure (Chapter 6). Little is known regarding the recovery of K-struvite, which evince the need for a theoretical approach, for later be modelled and experimentally adjusted.



# Chapter Three

## Methodology

---

### 3.1 Design of the crystallizer

A crystallizer was designed for nutrient recovery from wastewater, within the framework of the EU project ManureEcoMine (FP7 2013-2016, Grant Agreement n° 603744). MEM envisaged nutrient recovery from the liquid phase of digested livestock manure by chemical precipitation before or after a biological nitrogen removal to produce struvite or K-struvite, respectively.

According to the scopes of ManureEcoMine project, a design offering versatility in operation was essential. For this reason, a review of the state of the art regarding struvite crystallization processes' configurations and operational conditions was done to determine the basic principles on how nutrients could be recovered from wastewater in the form of struvite (Table 1. 1). Following the review, air-lift reactor was chosen as the optimal design to fulfill the aims of the project. Moreover, novelty was one of the characteristics sought, hence, the combination of an air-lift reactor plus a settler was the design chosen.

The crystallizer designed in this PhD thesis consisted of a square methacrylate crystallizer (21x21 cm) with a pyramidal base connected to a collector tube (Figure 3. 1). It was built on methacrylate to facilitate visual checking of the hydrodynamics and nutrient recovery performance. The total volume was 14.6 L, which later was increased to 14.79 L by enlarging the collector tube. The internal performance was based on the combination of an air-lift reactor with a settler.

The main reasons to design such crystallizer were related to the ManureEcoMine scopes: i) versatility in operation, either in terms of influent characteristics (centrate or permeate from digested manures), system operation (continuous versus batch operation), or targeted product (struvite or K-struvite); ii) high retention of the crystals produced to recover the maximum phosphorus possible; iii) promoting heterogeneous nucleation by the recirculation of crystal nucleus into the

supersaturated zone for better nutrient recovery efficiencies; and last but not least, iv) controlling the particles' size of the product recovered. Besides, the guiding compasses of the ManureEcoMine project were always considered: minimal energy and chemicals demand and recovery of valuable products for green fertilizers production.

In Figure 3. 1A, the three parts of the crystallizer are shown:

### 1) Riser

The riser was the channel for gas-liquid up-flow, where the air was injected at its bottom, and where crystallization took place. The parallel section was the downcomer, which was connected to the riser at the bottom and at the top.

Magnesium was introduced in the riser to ensure supersaturation conditions promoting the nucleation phase. In the upper part of the riser, particles were maintained fluidized by an air stream to promote its growth.

### 2) Clarifier

The clarifier was the upper part of the crystallizer. It consisted of a quiet zone, in which the up-flow velocity was kept constantly low ( $0.0177 \text{ m h}^{-1}$ ), even at high air-flow rates ( $0.0179 \text{ m h}^{-1}$ ) to prevent particles loss (only particles smaller than  $3\text{-}5 \mu\text{m}$  could be lost).

### 3) Collector

The bottom part of the crystallizer was the collector. The biggest particles (bigger than  $107.8 \mu\text{m}$ ) settled once their settling velocities were higher than the up-flow velocity ( $26.3 \text{ m h}^{-1}$ ). Product samples were collected periodically from this part to characterize the product formed.



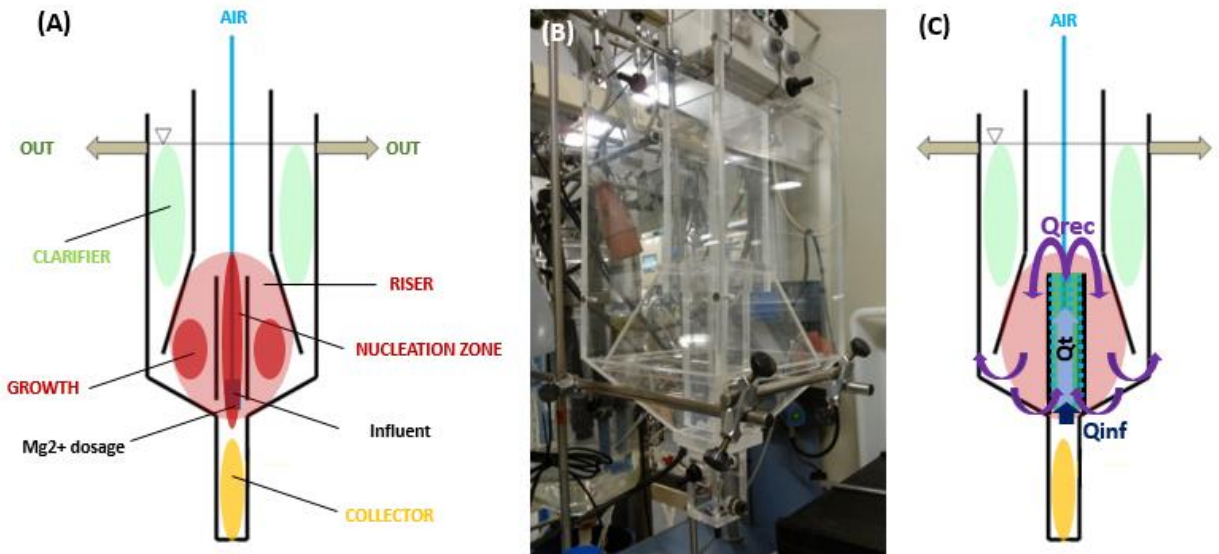


**Figure 3. 1** The designed crystallizer: (A) scheme with the three differentiated parts (clarifier in green, riser in red, and collector in yellow); (B) image of the crystallizer; and (C) hydraulics of the reactor, representing the aeration air and liquid flows ( $Q_t$ ,  $Q_{rec}$  and  $Q_{inf}$ ).

A general scheme of the crystallizer used is presented in Figure 3. 2, in which the influent and effluent flows are presented, along with the probes installed. The design was flexible regarding the aeration positions (modifying the hydrodynamics in the crystallizer) and feeding positions (varying the supersaturation zones) in order to study its effects on nucleation and growth of struvite and K-struvite crystals.

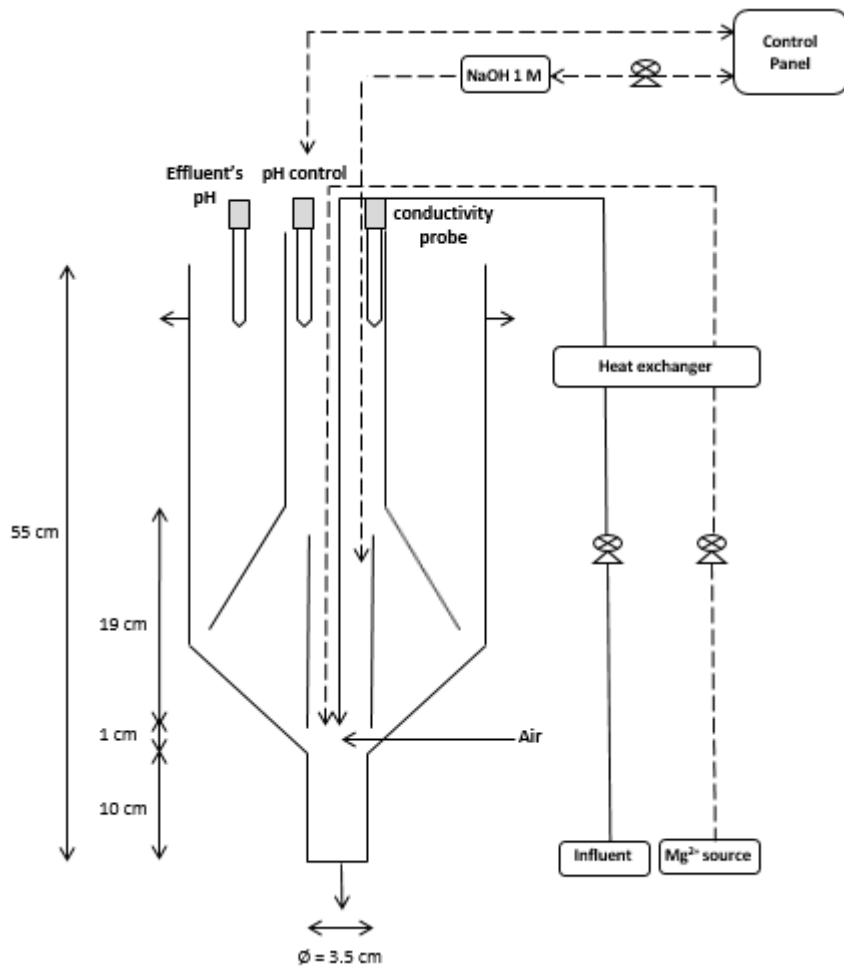


Figure 3. 2 General scheme of the crystallizer used as experimental set-up.

The influent was fed from the bottom of the riser. Different positions (depths) were tested to improve the crystallization process. Magnesium was also dosed in this zone, testing different magnesium reagents ( $\text{MgCl}_2 \cdot 6\text{H}_2\text{O}$ ,  $\text{MgSO}_4 \cdot 7\text{H}_2\text{O}$ ). The feeding solutions (influent and magnesium source) were heated up to  $35^\circ\text{C}$  using a heat exchanger (WB22, Memmert) to simulate the expected temperature of the influent in the MEM pilot plant.

Aeration was also applied in the riser through a tube with a diffuser to assure the homogenization of air bubbles. Different aeration positions and air-flow rates (1-10 L min<sup>-1</sup>) over the riser were assessed. The system was controlled by a mass flow meter (Rotameter, 2100/INOX). Finally, the effluent was continuously discharged by overflow from the top of the clarifier.

A pH control was implemented in the riser using a pH probe at the upper part connected to a control panel (Memograph; Endress+Hauser, RSG40). Hence, the pH in the riser could be maintained at a fixed set-point value by dosing 1M NaOH, being pH 8.5 for struvite recovery and pH 10.3 for K-struvite recovery (further explained in Chapter 4 and Chapter 6, respectively). Moreover, pH in the effluent (clarifier part) was also *on-line* monitored, as well as the conductivity in the riser.

### 3.2 Visual Minteq software

The freeware chemical equilibrium model Visual Minteq<sup>12</sup> was used to determine the speciation, the solubility and the equilibrium between solid and dissolved species in aqueous solutions, essential parameters in all the crystallization processes. Visual Minteq software included a large updated database, which could be modified by the user in order to use specific data needed.

The main screen of the program (Figure 3. 3) featured the input data for pH, temperature, ionic strength, and component's concentration as well as the desired units for concentration, which needs be introduced by the user. Moreover, more specific parameters could also be introduced, depending on the data available and the interests of the user. These parameters were: i) the inorganic carbon, when there is a measurement of the carbonate alkalinity; ii) the solid phases, distinguishing

---

<sup>12</sup> <https://vminteq.lwr.kth.se/>

between infinite, finite, possible and excluded solid phases; iii) adsorption, adding parameters and constants for several complexation models and empirical adsorption equations; iv) gases, stating fixed partial pressures of carbon dioxide; v) and redox, calculating the speciation of different redox-sensitive species.

Figure 3. 3 Visual Minteq's input interface.

Once the input data was introduced, the program could run, and the results were displayed in the output page, which could be exported to an excel file. This report contained a list with the concentration, activity and the logarithm of the activity for all species displayed. The results were also presented in three different formats:

- i. View species distribution, in which the percentage of each specie in solution that contribute to at least 0.01% of the total molar concentration is shown;
- ii. Display saturation indices (Figure 3. 4), in which a list of the possible compounds that could be formed as a function of the saturation index (SI) is shown. The SI is calculated according to Eq 3. 1, and determines if a product can precipitate. If  $SI > 0$ , the solution is oversaturated for that product (displayed in red), meaning that it can precipitate; if  $SI < 0$ , the solution is undersaturated for that product (displayed in blue), meaning that precipitation is not feasible; and if  $SI = 0$ , the solution is in apparent equilibrium with respect to the solid (displayed in green).

The stoichiometry and the mineral components are also displayed.

$$SI = \log IAP - \log K_s \quad \text{Eq 3. 1}$$

where, IAP is the Ion Activity Product, and  $K_s$  the temperature-corrected solubility constant.

- iii. Equilibrated mass distribution, in which the total concentration of each component was shown, classified into dissolved, adsorbed and precipitated phases.

Saturation indices for minerals - Visual MINTEQ

Mineral	log IAP	Sat. Index (=log IAP - log Ks)	Stoichiometry and mineral components														
Brucite	17.253	0.926	1	Mg+2	2	H2O	-2	H+1									
Halite	-3.466	-5.041	1	Na+1	1	Cl-1											
KCl(s)	-3.772	-4.672	1	K+1	1	Cl-1											
K-struvite	-10.247	3.250	1	Mg+2	1	K+1	1	PO4-3	6	H2O							
Mg(OH)2 (active)	17.253	-1.541	1	Mg+2	2	H2O	-2	H+1									
Mg2(OH)3Cl·4H2O(s)	22.711	-3.289	2	Mg+2	1	Cl-1	-3	H+1	7	H2O							
Mg3(PO4)2(s)	-19.277	4.003	3	Mg+2	2	PO4-3											
MgHPO4·3H2O(s)	-18.267	-0.092	1	Mg+2	1	H+1	1	PO4-3	3	H2O							
Periclase	17.253	-3.306	-2	H+1	1	Mg+2	1	H2O									
Struvite	-13.067	0.193	1	Mg+2	1	NH4+1	1	PO4-3									

Red text - oversaturation    Blue text - undersaturation    Green - apparent equilibrium

Back to main output menu    Print to Excel

Figure 3. 4 Visual Minteq's output of the saturation indices for minerals. Oversaturation in red, undersaturation in blue, and apparent equilibrium in green.

## 3.3 Calculations

### 3.3.1 Chemical calculations

Supersaturation is an essential parameter to be determined, as it is the driving force in crystallization processes (Pastor et al., 2008). The **relative supersaturation ( $S_r$ )** was calculated based on the methodology followed by Bergmans, 2011 (Eq 3. 2). The relative supersaturation is a function of the **dimensionless supersaturation ratio ( $S_c$ )**, which in turn depends on the analytical molar concentration of the targeted compound ( $P_{so}$ ) and the solution properties ( $P_{cs}$ ), as it can be deduced from Eq 3. 3.  $P_{cs}$  is a function of the minimum struvite solubility product ( $K_{so}$ ), as well as the ionization fraction ( $\alpha_i$ ) and the activity coefficients ( $\gamma_i$ ) of each struvite compound (Eq 3. 6). The ionization fractions are defined by the quotient of free ion concentration and the total concentration of each chemical component (Ali and Schneider, 2008).

The activity coefficients were calculated from the extended form of the Debye-Hückel equation proposed by Davies, 1962 (Eq 3. 5). According to this, the solution is supersaturated for  $S_r > 0$ , and undersaturated for  $S_r < 0$ .

$$S_r = S_c - 1 \quad \text{Eq 3. 2}$$

$$S_c = \left( \frac{P_{SO}}{P_{CS}} \right)^{1/3} \quad \text{Eq 3. 3}$$

$$P_{CS} = \frac{K_{sp}}{\alpha_{PO4} \cdot \alpha_{NH4} \cdot \alpha_{Mg} \cdot \gamma_{PO4} \cdot \gamma_{NH4} \cdot \gamma_{Mg}} \quad \text{Eq 3. 4}$$

$$-\text{Log}(\gamma_i) = A \cdot Z_i^2 \cdot \left( \frac{\sqrt{I}}{1 + \sqrt{I}} \right) - 0.3I \quad \text{Eq 3. 5}$$

The induction time is defined as the period time between the achievement of supersaturation and the appearance of crystal nuclei. Mehta and Batstone (2013) measured this parameter as the time for the first pH drop after the initial setting. This parameter was determined by monitoring *on-line* the pH in this PhD Thesis.

### 3.3.2 Up-flow velocity

The **up-flow velocity** in the riser was determined by the total flow in this zone and the section of the riser (Eq 3. 6).

$$\text{Up-flow velocity} = \frac{Q_t}{\text{Section}} \quad \text{Eq 3. 6}$$

The total flow ( $Q_t$ ) was the sum of the influent flow treated ( $Q_{inf}$ ) plus the recirculation flow ( $Q_{rec}$ ) induced by the aeration applied. The recirculation flow into the riser was calculated according to Merchuk and Gluz (1999), following the model of Chisti and Moo-Young (1988). They established that the **average superficial liquid velocity in the riser ( $U_{Lr}$ )** was function of the cross-sectional area of the riser ( $A_{riser}$ ) and the downcomer ( $A_{downcomer}$ ), the downcomer height ( $H_{downcomer}$ ), the hydraulic

pressure loss coefficients ( $K_b$  in the bottom, and  $K_t$  in the top), the riser gas holdup ( $\varphi_{riser}$ ) and the downcomer gas holdup ( $\varphi_{downcomer}$ ), according to Eq 3. 7:

$$U_{Lr} = \left( \frac{2gH_{downcomer}(\varphi_{riser} - \varphi_{downcomer})}{\frac{K_t}{(1 - \varphi_{riser})^2} + K_B \left( \frac{A_{riser}^2}{A_{downcomer}} \right) \frac{1}{(1 - \varphi_{downcomer})^2}} \right)^{0.5} \quad \text{Eq 3. 7}$$

where,  $K_b$ ,  $K_t$ ,  $\varphi_{riser}$ , and  $\varphi_{downcomer}$  are calculated according to Merchuk and Gluz (1999).

The product between the average superficial liquid velocity in the riser and the cross-sectional area of the riser was the total flow ( $Q_t$ ), which allowed to calculate the up-flow velocity to Eq 3. 6. In Figure 3. 1C, the flows in the crystallizer ( $Q_t$ ,  $Q_{inf}$  and  $Q_{rec}$ ) used to determine the up-flow velocity are presented.

### 3.3.3 Minimum theoretical equivalent diameter

The **minimum theoretical equivalent diameter (MTD)** is the minimum particle size that can be retained for a specific up-flow velocity. Particles smaller than the theoretical equivalent diameter remained in suspension (growth phase), while bigger particles settled in the collector. The MTD that can be retained in the riser was determined as a function of the up-flow velocity applied, according to Eq 3. 8:

$$MTD = \sqrt{\frac{v \cdot 18 \cdot \mu}{(\rho_p - \rho_L) \cdot g}} \quad \text{Eq 3. 8}$$

where, the critical settling velocity ( $v$ ) is assumed to be the up-flow velocity,  $\rho_p$  and  $\rho_L$  are the density of the particle and the liquid density;  $g$  is the standard acceleration due to gravity and  $\mu$  is the fluid viscosity (0.7978 mPa s<sup>-1</sup>).



The fluid density in the riser is also influenced by the air-flow, according to Eq 3. 9:

$$\rho_L = (\rho_{air} \cdot \varphi_{riser}) + (\rho_{fluid} \cdot (1 - \varphi_{riser})) \quad \text{Eq 3. 9}$$

where,  $\rho_{air}$  is the density of the air at 26.5°C (1.26 Kg m<sup>-3</sup> at the temperature of the air entrance),  $\varphi_{riser}$  is the gas holdup in internal air-lift reactors (determined by Merchuk and Gluz, 1999) and  $\rho_{fluid}$  is the fluid density (995.65 Kg m<sup>-3</sup> in water), which depends on the temperature inside the crystallizer.

### 3.4 Analytical methods

#### 3.4.1 Physical-chemical analysis

Standard wastewater analysis were carried out according to the standard methods (APHA, 2005). Solid content was determined as total solids, total suspended solids, volatile solids and volatile suspended solids (2540D and 2540E), and organic matter as total/soluble chemical oxygen demand (5220A and 5220 B) and/or biochemical oxygen demand (Methods 5210-A, 5210-B and 5210-C).

The concentrations of ions in the liquid phase were determined by Ion Chromatography (Dionex, IC5000), analyzing both anions (chloride, nitrite, nitrate, sulphate and phosphate) and cations (sodium, ammonium, potassium, calcium and magnesium). The principle of the method was the ion separation through an anion/cation exchanger, using potassium hydroxide as eluent for anions and methanesulfonic acid for cations, and a conductivity detector.

The pH (EC-Meter BASIC 20+, Crison, Spain) and the conductivity (EC-Meter BASIC 30+, Crison, Spain) were measured *on-line*.

### 3.4.2 Characterization of the product recovered

Different techniques were used for the complete characterization of the product recovered.

#### *X-ray diffraction (XRD) to determine crystal's structure*

The analysis by XRD was done with X-ray Diffractometer (Bruker, D8 Advance), with Bragg-Brentano geometry, Theta-2Theta, Reflection mode. The basic characteristics of X-ray Diffractometer are: Copper K<sub>alpha</sub> Radiation ( $\lambda = \text{\AA}$ ), Power 40KV-40mA, Secondary graphite monochromator, and Width Step 0.05°.

Ray powder diffraction is an analytical technique that is based on the phenomenon of X-ray diffraction by crystals. In the crystal, the interatomic distances are of the same order as X-ray wavelength, therefore, diffraction of these is more pronounced. Diffraction can be interpreted according to the Bragg law, such as the reflection of the beam incident on different crystal planes (planes where the electron density is high). The distance between these plans depends on the crystal structure. The beam reflects in different directions, according to the scattered reflection.

The technique uses a monochromatic incident ray which is diffracted by the sample. Different reflections are recorded with a detector X-ray point, moving circularly around the sample. So, a diffractogram X-ray is obtained, where the X axis is the position of the detector and Y is the intensity of the diffracted rays.

The position and intensity of the reflections depend on the structure and composition of the crystal, which is why by comparing diffractograms obtained with a database of diffraction patterns, the compounds present in the sample can be established. The identification of the crystals formed via X-ray diffractograms was done by matching the position and intensity of the peaks with the database (Powder Diffraction File, PDF) model of the reference.

XRD analysis determine the crystal structures in the sample. If amorphous substances are present, these are detected in the diffractograms as background noise, but are not identified. The samples used for XRD analysis were dried for 24 h at 45°C in an oven (UNB 400, Memmert, Germany; MM-UFB-400, Memmert, Germany) to not damage the crystalline structures, according to Crutchik and Garrido (2011).

### ***Particle Size Distribution (PSD) to determine crystals' size***

The analysis of particles' size were performed by Mastersizer (Beckman Coulter; LS 13320 MW Optical Bench). The analysis uses the theory of Mie- $D < \lambda$ , which describes the interaction between light and a particle smaller than the wavelength of incident light, as function of the angle. The wavelength and the polarization light are known, and the particle is considered to be soft, spherical, homogeneous and with a specific refraction index. This theory considers all the possible interactions between particles and light, although it is only applicable to spheres.

Spheres produce scattered light patterns, which are characterized by the presence of minimum and maximum scatters in different locations, depending on particles properties.

Determination of particles size distribution follows a dispersion pattern composed of 126 detectors in angles of 35° from the optical axis, which allows observing intensity in flow units. In order to calculate size distribution, dispersion pattern is transformed in many individual and additives functions, one for each size classification, and the relative amplitude of each pattern is used to measure the relative volume of spherical particles of that size. This decomposition is based on Mie's Theory explained above.

### ***Optic microscope to determine crystals' morphology and length***

Optic microscope (Nikon, Eclipse E2000) observation was used to determine the morphology, and occasionally the length, of the crystals recovered. In all cases, a systematic methodology was applied during the optical counting, taking representative pictures for each sample, and characterizing crystals for its morphology and size.

### ***Redissolution method to determine the composition of the product***

In all tests the product was redissolved in MilliQ water and decreasing the pH with HCl 2M, to determine the concentration of nutrients in the product recovered by Ion Chromatography (Dionex, IC5000), and compared to the results with the XRD.

As struvite and K-struvite have equimolar concentrations of magnesium, phosphate and ammonium/potassium, an excess of these compounds may indicate the co-precipitation of other products (i.e. magnesium phosphate and magnesium hydroxide). These other products can be detected by XRD analysis only if crystalline structure is achieved. If co-precipitation of amorphous substances took place, the redissolution method allowed to determine.



## Chapter Four

# Controlling struvite particles' size using the up-flow velocity

---

---

Tarragó, E., Puig, S., Rusalleda, M., Balaguer, M. D., Colprim, J. 2016. **Controlling struvite particles' size using the up-flow velocity**. Chem. Eng. J. 302, 819-827.

### 4.1 Overview

Phosphorus recovery from waste streams is considered to be an essential and significant breakthrough for assuring long-term and economical phosphorus supply (Liu et al., 2013), as the reserves may be depleted within around 200 years (Bergmans, 2011). For this reason, the actions for the coming 10-25 years must focus on its recovery, rather than its removal.

European cows and pigs jointly produce about 1.27 billion ton of manure each year. If this manure is directly applied to the soil, it can degrade water quality and represent an eutrophication threat in nitrate vulnerable zones (Menció et al., 2011). Traditionally, these nutrients were removed before the application, to diminish the environmental impact and prevent contamination of agricultural soils.

A new paradigm consists on the recovery of these nutrients, rather than its removal, to reduce the reliance on industrial fertilizers. Therefore, some European governments have been promoting new technologies to recycle P, a limited resource, from wastewater, sewage sludge and animal wastes (SCOPE Newsletter, 2001).

Phosphorus can be recovered from waste streams via struvite crystallization. Struvite is an effective slow-release fertilizer. Struvite offers many advantages versus conventional fertilizers: presents low leach rates and slowly release of nutrients (Münch and Barr, 2001); it is suitable in grasslands and forests where fertilizers are applied once in several years (Rahman et al., 2014); it does not damage growing plants when a single high dose is applied (De-Bashan and Bashan, 2004); represents an alternative for those crops that require magnesium, such as sugar beets (Gaterell et al., 2000); and, phosphorus uptake is higher in ryegrass when struvite is used as a fertilizer (Johnston and Richards, 2003).

Particle size is an important characteristic in fertilizers, as bigger particles will have longer effects on soil, increasing the nutrient uptake of plants/crops. It also affects

#### Chapter 4. Controlling struvite particles' size using the up-flow velocity

agronomic response, blending, storage, handling and application properties (UN Industrial Development Organization, 1998; Lu et al., 2012). Although there is no standard for particle size, it is identified as the most important factor in producing a stable, high-quality, blended fertilizer (Beegle, 1985). Ahmed et al., 2016 stated the need to focus future studies on determining the optimal placement and granule size to match the granule dissolution to the lifecycle of the plant.

Most probably, the product recovered from the waste streams will be used by the fertilizers producers as a green fertilizer blending, demanding for a stable particle size. Therefore, a methodology to control particle size could be helpful to adjust it in the range of customers' requirements.

How to increase particle size has been investigated in the literature. Two main methodologies were used: promote secondary nucleation or increase the reaction time. Seeding crystals or seeding inert materials can be used to promote secondary nucleation. Mehta and Batstone (2013) recovered struvite crystals with a volume median size of  $100 \pm 5 \mu\text{m}$  by using struvite crystals of  $35 \pm 3 \mu\text{m}$  as seeds. Wang et al., 2006 compared between seeded and unseeded experiments, and concluded that the production of large particles ( $350 \pm 32 \mu\text{m}$ ) is likely unfeasible in a reasonable operation time (1 h) without seeding. Suzuki et al., 2005 assessed different inert materials (stainless steel, wood and rubber) for struvite accumulation on their surface at different reaction times (from 5 to 42 days). They showed that after 5 days in an aeration column, the 80% (weight) of struvite were under  $1000 \mu\text{m}$ , whereas after 42 days, the 65% were over  $2000\mu\text{m}$ .

However, some authors stated that these methodologies may increase the operational costs, may end into materials interferences or low accumulation efficiencies depending on the seeding materials used (Suzuki et al., 2005) and decrease the purity of the struvite crystals (Liu et al., 2013).

On the other hand, Ronteltap et al., 2010 assessed the effect of some operational factors (type of stirrer, pH and temperature) on struvite particle size recovered from



## Chapter 4. Controlling struvite particles' size using the up-flow velocity

urine in a CSTR. They found that the use of a magnetic stirrer increased the supersaturation of the solution, preferring nucleation over crystal growth, and therefore, recovering smaller crystal sizes. Nevertheless, some of the developed crystallizers (such as air-lift reactors) do not have/use mechanical agitation. Therefore, alternative approaches should be put in practice, such as using hydrodynamics to control struvite particle size.

As stated, many studies have investigated the parameters affecting crystal growth. But, none of them, under our concern, suggest a methodology to control particle size. In this study, the up-flow velocity is assessed as a control parameter for the growth of struvite particles, in a combined air-lift reactor. By modifying the air-flow rate applied, the up-flow velocity can be controlled. It is hypothesized that the up-flow velocity determined the minimum theoretical equivalent diameter that can be recovered. This theoretical diameter was contrasted with the experimental results, promoting both struvite nucleation and growth. The performance of the designed crystallizer was evaluated in terms of particle size and characterization of the product recovered.

### 4.2 Materials and methods

#### 4.2.1 Experimental set-up

A methacrylate crystallizer was designed as an air-lift reactor plus a settler (Figure 4. 1). Three differentiated zones could be distinguished in the crystallizer: riser, clarifier and collector. Supersaturated conditions were ensured in the riser zone. Struvite growth was promoted in this zone thanks to the recirculation and fluidization of small particles from zone 2. The clarifier consisted of a quiet zone to prevent particles loss as the up-flow velocity was kept constantly low ( $0.0177 \text{ m h}^{-1}$ ), even at higher air-flow rates ( $0.0179 \text{ m h}^{-1}$ ).

## Chapter 4. Controlling struvite particles' size using the up-flow velocity

The collector, where the particles settled once their settling velocity was higher than the up-flow velocity.

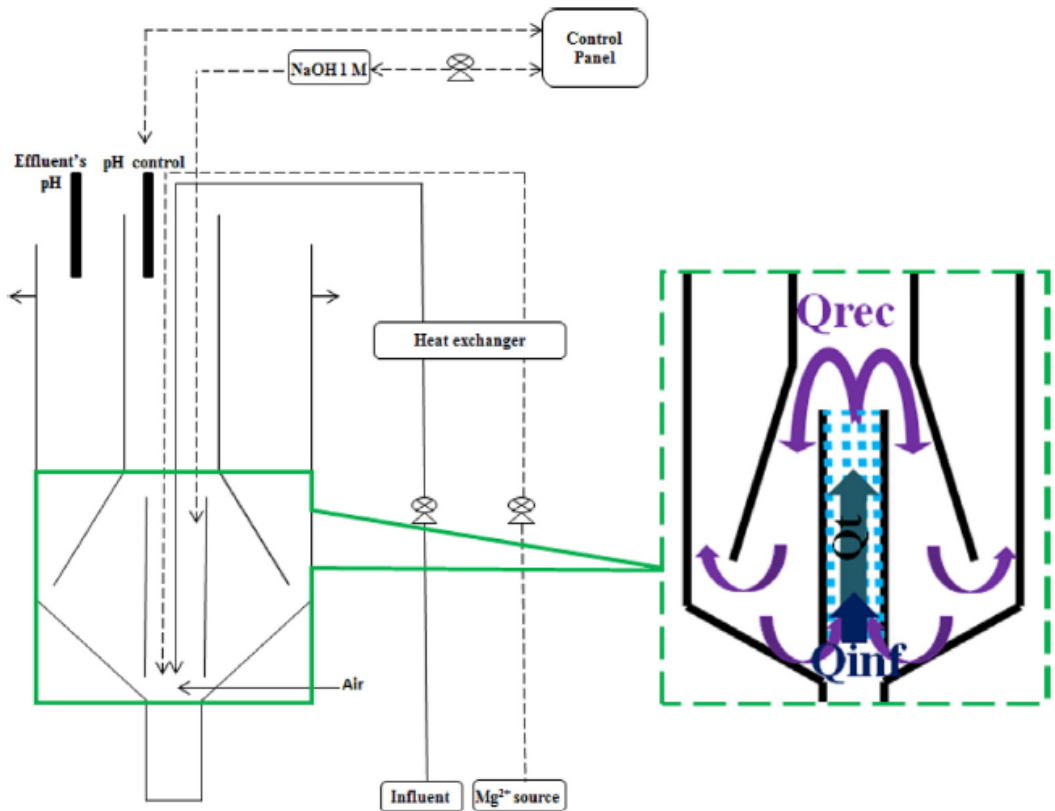


**Figure 4. 1** Scheme of the crystallizer designed for struvite recovery. Crystallizer's parts: riser (1), clarifier (2) and collector (3). In the zoom, crystallizer's hydrodynamics in the riser: recirculation flow ( $Q_{rec}$ ), induced by the air-flow rate applied; influent flow ( $Q_{inf}$ ); and total flow ( $Q_t$ ) as the sum of  $Q_{rec}$  and  $Q_{inf}$ .

The total volume of the crystallizer was 14.6 L with an hydraulic retention time (HRT) of 3.5 h. The influent wastewater was heated up to  $30.5 \pm 1.0$  °C, to simulate the temperature of the digester supernatant, and fed continuously ( $4.13 \pm 0.04$  L h<sup>-1</sup>) into the crystallizer (riser zone). A magnesium solution was added to allow struvite

## Chapter 4. Controlling struvite particles' size using the up-flow velocity

precipitation at a ratio  $\text{Mg}^{2+}/\text{PO}_4^{3-}$  of 2.5. Aeration in the riser was controlled by means of a mass flow meter (Rotameter, 2100/INOX). pH was controlled in the riser at 8.5 using a control panel (Memograph; Endress+Hauser, RSG40), dosing NaOH (1M). Struvite particles settled in the bottom part of the crystallizer (collector) and were recovered at the end of the experiments, while the effluent wastewater was continuously discharged by overflow.

### 4.2.2 Experimental procedure

Six tests of 1 h were carried out in duplicate at six up-flow velocities (13.3, 15.4, 17.0, 22.6, 24.9 and 26.3  $\text{m h}^{-1}$ ) to find out the influence of the up-flow velocity on struvite particles' size. The up-flow velocity was controlled by modifying the air-flow applied at 1, 1.5, 2, 5, 7.5 and 10  $\text{L min}^{-1}$ , respectively.

Then, a continuous mode test at the up-flow velocity of 22.6  $\text{m h}^{-1}$  was carried out, in duplicate, to study the influence of increasing the particle residence time to 138.6 h on particle size distribution. Samples were taken periodically (25.5, 48.5, 69.5 and 138.6 h) from the collector to determine particle size distribution through time.

In all tests, struvite crystal size, recovery efficiency and purity conditions were analyzed.

### 4.2.3 Influent wastewater

Effluent from the wastewater treatment plant of Girona (Spain) was used as media to prepare the influent wastewater. The concentrations of ammonium and phosphate were adjusted to  $929.3 \pm 26.9 \text{ mg NH}_4^+ \cdot \text{L}^{-1}$  and  $368.5 \pm 14.9 \text{ mg PO}_4^{3-} \cdot \text{L}^{-1}$ , respectively. Those concentrations simulated the characteristics of cow and pig manure samples from Spain and The Netherlands, previously characterized (digested manure after a solid/liquid separation unit). Table 4. 1 presents the main physico-chemical characteristics of the influent.

## Chapter 4. Controlling struvite particles' size using the up-flow velocity

**Table 4. 1** Physico-chemical characteristics of the influent. The results are presented as mean  $\pm$  standard deviation.

	Units	Influent
pH	–	8.45 $\pm$ 0.02
Conductivity	mS cm <sup>-1</sup>	5.56 $\pm$ 2.95
Temperature	°C	30.5 $\pm$ 1.0
Total suspended solids (TSS)	mg TSS L <sup>-1</sup>	167 $\pm$ 71
Volatile suspended solids (VSS)	mg VSS L <sup>-1</sup>	83 $\pm$ 21
Magnesium	mg Mg <sup>2+</sup> L <sup>-1</sup>	236.9 $\pm$ 19.2
Ammonium	mg NH <sub>4</sub> <sup>+</sup> L <sup>-1</sup>	929.3 $\pm$ 26.9
Phosphate	mg PO <sub>4</sub> <sup>3-</sup> L <sup>-1</sup>	368.5 $\pm$ 14.9
Potassium	mg K <sup>+</sup> L <sup>-1</sup>	21.8 $\pm$ 7.3
Calcium	mg Ca <sup>2+</sup> L <sup>-1</sup>	66.5 $\pm$ 19.9

The average Mg<sup>2+</sup>:NH<sub>4</sub><sup>+</sup>:PO<sub>4</sub><sup>3-</sup> molar ratio in the influent was 2.5:13.3:1.0. Mg<sup>2+</sup>/PO<sub>4</sub><sup>3-</sup> molar ratio was 2.5, similar to the ratios found in the literature for similar influents: Mg<sup>2+</sup>/PO<sub>4</sub><sup>3-</sup> of 1.79 from digested swine wastewater (Yong-Hui Song et al., 2011), 2.14 from synthetic swine wastewater (Capdevielle et al., 2013), 3.29 (calculated) from anaerobic digested sludge (Martí et al., 2008) and 4.8 from anaerobically digested dairy manure (Huchzermeier and Tao, 2012).

### 4.2.4 Calculations

The up-flow velocity in the riser was calculated according to Eq 4. 1. This parameter was function of the total flow inside the riser and the section of the riser. In the designed crystallizer, the total flow (Qt) was the sum of the influent flow treated (Qinf) plus the recirculation flow (Qrec) induced by the aeration applied. The recirculation flow into the riser was calculated according to Merchuk and Gluz (1999), taking into account the superficial gas velocity (J<sub>G</sub>). By determining the recirculation and the influent flow, the total flow (Qt) was obtained, and the up-flow velocity was calculated according to Eq 4. 1.

#### Chapter 4. Controlling struvite particles' size using the up-flow velocity

$$\text{Up-flow velocity} = \frac{\text{Total flow}}{\text{Section}} \quad \text{Eq 4. 1}$$

The up-flow velocity determines the minimum theoretical equivalent diameter (MTD) that can be recovered. The MTD was calculated according to Eq 4. 2. Particles smaller than the theoretical equivalent diameter remain in suspension, while bigger particles settle in the collector. The MTD that can be retained in the riser is determined as a function of the up-flow velocity applied (Figure 4. 2).

$$\text{MTD} = \sqrt{\frac{v \cdot 18 \cdot \mu}{(\rho_p - \rho_L) \cdot g}} \quad \text{Eq 4. 2}$$

where the critical settling velocity ( $v$ ) was assumed to be the up-flow velocity,  $\rho_p$  and  $\rho_L$  were the density of the particle and the fluid density ( $995.65 \text{ kg m}^{-3}$ );  $g$  was the standard acceleration due to gravity and  $\mu$  was the fluid viscosity ( $0.7978 \text{ mPa s}^{-1}$ ). The fluid density in the riser was also influenced by the air-flow according to Eq 4. 3.

$$\rho_L = (\rho_{\text{air}} \cdot \phi_{\text{riser}}) + (\rho_{\text{fluid}} \cdot (1 - \phi_{\text{riser}})) \quad \text{Eq 4. 3}$$

where  $\rho_{\text{air}}$  is the density of the air at  $26.5 \text{ }^\circ\text{C}$  (temperature of the air entrance),  $\phi_{\text{riser}}$  is the gas holdup in internal air-lift reactors (Merchuk and Gluz, 1999) and  $\rho_{\text{fluid}}$  is the fluid density at  $30.5 \text{ }^\circ\text{C}$  (average temperature inside the crystallizer).

## Chapter 4. Controlling struvite particles' size using the up-flow velocity

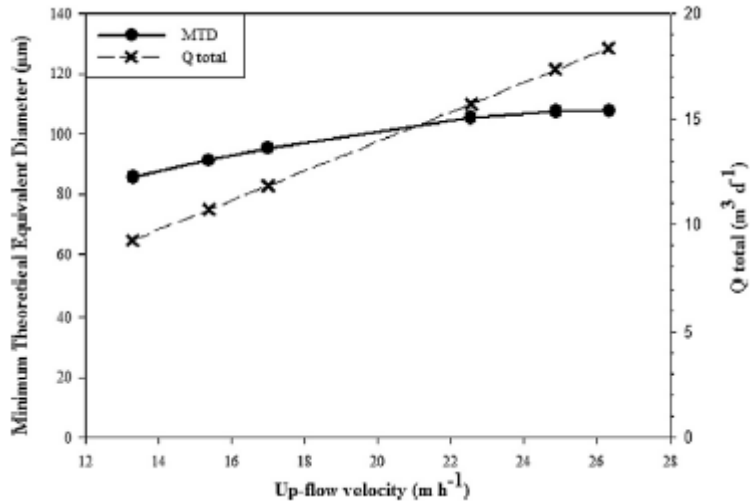


**Figure 4. 2** Minimum theoretical equivalent diameter (MTD), in  $\mu\text{m}$ , that can be retained in the riser as a function of the up-flow velocity ( $\text{m h}^{-1}$ ). The total flow ( $\text{m}^3 \text{d}^{-1}$ ), as a sum of the recirculation ( $Q_{\text{rec}}$ ) and the influent flow ( $Q_{\text{inf}}$ ), is represented as  $Q_{\text{total}}$ .

The driving force for struvite formation, and for all crystallization processes, is the supersaturation (Pastor et al., 2008). The relative supersaturation ( $S_r$ ) was calculated based on the methodology followed by Bergmans, 2011 (Eq 4. 4). The relative supersaturation is a function of the dimensionless supersaturation ratio ( $S_c$ ), which in turn depends on the analytical molar concentration ( $P_{\text{SO}}$ ) and the solution properties ( $P_{\text{CS}}$ ).  $P_{\text{CS}}$  is a function of the minimum struvite solubility product ( $K_{\text{SO}}$ ), as well as the ionization fraction ( $\alpha_i$ ) and the activity coefficients ( $\gamma_i$ ) of each struvite compound (Eq 4. 5). The activity coefficients were calculated from the extended form of the Debye-Hückel equation proposed by Davies, 1962. Accordingly, the solution is supersaturated for  $S_r > 0$  and undersaturated for  $S_r < 0$ .

$$S_r = S_c - 1 \quad \text{Eq 4. 4}$$

$$S_c = \left( \frac{P_{\text{SO}}}{P_{\text{CS}}} \right)^{1/3} \quad \text{Eq 4. 5}$$

## **Chapter 4. Controlling struvite particles' size using the up-flow velocity**

The induction time was determined by monitoring on-line pH. Mehta and Batstone (2013) defined the induction time as the period time between the achievement of supersaturation and the appearance of crystal nuclei, which can be measured as the time for the first pH drop after the initial setting.

### **4.2.5 Analytical methods**

Influent and effluent liquid samples were taken periodically and analyzed to determine the nutrient recovery efficiency of the process. The concentrations of ammonium, phosphate, magnesium, potassium and calcium in the liquid phase were determined by Ion Chromatography (Dionex, IC5000). Total suspended solids (TSS) and volatile suspended solids (VSS) were determined according to standard methods (APHA, 2005). pH (EC-Meter BASIC 20+, Crison, Spain) and conductivity (EC-Meter BASIC 30+, Crison, Spain) were measured on-line and periodically, respectively. The product (precipitate) obtained was characterized by X-ray diffraction analysis (X-ray Diffractometer, Bruker, D8 Advance) to determine crystal's structure. Laser diffraction (Beckman Coulter, LS 13320MW Optical Bench) and optical counting (Nikon, Eclipse E2000) were used to determine the size distribution of the crystals.

## **4.3 Results and discussion**

### **4.3.1 MTD as a function of the up-flow velocity**

The up-flow velocity determines the minimum theoretical equivalent struvite diameter that can be recovered. Figure 4. 2 presents the MTD versus the up-flow velocity. The MTD increased at the highest up-flow velocities. By increasing the air-flow rate (so the up-flow velocity), the density of the liquid is decreased and a higher recirculation flow is induced, increasing the minimum theoretical equivalent diameter that can be recovered. Therefore, only particles with the minimum

## Chapter 4. Controlling struvite particles' size using the up-flow velocity

diameter could settle in the collector, whereas smaller particles were recirculated into the riser and maintained in fluidization, while growing until the critical diameter was reached. The methodology used, based on Merchuk and Gluz (1999) calculation for the recirculation flow induced in an air-lift reactor, allowed to determine the minimum theoretical equivalent diameter that could be recovered. It was a useful tool, both for operational conditions and product recovery. This theoretical approach was confirmed with the experimental results for the different up-flow velocities tested, as only bigger particles than the minimum theoretical equivalent diameter were recovered.

### 4.3.2 Struvite recovery performance at different up-flow velocities

Table 4. 2 compares the struvite recovery performance at different up-flow velocities. Its recovery performance was not influenced in any of the up-flow velocities applied, in terms of supersaturation, phosphate recovery and struvite production.

**Table 4. 2** Relative supersaturation, induction time, struvite production and phosphate recovery efficiency for each up-flow velocity studied. Also, volatile suspended solids (VSS) in the effluent of each test are presented.

Up-flow velocity (m h <sup>-1</sup> )	Air-flow (L min <sup>-1</sup> )	Sr (mol L <sup>-1</sup> )	Induction time (min)	Struvite production (g L <sup>-1</sup> treated)	PO <sub>4</sub> <sup>3-</sup> recovery efficiency (%)	VSS in the effluent (mg VSS L <sup>-1</sup> )
13.3	1	0.25	2.17	1.26	92.3	35
15.4	1.5	0.12	2.33	1.74	94.5	68
17.0	2	0.22	0.67	1.76	94.6	54
22.6	5	0.22	0.34	1.67	95.4	108
24.9	7.5	0.27	0.54	1.55	95.0	93
26.3	10	0.27	0.67	1.70	95.4	71

The design of the crystallizer as an air-lift reactor plus a settler was proved to be effective for P-recovery as struvite from simulated digested manure after a solid/liquid separation. High P-recovery efficiency (94.4 ± 1.3%, on average) was achieved by minimizing the reagents consumption (Mg<sup>2+</sup>/PO<sub>4</sub><sup>3-</sup> ratio of 2.5).



#### Chapter 4. Controlling struvite particles' size using the up-flow velocity

Phosphate was recovered as struvite in the collector, achieving an average struvite production of  $1.63 \pm 0.21 \text{ g L}^{-1}$  treated. These results are in agreement with Stumpf et al., 2008 that recovered struvite from a synthetic solution, in a similar air-lift reactor (with a diameter of 30 cm) at different air-flow rates (from  $1.7$  to  $8.3 \text{ L min}^{-1}$ ). They established that P-recovery was dependent on the amount of the stripped  $\text{CO}_2$ , increasing at higher air-flow rates (from 58% of P-recovery in 1 h at  $1.7 \text{ L min}^{-1}$ , to 90% at  $8.3 \text{ L min}^{-1}$ ). In the present study, P-recovery efficiency at all the up-flow velocities studied, and consequently, in all the air-flow rates applied, was approximately 95% in 1 h.

X-ray diffraction (XRD) analysis confirmed that the crystals recovered in the collector were pure struvite. Figure 4. 3A presents a representative XRD diffractogram of the particles recovered at the up-flow velocity of  $22.6 \text{ m h}^{-1}$ . These results confirmed that the quality of the struvite recovered was not affected by the presence of suspended solids ( $83 \pm 21 \text{ mg L}^{-1}$ ) or calcium concentration ( $66.5 \pm 19.9 \text{ mg Ca}^{2+} \text{ L}^{-1}$ ) in the influent (Ca/Mg ratio of 0.17). The suspended solids in the influent were mainly colloidal (as it would be expected after a solid/liquid separation unit) and just passed through the system without being settled in the collector nor captured into the crystals. Thus, the effluent VSS concentration was similar ( $75 \pm 23 \text{ mg L}^{-1}$ ), except in the lowest up-flow velocity of  $13.3 \text{ m h}^{-1}$  (Table 4. 2). The concentration of calcium was around  $66.5 \text{ mg Ca}^{2+} \text{ L}^{-1}$ , which came from the treated effluent from Girona's WWTP, used as a media to prepare the synthetic swine wastewater. The product obtained in all the studies was characterized by X-ray diffraction (XRD) analysis as pure struvite crystals, showing no presence of amorphous substances, contrasted with optic microscope observations. Our results are in concordance with Crutchik and Garrido (2011), Hwang and Choi (1998), Le Corre et al., 2005 and Stratful et al., 2004, in which struvite formation was enhanced by having a  $\text{Ca}^{2+}/\text{Mg}^{2+}$  molar ratio below 1 (Crutchik and Garrido, 2011; Hwang and Choi, 1998; Le Corre et al., 2005) (0.17 in our study), and/or a high ammonium concentration in the influent, in a  $\text{NH}_4^+/\text{PO}_4^{3-}$  ratio of 9.4

#### Chapter 4. Controlling struvite particles' size using the up-flow velocity

(Stratful et al., 2004) (13.3 in our study). Therefore, nutrients were always recovered as pure struvite crystals, without any interference of influent's colloidal suspended solids or the presence of calcium in the influent used.

The air-lift configuration allowed the recirculation of small particles into the riser, promoting heterogeneous nucleation and crystal growth due to the recirculation flow induced by the air-flow applied in the riser. The crystallizer configuration promoted supersaturated conditions in the riser, where the influent wastewater was fed, the magnesium solution dosed and pH was adjusted. Consequently, struvite's nuclei were formed in the riser, where it had the highest availability of nutrients and supersaturation conditions ( $S_r$  of  $0.21 \pm 0.06$ , on average). The values of relative supersaturation obtained in this study were similar to the ones obtained by Kofina and Koutsoukos (2005) in their study of spontaneous precipitation of struvite, as similar operational conditions were used, such as pH, temperature and concentrations of the influent (considering the phosphate, the limiting compound in our study).

The induction time (the time lapse until the first pH drop of 0.05 is detected) was always short, between 0.34 and 2.33 min (Table 4. 2). However, the induction time was reduced when the up-flow velocity was increased, meaning that first nuclei were formed faster at higher up-flow velocities. Hence, the induction time depended on the air-flow rate applied in the riser. Higher up-flow velocities led to lower induction times, as the mixing energy, one of the parameters affecting induction time (Liu et al., 2013), was supposed to be higher and favored nucleation.

The applicability of the designed crystallizer is proved, showing good performance results, both in batch and continuous mode, without affecting the production and the quality of the product recovered. The results obtained in this study were compared to the performance of similar reactors, in terms of P-recovery, operation conditions (HRT) and the average particle size of the product recovered (Table 4. 3). High P-recoveries were achieved, both in batch and continuous mode tests, in

## Chapter 4. Controlling struvite particles' size using the up-flow velocity

comparison with other studies (Bergmans, 2011; Martí et al., 2010; Stumpf et al., 2008). The system was able to operate at low HRT, compared to Ueno and Fujii (2001), without affecting the system performance.

The air-lift configuration allowed the possibility of controlling particle size, which will be further analyzed in the following sections.

**Table 4.3** Comparison between performances of the designed crystallizer and similar reactors available in the literature cited. Adapted from Tarragó et al., 2016.

Reference	Type of crystallizer	Stream treated	HRT	P-recovery (%)	Induction time (min)	Sr	Seeding	Mean particle size recovered ( $\mu\text{m}$ )
Present study	Air-lift reactor combined with a settler	Synthetic wastewater (treated effluent of WWTP as a media)	3.5h	> 95%	0.34 – 2.33	0.24 $\pm$ 0.02	No	Batch: 112.6-242.6 $\mu\text{m}$ Continuous: 314 $\mu\text{m}$
Bergmans, 2011	Short-Long column	WWTP's digested sludge	n.d.	70-90%	n.d.	n.d.	No	n.d.
Martí et al., 2010	Stirred tank reactor (reaction and Settling zone)	Rejected liquors of different strategies of the sludge treatment line	2.5h (reaction zone)	70-90%	n.d.	n.d.	No	n.d.
Soare et al., 2012	Air-lift crystallizer	Synthetic saturated solution	n.d.	n.d.	n.d.	0.5 - 1	Yes (average seed size of 110 $\mu\text{m}$ )	400-600 $\mu\text{m}$
Stumpf et al., 2008	Batch tests and Pilot reactor (air-lift)	WWTP's digested sludge	n.d.	Batch: 85% Pilot reactor: 58-90%	n.d.	n.d.	No	90-150 $\mu\text{m}$
Ueno and Fujii (2001)	Fluidized Bed Reactor (FBR)	Dewatered filtrate from anaerobic digestion	10 days	90%	n.d.	n.d.	Yes	500-1000 $\mu\text{m}$

## Chapter 4. Controlling struvite particles' size using the up-flow velocity

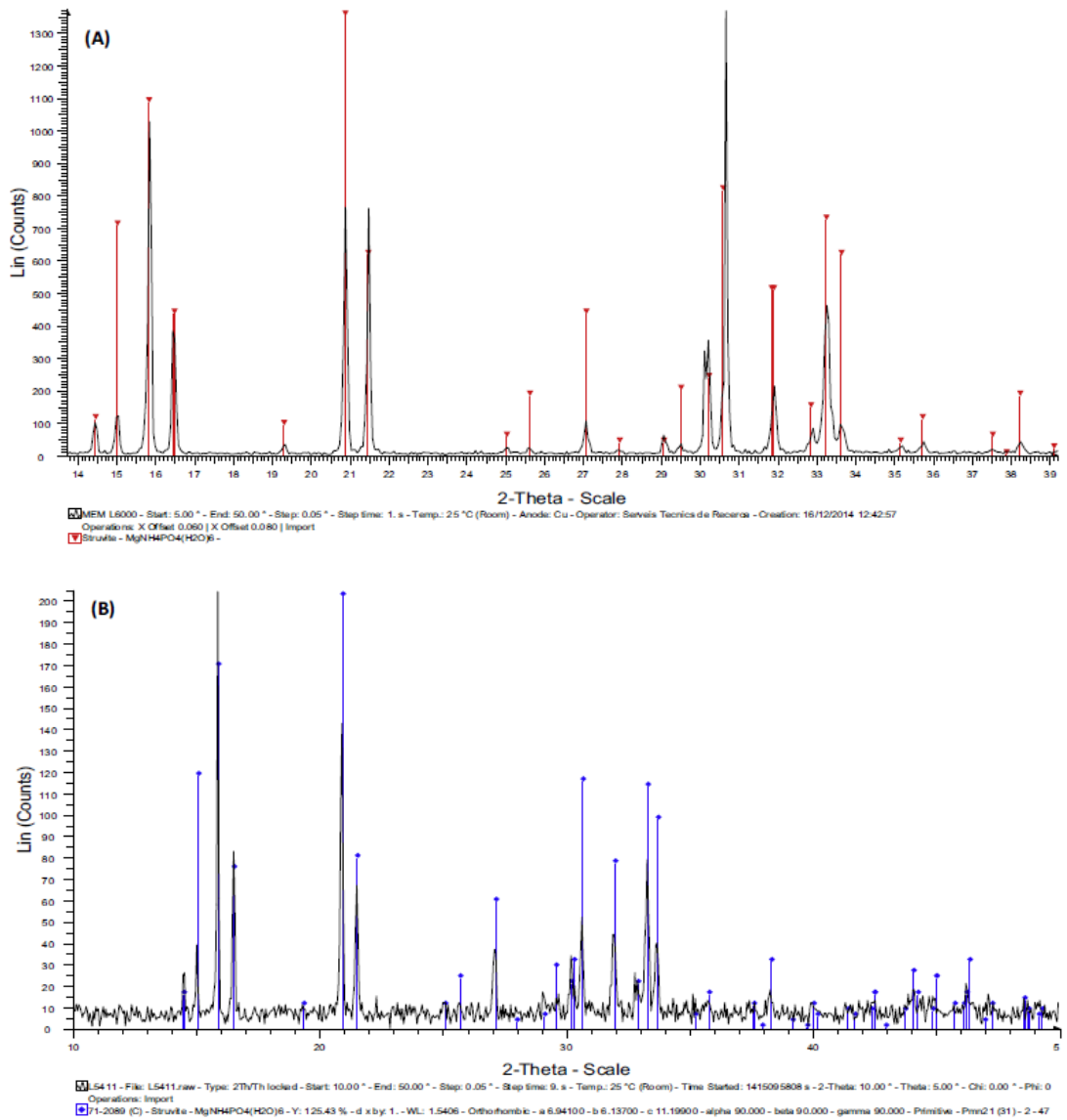


**Figure 4. 3** XRD diffractograms of the precipitates settled in the collector of the crystallizer at the up-flow velocity of  $22.55 \text{ m h}^{-1}$ . (A) Test for struvite recovery at different up-flow velocities (1 h tests); (B) continuous mode tests.

### 4.3.3 Experimental size of struvite particles

The design of the crystallizer allowed the control of the up-flow velocity in the riser, by applying a specific air-flow rate. The up-flow velocity could have an influence in the size of the particles' recovered in the collector. As stated in Figure 4. 2, only bigger particles with a settling velocity equal or higher than the up-flow velocity can settle at the collector. Different up-flow velocities were tested (from 13.3 to 26.3 m h<sup>-1</sup>) by increasing the air-flow rate from 1 to 10 L min<sup>-1</sup>.

Table 4. 4 presents both the theoretical approach about the MTD that can be recovered and the experimental results of particle size (mean equivalent diameter recovered). In all tests, the theoretical approach was confirmed experimentally, recovering a mean equivalent diameter (Mean Deq) bigger than the MTD calculated by Eq 4. 2.

**Table 4. 4** Comparison between the MTD and the experimental mean equivalent diameter recovered (Mean Deq) for each up-flow velocity studied.

Up-flow velocity (m h <sup>-1</sup> )	MTD (μm)	Mean D <sub>eq</sub> (μm)
13.3	85.7	112.2 ± 0.6
15.4	91.4	126.5 ± 7.3
17.0	95.4	136.9 ± 4.9
22.6	105.5	148.5 ± 6.4
24.9	107.5	201.9 ± 7.0
26.3	107.8	244.0 ± 2.0

The results obtained showed that the up-flow velocity in the riser is directly correlated with the particle size of the struvite recovered. Figure 4. 4 shows the experimental particle size recovered as a function of the up-flow velocity, including 95% confidence and prediction bands. All particle sizes recovered are in the zone of 95% confidence, except for the particle size recovered at the up-flow velocity of 22.6 m h<sup>-1</sup>, which differs slightly. This up-flow velocity is enclosed in the 95% prediction band, due to the standard deviation between duplicates.

## Chapter 4. Controlling struvite particles' size using the up-flow velocity

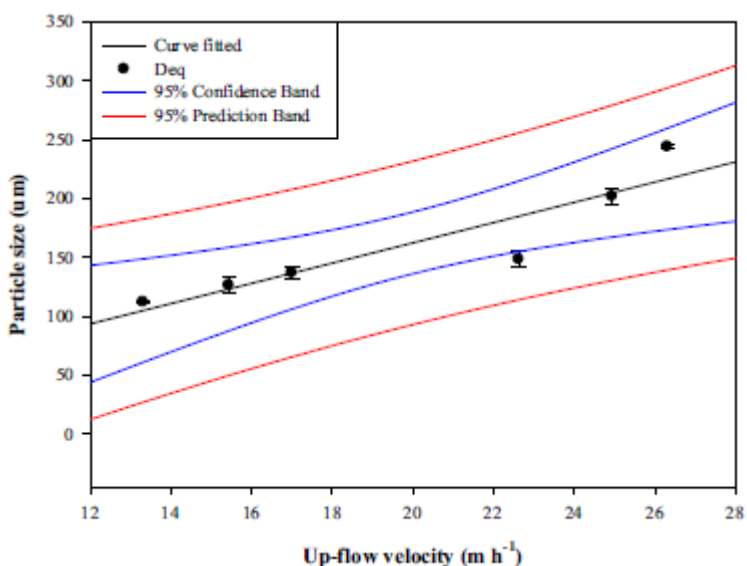


**Figure 4. 4** Particle size recovered (Deq) as a function of the up-flow velocity. The curve fitted is showed in black, the 95% confidence band in blue, and the 95% prediction band in red.

Therefore, by increasing the up-flow velocity from 13.3 to 26.3 m h<sup>-1</sup> (air-flow rate from 1 to 10 L min<sup>-1</sup>), the average diameter of the crystals recovered increased from 112.6 to 242.6 µm (46%). Besides, the increase of the up-flow velocity in the riser resulted in an increase of the recirculation flow, promoting heterogeneous nucleation and crystal growth.

A wide range of struvite particles' sizes were recovered in the literature, from 0.5 mm to 6.5 mm (Fattah, 2004). Nevertheless, few studies have been able to deal with the production of fines and growing large pellets, mainly by using fines as seeding material and increasing the retention time (longer periods of time). For example, Ueno and Fujii (2001) recovered particles up to 500-1000 µm in a fluidized bed reactor treating dewatered filtrate from anaerobic sludge digestion and using the fines produced as seeding materials, at a retention time of 10 days. In comparison with our results, as the designed crystallizer allowed the recirculation of small particles, and therefore, enhanced struvite growth, a mean particle size of 250 µm

#### Chapter 4. Controlling struvite particles' size using the up-flow velocity

(mean equivalent diameter) was recovered in a retention time of 3.5 h. The low retention time applied can be a key point for the application of the technology, having a compact system which can treat bigger flow volumes (e.g. 100 L day<sup>-1</sup>), without affecting the growth phase. Then, the results presented in this paper prove that particle size can be increased in the designed crystallizer at lower retention times and without seeding, by controlling the up-flow velocity applied and thanks to the design.

Soare et al., 2012 introduced the effect of the air-flow to the final crystal size and shape, in an air-lift reactor, applying different air-flow rates (from 1.6 to 13.3 L min<sup>-1</sup>) and seeding loads, and obtaining a narrower distribution size at the lowest up-flow velocities (lowest air-flow rates). The differences remain in particle size distribution. Soare et al., 2012 recovered largest particles at the lowest air-flow rates, as well as a better quality of the crystals; whereas the results presented in this study showed a narrower distribution (Figure S4. 1) and largest particles recovered at higher up-flow velocities, without affecting the quality. These differences can be explained by the superficial gas velocity of both systems. The gas velocity must be sufficient to generate an upward liquid velocity in the riser that is equal to the particle swarm velocity (Soare et al., 2012). Low velocities might only fluidize a fraction of the crystals, depending of its size. In the present study, slightly higher gas velocities were obtained, allowing the recovery of bigger particles at higher air-flow rates (higher up-flow velocities).

In all the up-flow velocities tested, the crystals recovered in the collector zone had mainly rectangular type morphology (elongated crystals), with a minor fraction of coffin shaped (trapezoidal shape) crystals. The morphology observed in this study is in agreement with Le Corre et al., 2005 which established that elongated crystals are the typical morphology for crystals recovered from synthetic wastewater using magnesium chloride as an additional chemical. Struvite crystals are rod-like, orthorhombic and ranging from X-shaped to flat trapezoidal (Münc and Barr, 2001),

being the coffin, the needle and the trapezoidal shape the typical forms (Ronteltap et al., 2010). These differences in struvite morphology are due to some operational conditions, such as the initial concentration of the compounds (Le Corre et al., 2005) or the supersaturation ratio (Fattah et al., 2012), among others. Shikazono, 2003 stated that rectangular type precipitation form might be due to heterogeneous nucleation and growth of crystals on the surface of pre-existing crystals. This concurred with our results, as the design of the crystallizer allowed the recirculation of formed nuclei.

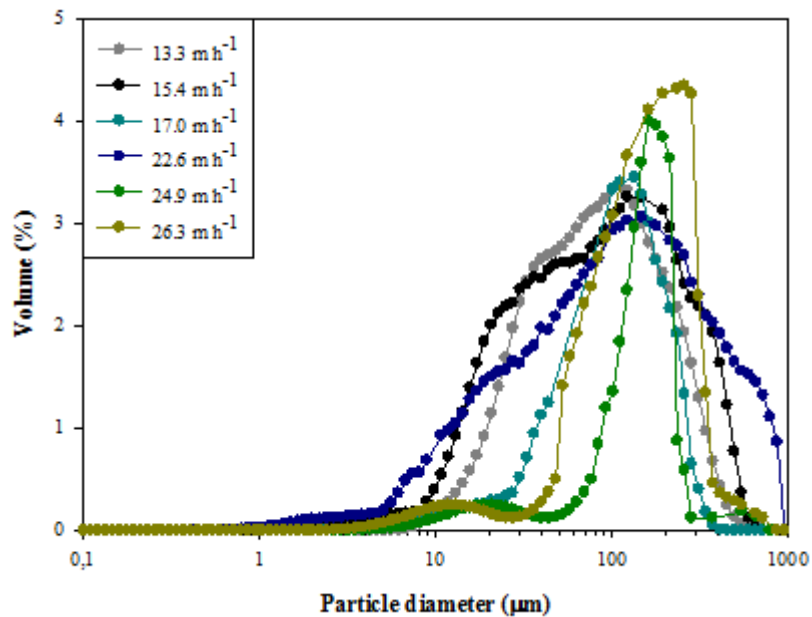


**Figure S4. 1** Particle size distribution results, by the laser diffraction method, for each up-flow velocity studied.

### 4.3.4 Promoting the growth of struvite particles by operating the crystallizer in continuous mode

The up-flow velocity determines the minimum theoretical equivalent diameter that can be recovered. Particle size can be increased enhancing growth phase, for



#### Chapter 4. Controlling struvite particles' size using the up-flow velocity

example, by operating in continuous mode. For this reason, the system was switched from batch mode (experiments of few hours) to continuous mode operation to enhance growth phase (to reach metastable conditions) and test the implications for struvite particles' size. Metastable zone can be defined as the period of time in which crystal growth preferably takes place over nucleation (Bergmans, 2011), being the area between supersolubility and solubility curves (Bhuiyan et al., 2008). For continuous mode experiments, the up-flow velocity was kept at  $22.6 \text{ m h}^{-1}$  during 138.6 h, and particle size distribution was analyzed periodically.

Phosphate's concentration in the effluent was periodically analyzed (Figure 4. 5). An immediate phosphate removal was observed, remaining constant in time despite the continuous feeding. Despite the fact that the metastable zone was not determined experimentally, the results of the continuous mode experiments might prove that they were carried out close to the metastable zone. The immediate decrease of the concentration of phosphate ( $330 \text{ mg PO}_4^{3-} \text{ L}^{-1}$  in 15 h) and the highest phosphate recovery rate at the end of the experiments ( $95.4 \pm 0.3\%$ ) were due to the continuous mode operation, in which steady state was achieved, enhancing crystal growth. pH control at 8.5 ensured the optimal conditions for struvite formation. XRD confirmed that only pure struvite was recovered during continuous mode operation tests (Figure 4. 3B). Samples of the product obtained in the collector were taken at different times (25.5, 48.5, 69.5 and 138.6 h) and analyzed for particle size distribution. Figure 4. 6 depicts the particle size evolution over time. Fourteen particle size ranges (from  $0\text{-}50 \text{ }\mu\text{m}$  to  $900\text{-}1000 \text{ }\mu\text{m}$ ) were obtained from an optical counting. The average crystal size increased in time:  $201 \text{ }\mu\text{m}$  at 25.5 h,  $219 \text{ }\mu\text{m}$  at 48.5 h,  $237 \text{ }\mu\text{m}$  at 69.5 h and  $314 \text{ }\mu\text{m}$  at 138.6 h (end of the study), meaning that struvite particle size increased in time ( $113 \text{ }\mu\text{m}$  in 113 h) as growth phase was enhanced.

Besides, there was a displacement of the particles' size ranges and the abundance of particles at higher ranges increased in time. As an example, the abundance of

## Chapter 4. Controlling struvite particles' size using the up-flow velocity

particles in the range of 300-400  $\mu\text{m}$  was duplicated at the end of the experiment, and moreover, bigger particles (ranges from 500 to 1000  $\mu\text{m}$ ) only appeared at the end of the experiment, reaffirming the previous statement. This means that the small particles could grow in time and increase its size due to heterogeneous nucleation favored for the design of the crystallizer and the continuous mode operation. Nevertheless, small particles (range 0-50  $\mu\text{m}$  and 50-100  $\mu\text{m}$ ) were found at the end, as they were the new nuclei formed that could settle in the collector either because they were attached to bigger particles (aggregation) or due to some part of the crystallizer with a velocity equals to zero. Soare et al., 2012 also observed the presence of small particles at high air-flow rates, indicating nucleation at the end of the batch, which is in agreement of the results obtained in this study. The results obtained from batch and continuous mode operation were consistent with those of Stratful et al., 2001 and De-Bashan and Bashan, 2004, who reported that on increasing reaction time from 1 to 180 min, crystal size increased significantly. In our case, from 1 h to 6 days length tests, particle size increased from 150  $\mu\text{m}$  to 300  $\mu\text{m}$ .

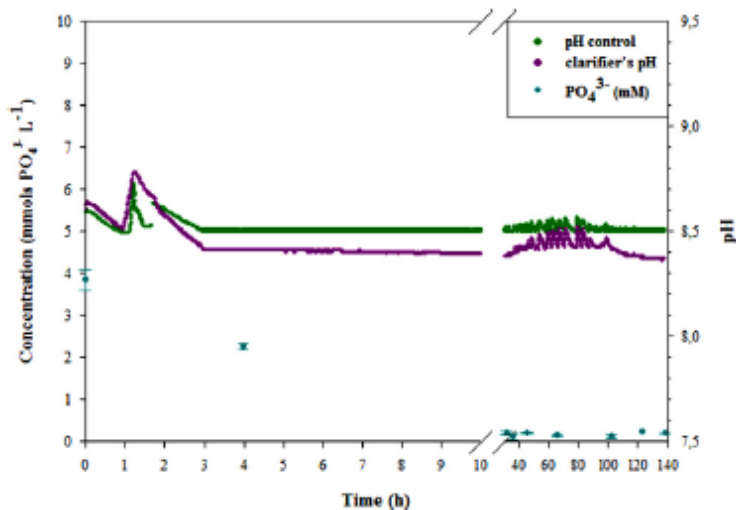


**Figure 4. 5** Average phosphate's concentration during the tests of 138.6 h at the up-flow velocity of 22.6  $\text{m h}^{-1}$ . pH control (pH in the riser) is presented in green and pH in the clarifier zone in pink, for one of the replicates.

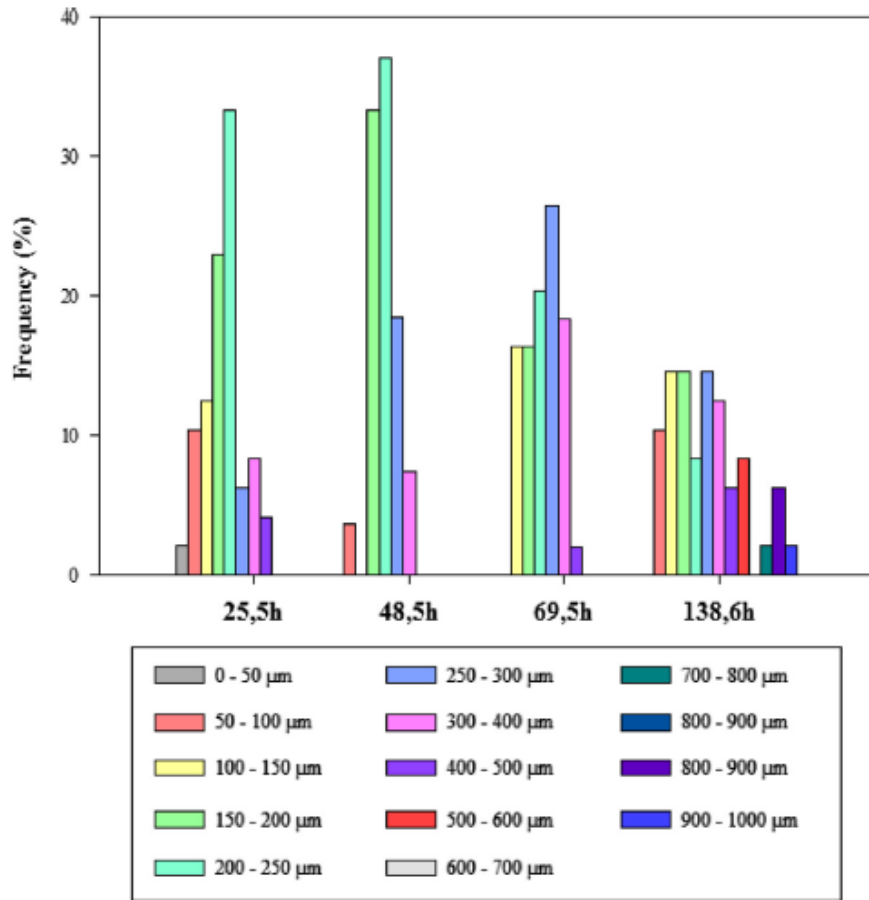


Figure 4. 6 Particle size distribution results over time in 14 particle size ranges (from 0-50 μm to 900-1000 μm), from the continuous mode experiments at the up-flow velocity of 22.6 m h<sup>-1</sup>. The results presented are the average of replicates.

#### 4.4. Conclusions

This study proves that the up-flow velocity has a direct effect on the minimum theoretical equivalent struvite particle diameter that can be recovered. The theoretical approach was confirmed experimentally, recovering a mean equivalent diameter bigger than the theoretical.

By applying higher up-flow velocities, bigger struvite particles were recovered, without affecting recovery efficiency. Struvite particle size can be promoted up to 800-1000  $\mu\text{m}$  by operating the crystallizer in continuous mode.

The excellent system performance, both in terms of process efficiency and quality of the harvested product, was confirmed, as high phosphate recovery rates were achieved. This study opens the door to use the up-flow velocity as a controlling parameter of particle size to the customers' requirements for fertilizer application (e.g. particle size).



## Chapter Five

# Effect of suspended solids on struvite formation from digested manure supernatant

---

---

Effect of solids on struvite formation from digested manure supernatant.

*Submitted*

Submitted paper. Embargoed until publication date





## Chapter Six

# Towards a methodology for recovering K-struvite from manure

---

---

E. Tarragó, M. Rusalleda, J. Colprim, M. D. Balaguer, S. Puig, 2017. **Towards a methodology for recovering K-struvite from manure.** Journal of Chemical Technology & Biotechnology, DOI: 10.1002/jctb.5518. *Accepted article*

### 6.1 Overview

Synthetic fertilizers contain mainly three essential macronutrients for plants/crops (nitrogen, N; phosphate, P; and potassium, K) (Manning, 2015). Traditionally, manure (liquid and solid fractions) was directly applied to the soil. The high content of N respect to P and the low kinetics of nutrient uptake of plants results in an overdosing of N in soils, and consequently, the leaching of nutrients to the water bodies (Menció et al., 2011) (i.e. eutrophication), contributing to the balance of its global offtake. Phosphate fertilizers' production is mainly dependent on extraction of phosphorus from guano and apatite; and potassium (K) fertilizers are extracted from potash ore (Manning, 2015). As limited resources, the community should push towards the desired sustainable technologies, including recovery of nutrients from waste.

Anaerobic digestion is a well-established technology for the valorisation manure's organic content in form of biogas (Pintucci et al., 2016). Its supernatant is rich in nutrients (N, P, K) and other ions. Autotrophic nitrogen removal technologies (e. g. partial nitrification plus Anammox) are proposed as an economical process before being discharged to water bodies (Ruscalleda et al., 2010; Gabarró et al., 2014;). This creates a potential for new business opportunities for nutrient recovery as K-struvite ( $\text{MgKPO}_4 \cdot 6\text{H}_2\text{O}$ ) from this stream, in the context of circular economy.

K-struvite is an inorganic phosphate mineral that contains equimolar concentrations of magnesium ( $\text{Mg}^{2+}$ ), potassium ( $\text{K}^+$ ) and phosphate ( $\text{PO}_4^{3-}$ ). Its composition is similar to struvite ( $\text{MgNH}_4\text{PO}_4 \cdot 6\text{H}_2\text{O}$ ), but it contains the most limited macronutrient in soils (potassium) instead of nitrogen, and is also considered an efficient fertilizer (Fernández-Lozano et al., 1999; Xu et al., 2011, 2015). In spite of this, K-struvite has been hardly investigated, and mainly from synthetic urine (Wilsenach et al., 2007; Xu et al., 2011, 2012,

2015) or real urine (Sun et al., 2010). Only two studies (Zeng and Li, 2006; Bao et al., 2011), under our concern, introduced some formation of K-struvite from manure. Bao et al., 2011 focused on studying the optimal conditions to obtain a highly pure struvite crystal product from swine wastewater, and observed possible co-precipitation of K-struvite formation when pH increased from 9 to 11. Zeng and Li (2006) investigated nutrient recovery for simultaneous removal of P, N and K from digested cattle manure after a centrifugation process. As reported by several authors (Schuiling and Andrade, 1999; Wilsenach et al., 2007; Barat et al., 2009; Xu et al., 2011), they determined the competition between struvite and K-struvite formation, and concluded that K-struvite formation only occurs at low concentrations of ammonium, when the reactivity of K-struvite formation surpasses that of struvite (Zeng and Li, 2006). Therefore, in the present study, a combination of different technologies is used for manure treatment in the framework of an European project (ManureEcoMine, FP7/2007-2013; <http://www.manureecomine.ugent.be/>). The process flow allowed the recovery of energy (anaerobic digestion), ammonium sulphate (stripping unit), water (secondary N removal unit with partial nitrification plus Anammox) and struvite and/or K-struvite (crystallizer) (Pintucci et al., 2016). The present work paves the way for K-struvite recovery from manure by establishing a methodology to determine the suitable operational conditions (pH and temperature) to enhance its recovery. The theoretically operational conditions were established by modelling and experimentally adjusted with the ADOx manure (digested and centrifuged manure, after a partial nitrification plus Anammox process).

## 6.2 Experimental

### 6.2.1 Visual Minteq software

The freeware Visual Minteq software (<https://vminteq.lwr.kth.se/>) was used to determine the speciation, the solubility and the equilibrium between solid and dissolved phases in aqueous solutions. Minteq displays the saturation index (SI) of the possible compounds that can be formed (Eq 6. 1), which can be defined as:

$$SI = \log IAP - \log K_s \quad \text{Eq 6. 1}$$

where, IAP the Ion Activity Product, and  $K_s$  the temperature-corrected solubility constant.

If  $SI > 0$ , it means oversaturation for that product; if  $SI < 0$ , undersaturation; and if  $SI = 0$ , apparent equilibrium with respect to the solid.

### 6.2.2 Experimental procedure

Batch tests were carried out to determine the effect of pH on K-struvite formation. Ten tests at the fixed temperature of 38°C (assumed temperature of the mesophilic ADox manure) were performed in 1L beakers in triplicate, in which a range of pH from 9 - 12 was studied, using a 10% manure (ADox) solution to decrease the interferences due to the solid content in manure.  $K^+$  and  $PO_4^{3-}$  were adjusted (using KCl and  $Na_3PO_4 \cdot H_2O$ , respectively) to the concentrations of the real ADox manure (500 mg  $K^+ L^{-1}$ , 250 mg  $PO_4^{3-} L^{-1}$  and  $< 10$  mg  $NH_4^+ L^{-1}$ ), being the phosphate the limiting compound. Magnesium was dosed in excess to ensure the formation of K-struvite, in a Mg/P molar ratio around 2 (Tarragó et al., 2016).

## Chapter 6. Towards a methodology for recovering K-struvite from manure

Finally, the established operational conditions were evaluated using 0-10-50-100% solutions of the ADox manure to assess the viability of K-struvite recovery from manure. The physico-chemical characteristics of the solutions used are shown in Table 6. 1. The concentrations of magnesium, potassium and phosphate were adjusted to have similar concentrations in all the solutions used, whereas ammonium and calcium concentrations increased from 10-100% solution due to the presence of this compounds in the ADox manure.

**Table 6. 1** Physico-chemical characteristics of the ADox solutions used (0-10-50-100%). The results are presented as mean  $\pm$  standard deviation.

		<b>0% ADox solution (control)</b>	<b>10% ADox solution</b>	<b>50% ADox solution</b>	<b>100% ADox solution</b>
<b>pH</b>	<b>un. pH</b>	10.34 $\pm$ 0.02	10.35 $\pm$ 0.08	10.41 $\pm$ 0.09	10.32 $\pm$ 0.02
<b>Temperature</b>	<b>°C</b>	37.4 $\pm$ 1.2	38.4 $\pm$ 2.2	36.9 $\pm$ 0.6	36.8 $\pm$ 0.4
<b>Mg<sup>2+</sup></b>	<b>mg Mg<sup>2+</sup> L<sup>-1</sup></b>	160.2 $\pm$ 3.5	162.4 $\pm$ 5.6	161.1 $\pm$ 1.1	163.1 $\pm$ 1.7
<b>K<sup>+</sup></b>	<b>mg K<sup>+</sup> L<sup>-1</sup></b>	584.3 $\pm$ 30.2	572.3 $\pm$ 25.8	501.1 $\pm$ 3.3	609.2 $\pm$ 7.9
<b>PO<sub>4</sub><sup>3-</sup></b>	<b>mg PO<sub>4</sub><sup>3-</sup> L<sup>-1</sup></b>	294.6 $\pm$ 5.8	283.8 $\pm$ 9.7	298.7 $\pm$ 1.1	332.3 $\pm$ 4.8
<b>NH<sub>4</sub><sup>+</sup></b>	<b>mg NH<sub>4</sub><sup>+</sup> L<sup>-1</sup></b>	n.d.	1.3 $\pm$ 0.3	6.5 $\pm$ 0.4	10.7 $\pm$ 0.8
<b>Ca<sup>2+</sup></b>	<b>mg Ca<sup>2+</sup> L<sup>-1</sup></b>	n.d.	6.8 $\pm$ 0.8	64.6 $\pm$ 1.8	35.7 $\pm$ 3.0
<b>TSS</b>	<b>mg TSS L<sup>-1</sup></b>	3.5 $\pm$ 0.7	30 $\pm$ 2	293 $\pm$ 71	500 $\pm$ 40

### 6.2.3 Analytical methods

In all tests, pH was monitored and controlled by a control panel (Memograph; Endress+Hauser, RSG40) dosing NaOH 1M if needed, and temperature by a heat exchanger (Mettmert, WB22) at the desired temperature for the study. The concentrations of Mg<sup>2+</sup>, K<sup>+</sup>, PO<sub>4</sub><sup>3-</sup> and ammonium (NH<sub>4</sub><sup>+</sup>) in the liquid phase

were analyzed by Ion Chromatography (Dionex, IC5000) to determine the nutrient recovery efficiencies. The product recovered in all tests was characterized by X-ray diffraction analysis (X-ray Diffractometer, Bruker, D8 Advance) to determine the crystal structure, and optical microscopy (Nikon, Eclipse E2000) was used to determine the morphology and length of the crystals recovered. The amount of nutrient recovered ( $\text{mmols L}^{-1}$  treated) were calculated as the difference between the initial and the final concentration of each compound per unit of liquid volume treated.

### 6.3 Results and Discussion

#### 6.3.1 Theoretical approach

Figure 6. 1 presents the saturation index (SI) of K-struvite calculated by Visual Minteq software at different pHs values, ranging from pH 8 to 12, and temperatures, from 20°C to 50°C. In general, K-struvite formation was reinforced at both alkaline pHs and high temperatures, due to the pH dependence of orthophosphates. In all the temperatures simulated, the SI increased with the temperature, reaching a plateau at the highest pHs (pH 11-12), meaning that even by increasing the pH, K-struvite saturation did not increase.

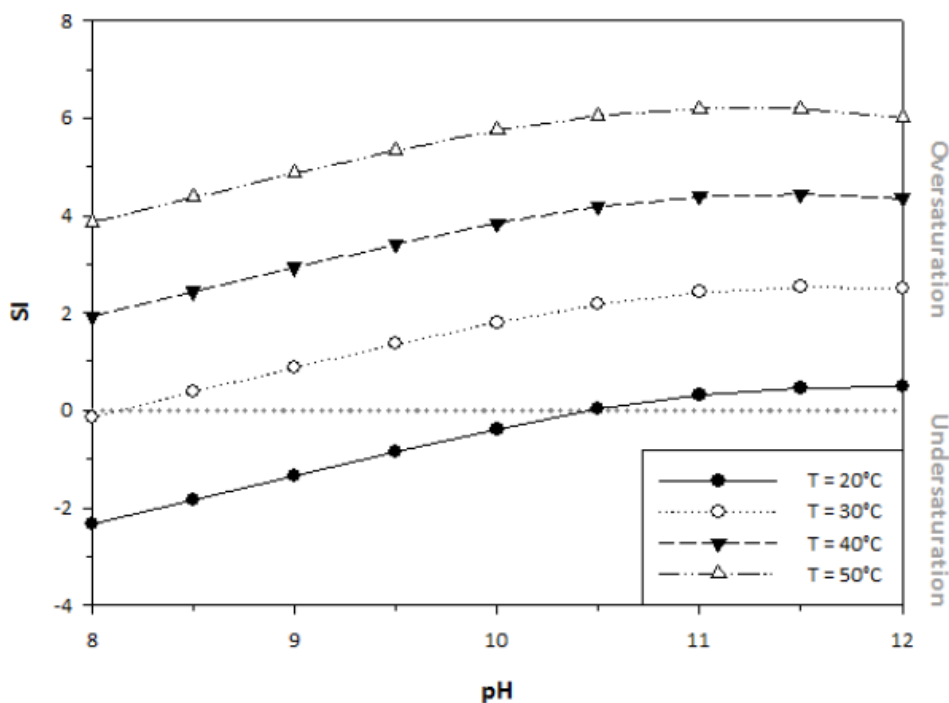


Figure 6. 1 Saturation Index (SI) of K-struvite as a function of pH, for a range of temperatures from 20°C to 50°C.

Considering the temperature of the ADox manure, the products that can be obtained at 38°C according to Visual Minteq software are presented in Table 6. 2. Minteq showed the SI of the different compounds (K-struvite, magnesium phosphate and magnesium hydroxide) as a function of the pH, in a pH range from 8-12. Even though SI can not quantify the amount of product precipitated, it is useful to determine which compounds (e.g. products) can precipitate under the specified conditions. The SI of K-struvite and magnesium phosphate ( $Mg_3(PO_4)_2$ ) increased with the pH up to pH 11, and then stabilized at pH 11-12. The SI of the magnesium hydroxide ( $Mg(OH)_2$ ) showed undersaturated conditions for  $pH < 10$ , and supersaturated conditions at  $pH > 10$ , increasing the SI with the increase of pH (direct correlation). Then, accordingly to the SI, the maximum K-struvite precipitation would be between

## Chapter 6. Towards a methodology for recovering K-struvite from manure

pH 10 and 11, but with the co-precipitation of other magnesium compounds ( $\text{Mg}_3(\text{PO}_4)_2$  and  $\text{Mg}(\text{OH})_2$ ).

Thus, Visual Minteq software suggested the possible compounds that could be formed at the assumed temperature of the influent for K-struvite recovery.

**Table 6. 2** SI of the three compounds that can be formed at 38°C, according to Visual Minteq software.

pH	SI of K-struvite	SI of $\text{Mg}_3(\text{PO}_4)_2$	SI of $\text{Mg}(\text{OH})_2$
8	1,528	0,206	-2,970
9	2,534	2,210	-0,977
10	3,450	4,002	0,984
11	4,005	4,878	2,750
12	4,001	4,270	4,103

### 6.3.2 pH effect on K-struvite formation

The operational conditions for K-struvite recovery were determined through batch tests, using a 10% manure (ADox) solution. A wide range of pHs, from 9-12, were studied in triplicate at 38°C. Figure 6. 2 presents the amount of nutrients recovered ( $\text{mmols L}^{-1}$  treated) for each pH studied. As K-struvite is composed of equimolar concentrations of  $\text{Mg}^{2+}$ ,  $\text{K}^+$  and  $\text{PO}_4^{3-}$ , the results showed an equimolar recovery of  $\text{K}^+$  and  $\text{PO}_4^{3-}$  between pH 9-9.5, indicating that K-struvite was formed, and recovering up to 60-80% of  $\text{PO}_4^{3-}$  in the form of K-struvite.

Furthermore, as the Mg/P molar ratio in the influent was 2, this resulted in the co-precipitation of magnesium phosphate and magnesium hydroxide.  $\text{Mg}_3(\text{PO}_4)_2$  was formed as demonstrated for the difference in the amount of P and K at  $\text{pH} > 9.5$ , and confirmed by the XRD results analysis of the products (Figure S6. 1).



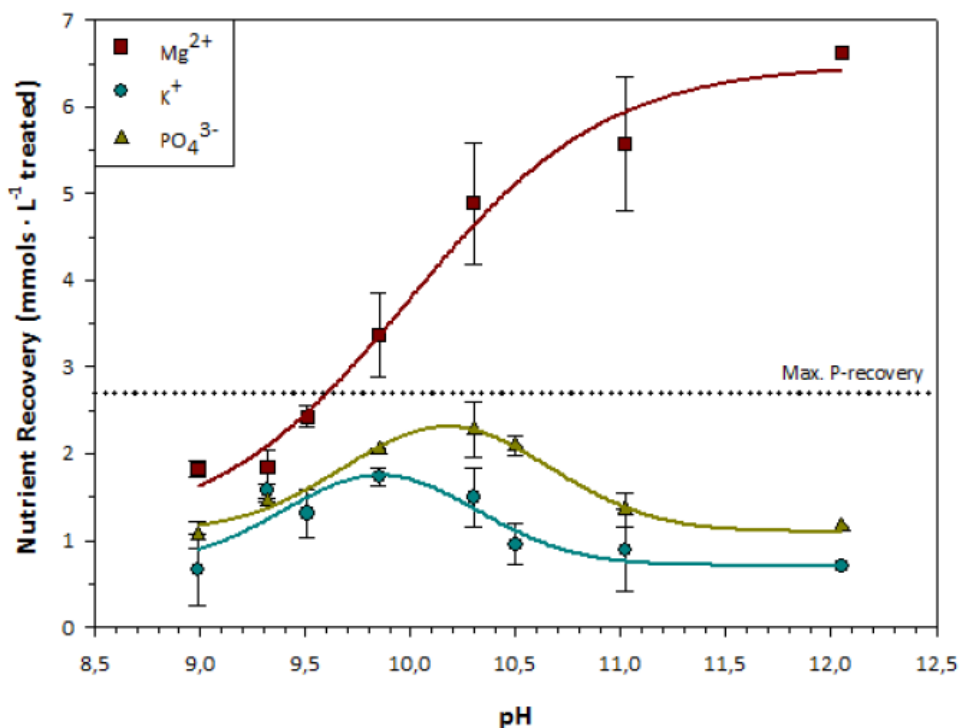
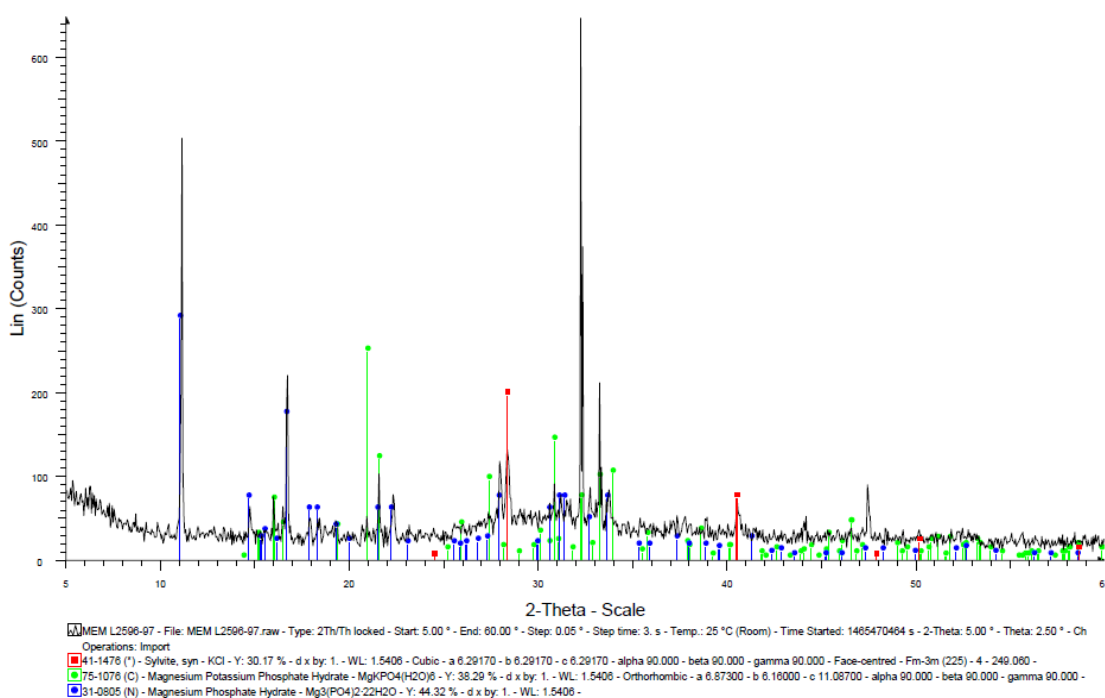


Figure 6. 2 Nutrient recoveries in mmols recovered per liter treated of the 10% ADOx manure solution, obtained during the batch tests performed in a range of pH from 9 to 12 to determine the effect of pH on K-struvite formation. Dot line represents the maximum P-recovery, assuming 100% P-recovery.

XRD analysis also showed the presence of potassium chloride due to the drying process of the product recovered. Values of pH higher than 10.5 favoured the formation of magnesium hydroxide over the formation of K-struvite, because the percentage of P-recovery decreased significantly, whereas the recovery of magnesium increased exponentially. Thus, the solution was oversaturated for magnesium hydroxide at pHs > 10.5, corroborated with Minteq software as higher saturation index (SI) for magnesium hydroxide were achieved. This is in concordance with Wilsenach et al., 2007 who found that PO<sub>4</sub><sup>3-</sup> removal efficiencies at room temperature (23-24°C) increased with alkaline pHs (7.4-

9.4). They found co-precipitation of struvite and K-struvite at pH 9 when synthetic urine was used. Xu et al., 2011 found that the optimum pH for  $\text{PO}_4^{3-}$  and  $\text{K}^+$  removal in synthetic urine was pH=10-11 (temperature not specified). In our study, the highest percentage of  $\text{PO}_4^{3-}$  and  $\text{K}^+$  recovered was at pH between 9.8-10.3 (pH around 10), which could concur with the results of Xu et al., 2011, despite the difference in the matrix of the solution used and the temperature.



**Figure S6. 1** XRD diffractogram of the product recovered at pH 10, during the batch tests carried out to determine the effect of pH on K-struvite formation. K-struvite is identified in green, magnesium phosphate in blue, potassium chloride in red and the background noise indicates an amorphous substance, most likely magnesium hydroxide (typically found as amorphous).

Therefore, pH control around 10 was found to be the optimal for K-struvite recovery at the temperature of 38°C, as higher K<sup>+</sup> recovery efficiencies were obtained in comparison to the other pHs studied, and the highest P-recovery (limited resource) was achieved, which together with K, both are essential nutrients for plants.

### 6.3.3 Influence of manure matrix on K-struvite formation

#### 6.3.3.1 Nutrient recovery efficiencies

Once the operational conditions were established, the influence of manure's matrix on nutrient recovery performance was tested in triplicate. Several solutions were used, containing 0% (synthetic), 10%, 50% and 100% of ADox manure to assess the viability of K-struvite recovery from manure. In Figure 6.3, the composition of the product recovered in each ADox solution studied is presented. The composition was determined through a balance of nutrient recovery efficiencies and accordingly to the stoichiometry of the products. In all the tests, the removal of K<sup>+</sup> was lower, indicating that all the K<sup>+</sup> recovered was in the form of K-struvite, corroborated with Minteq software. The rest of Mg<sup>+</sup> and PO<sub>4</sub><sup>3-</sup> could precipitate in other forms.

In the tests at 50-100% manure solution, the recovery of phosphate and potassium was equimolar, indicating that all the PO<sub>4</sub><sup>3-</sup> was recovered as K-struvite, and not as other phosphate precipitates; while during the tests at 0-10% manure solution, phosphate recovery was through the co-precipitation of K-struvite and Mg<sub>3</sub>(PO<sub>4</sub>)<sub>2</sub>, as more phosphate than potassium was recovered than the stoichiometrically for K-struvite formation.

In all the tests, Mg<sup>2+</sup> recovery was higher than PO<sub>4</sub><sup>3-</sup> and K<sup>+</sup> recovery, as there was an excess of Mg<sup>2+</sup> due to the Mg/P molar ratio in the influent, resulting in

the formation of  $Mg(OH)_2$  with the residual excess of magnesium. These results were in concordance with the XRD results of the products recovered in each test. As an example, XRD results of the product recovered when using 50-100% (Figure S6. 2) showed the presence of K-struvite and magnesium hydroxide, and some impurities (sodium chloride and potassium chloride) due to the drying process of the product recovered.

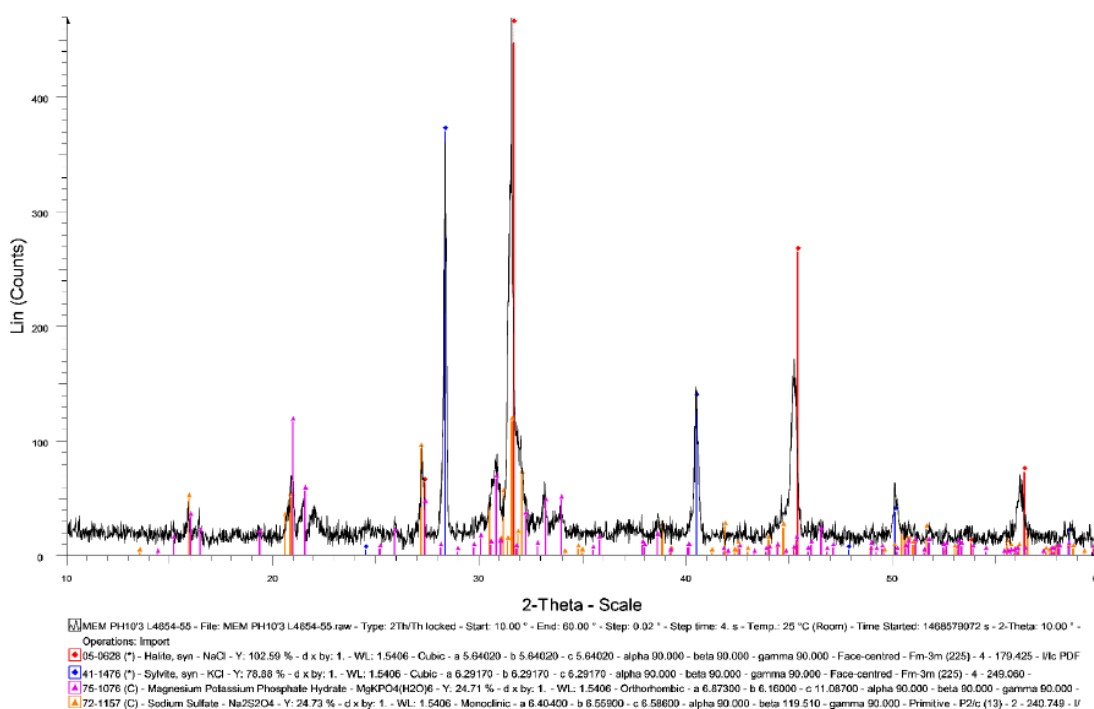


**Figure S6. 2** XRD diffractogram of the product recovered using a 100% manure solution, during the tests to determine the influence of manure’s matrix on nutrient recovery performance. K-struvite is identified in purple, sodium chloride in red, potassium chloride in blue, and the background noise indicates an amorphous substance, most likely magnesium hydroxide (typically found as amorphous).

## Chapter 6. Towards a methodology for recovering K-struvite from manure

The results obtained in this study are in accordance with Zeng and Li (2006). They observed low P-recoveries using anaerobically digested and centrifuged manure effluents, and related this to other parameters affecting the process, more likely, the complex matrix and the high suspended solids content. In our study, half of the phosphate was recovered at the 50-100% manure solutions ( $1.09 \pm 0.12$  mmols  $\text{PO}_4^{3-} \cdot \text{L}^{-1}$  treated) than at the 0-10% manure solution ( $2.24 \pm 0.06$  mmols  $\text{PO}_4^{3-} \cdot \text{L}^{-1}$  treated). Therefore, the decrease of the phosphate recovery efficiencies was related with the increase of solids in the feed solution. The ionic strength of the matrix could also have an effect on nutrient recovery efficiencies (e.g. P-recovery).

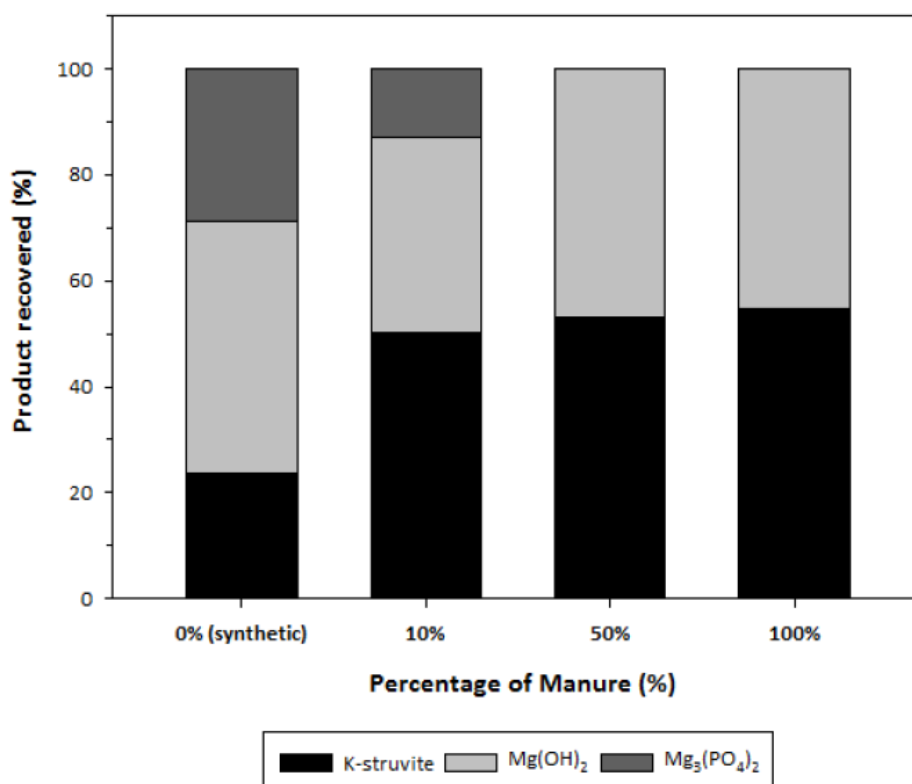


**Figure 6. 3** Composition of the product recovered, for each manure level tested, expressed in percentage of mmols per liter of feed solution.

### 6.3.3.2 Morphology of the crystals recovered

By using a solution with a higher content of manure, not only the nutrient recovery efficiencies were affected, but also the morphology of the crystals formed. At a low solid content (0-10% manure solution), individual needle-like crystals, typical form of K-struvite crystals (Graeser et al., 2008; Shih and Yan, 2016), were formed in the range of 50-100  $\mu\text{m}$  (Figure S6. 3). When the solid content increased, aggregation of the needle-like crystals formed took place, resulting in a star/asterisk form (Figure S6. 4 and Figure S6. 5), and crystal size was slightly increased to 100-200  $\mu\text{m}$  (50% and 100% manure solution, respectively). Thus, the influence of the matrix was evaluated, and the presence of suspended particles not only favored the nucleation phase, acting as the nuclei for heterogeneous nucleation (Liu et al., 2013), but also crystal growth. Suspended particles favored the formation of linking bonds between crystals, enhancing its aggregation and resulting in a change of the morphology.

As standard qualities for marketing K-struvite selling and its use as a fertilizer have not been yet established, the feasibility of the process in terms of quality of the product recovered will be up to the customers' requirements.

**Chapter 6. Towards a methodology for recovering K-struvite from manure**

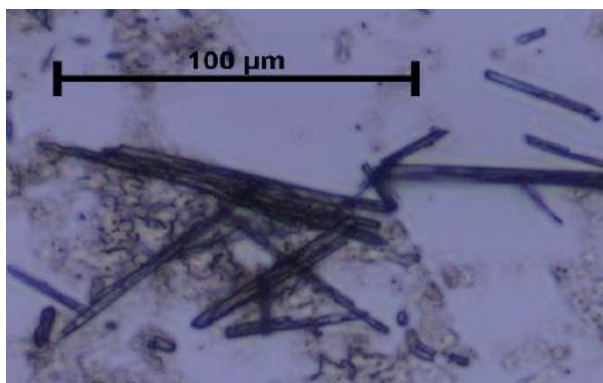


**Figure S6. 3** Images of crystals' morphology obtained through optic microscope observation (10x) for the test using 10% manure solution.

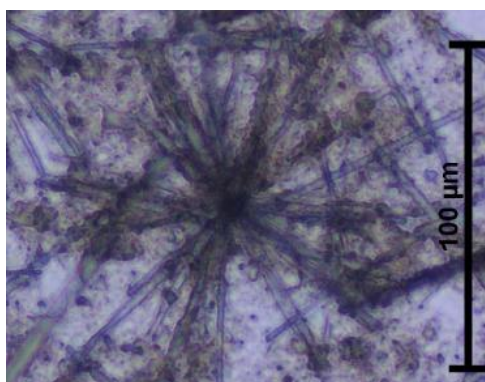


**Figure S6. 4** Images of crystals' morphology obtained through optic microscope observation (10x) for the test using 50% manure solution.

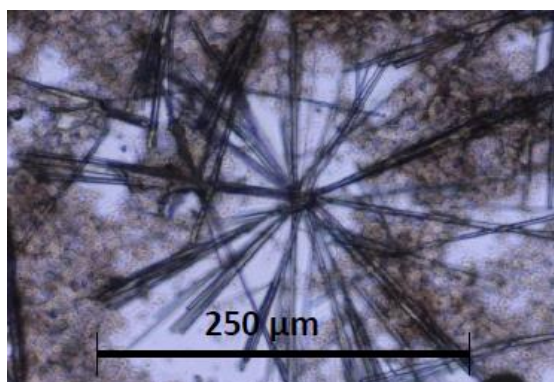


**Figure S6. 5** Images of crystals' morphology obtained through optic microscope observation (20x) for the test using 100% manure solution.

## 6.4 Conclusions

In conclusion, this study established and validated a methodology for K-struvite recovery from manure. The theoretical operational conditions were established by modelling and adjusted experimentally using batch tests at different fractions of manure. Temperature and pH were defined as key operational conditions in the recovery of potassium struvite. The best recovery performance was achieved at pH 10 and 38°C. The viability of the process was proved recovering K-struvite directly from digested manure after S/L separation and N removal through Anammox process to diminish the co-precipitation of struvite. Therefore, the results obtained so far opened the door to develop a sustainable technology for nutrient recovery from complex waste streams, such as manure.



## Chapter Seven

# General discussion

---

## 7.1 From waste to resource

Both the rising pressure on natural resources and the increasing environmental concerns stress the need for a paradigm shift in resource management towards greater resource efficiency (Sutton et al., 2012; European Commission, 2015 and 2016). This represents a key nexus point between economic, social, technological and environmental challenges.

In this sense, macronutrient recovery, especially phosphorus and potassium, from waste streams is considered to be a suitable option to assure at long-term the supply of nutrients. Nutrient recovery from manure can be through struvite and K-struvite crystallization, in which a valuable product can be obtained from a waste stream that needs to be treated to diminish its environmental impact.

## 7.2 The scope of this PhD thesis: ManureEcoMine project

In the framework of the EU FP7 ManureEcoMine project (Grant Agreement n°603744), an integrated approach to the treatment and reuse of manure was proposed, by combining different technologies and several process configurations. In this frame, the present study was focused on nutrient recovery from manure, by establishing the operational conditions for ammonium struvite and potassium struvite crystallization.

Swine manure was initially digested anaerobically to stabilize the organic matter and transform organic nitrogen into ammonium, and organic phosphorus into orthophosphate. Following, a stripping unit decreased the concentration/load of ammonium, and a centrifuge process separated the solid/liquid fraction.

ManureEcoMine considered two different scenarios for nutrient recovery from swine manure (Figure 1. 5 in Chapter 1):

- 1) Struvite recovery from the digested and centrifuged manure, and a polishing nitrogen removal step using a partial nitritation plus Anammox process.
- 2) K-struvite recovery from the ADox manure (digested and centrifuged manure, after a partial nitritation plus Anammox process).

In both scenarios, green fertilizers were obtained, which differed in the nutrient content: a fertilizer with magnesium, ammonium and phosphate (scenario 1, product: ammonium struvite), or a fertilizer with magnesium, potassium and phosphate (scenario 2, product: potassium struvite). Both products present good qualities to be used as fertilizers.

### **7.3 The up-flow velocity as the parameter to control particle size**

A crystallizer was designed in this PhD thesis not only to recover nutrients, but also to control the particle size of the resulting product. It consisted of an air-lift reactor plus a settler, for its versatility in operation and its capacity for crystals' retention (see section 3.1), having three different zones for different functions: the riser (the liquid-gas channel flow), the clarifier (a quiet zone to prevent particles' loss) and the collector (where particles settled). For the operational temperature of the influent (between 30-35°C), the optimal pH for struvite recovery was established at pH 8.5 (dosing NaOH 1M), as the highest P-recovery efficiencies were achieved. Magnesium was always the limiting compound in manure, and was overdosed in a  $Mg^{2+}/PO_4^{3-}$  molar ratio of 2-2.5, in agreement with other studies, which highlighted that a  $Mg^{2+}/PO_4^{3-}$  molar ratio higher than 1 was needed for struvite crystallization (Le Corre et al., 2005; Huchzermeier and Tao, 2012; Liu et al., 2013).

The designed crystallizer aimed to increase particle size, as the strategies used so far were reduced to the promotion of secondary nucleation (Mehta and Batstone, 2013; Wang et al., 2006), or to the increase of the reaction time (Suzuki et al., 2005).

A methodology to control the particle size of the product is of high interest, as particle size is an important characteristic in fertilizers, because the agronomic response, blending, storage, handling and application depend on it (Lu et al., 2012; UN Industrial Development Organization, 1998). Therefore, in Chapter 4, different up-flow velocities (ranging from 13.3 to 26.3 m·h<sup>-1</sup>) were studied using an influent solution that simulated digested manure after a solid/liquid separation. First, the theoretical equation was adapted to calculate the up-flow velocity of the crystallizer used, which allowed to determine the minimum crystal size that could be recovered during the study, establishing a direct correlation between the up-flow velocity and the crystal size recovered.

For each velocity, the minimum theoretical equivalent diameter (MTD) was determined (methodology based on Merchuk and Gluz, 1999), considering that particles smaller than the theoretical equivalent diameter remained in suspension, while bigger particles settled in the collector. This methodology was proven experimentally, as only bigger particles (from 112 µm to 244 µm) than the minimum theoretical equivalent diameter (from 85 µm to 108 µm) were recovered.

The results from the batch tests showed that the air-lift configuration allowed the recirculation of small particles into the riser, promoted heterogeneous nucleation and crystal growth due to the recirculation flow induced by the air-flow applied in the riser. Therefore, it was concluded that the up-flow velocity in the riser was directly correlated with the particle size of the struvite recovered, as the average diameter of the crystals recovered increased 46% (from 112.6 to 242.6 µm) by increasing the up-flow velocity from 13.3 to 26.3 m h<sup>-1</sup> (air-flow rate from 1 to 10 L min<sup>-1</sup>).

In literature, particles' up to 6.5 mm can be recovered (Fattah, 2004), but mainly using two strategies: either using seeding crystals and/or materials, or increasing the retention time. Ueno and Fujii (2001) recovered bigger particles (500-1000  $\mu\text{m}$  range) from dewatered filtrate from anaerobic sludge digestion, but using fines produced as seeding materials and at a retention time of 10 days (Table 7.1).

Only Soare et al., 2012 introduced the effect of the air-flow to the final crystal size, shape and quality. They tested different air-flow rates (from 1.6 to 13.3  $\text{L min}^{-1}$ ) and seeding loads (110-240  $\mu\text{m}$ ) in an air-lift reactor. They recovered bigger particles (around 500  $\mu\text{m}$ ) at the lowest air-flow rates (1.6-3.3  $\text{L min}^{-1}$ ), and smaller particles (around 400  $\mu\text{m}$ ) at the highest air-flow rates (6.6-13.3  $\text{L min}^{-1}$ ). The results obtained by Soare et al., 2012 are not in accordance with the results obtained in this PhD thesis, as high air-flow rates, so, up-flow velocities, led to the recovery of largest particles (242  $\mu\text{m}$ ), even without using the seeding method, and without affecting the quality of the product recovered. The explanation behind this difference can be due to: i) the seeding of struvite crystals, in Soare et al., 2012; and ii) the higher gas velocity achieved in this PhD thesis, because an upward liquid velocity in the riser higher than the particle swarm velocity allowed the recovery of bigger particles at the highest air-flow rates.

On the other hand, strategies to enhance crystal growth were also studied by operating the crystallizer in continuous mode (daily flow of  $99 \pm 1 \text{ L d}^{-1}$ ). The results obtained during the continuous mode tests demonstrated that the average crystal size increased in time, having a displacement of the particles' size ranges, and increasing the abundance of particles at the highest ranges (Table 7.1).

Particles up to 800-1000  $\mu\text{m}$  were recovered due to the continuous-mode operation, which promoted growth phase of the particles. The performance of the crystallizer in the present PhD thesis demonstrated that even at high up-flow velocities, high P-recovery efficiencies can be achieved (>95%), and an average particle size of 250  $\mu\text{m}$

(batch tests) or 314  $\mu\text{m}$  (continuous mode tests) can be recovered at low HRTs (3.5h) without seeding (Table 7.1).

Thus, the viability for the application of the technology was proved, as high P-recoveries were achieved, even when treating high flows (e.g. 100 L day<sup>-1</sup>), and crystals' growth phase was enhanced.

In comparison with other studies in similar crystallizers, smaller particles in a range of 90-150  $\mu\text{m}$  were recovered from WWTP's digested sludge by Stumpf et al., 2008, and particles around 600  $\mu\text{m}$  were recovered from a synthetic saturated solution by Soare et al., 2012 as seeding of 110  $\mu\text{m}$  was used to enhance crystal growth. The same methodology was used by Ueno and Fujii, 2001, recovering particles in a range of 500-1000  $\mu\text{m}$  from dewatered filtrate from anaerobic digestion in a FBR.

The results obtained were outstanding and proved the viability to control particle size using the up-flow velocity as a control parameter, as similar particles sizes were recovered when compared with other studies that promoted secondary nucleation by seeding with already formed crystals. Thus, due to the design of the crystallizer and the operational conditions applied, particle size could be controlled adjusting the up-flow velocity in the riser.

Therefore, the results allowed to establish that particle size can be adjusted to customers' requirements for fertilizer application, either obtaining bigger and more homogeneous size of particles at higher up-flow velocities, or obtaining smaller and more heterogeneous size of particles at lower up-flow velocities.

**Table 7. 1** Comparison between performances of the designed crystallizer and similar reactors available in the literature cited. Adapted from Chapter 4 (Table 4.3)

References	Feedstock	Technology type	HRT	P-recovery efficiency (%)	Seeding	Product recovered	Mean particle size recovered ( $\mu\text{m}$ )
<b>Present study</b>	Synthetic WW (WWTP's effluent as media) to simulate digested manure after a S/L separation	Air-lift reactor combined with a settler	3.5 h	> 95%	No	Struvite	Batch: 112.6-242.6 $\mu\text{m}$ Continuous: 314 $\mu\text{m}$
<b>Bergmans, 2011</b>	WWTP's digested sludge	Batch tests in a short-long column	n.d.	70-90%	No	Assumed to be struvite	n.d.
<b>Cerrillo et al., 2015</b>	Synthetic solution for batch tests, and centrifuged digested pig slurry for continuous essays	20L-reactor with a reaction and a settling zone	20 h	> 95% in batch tests (n.d. for continuous essays)	No	Struvite, hydroxyapatite, dolomite, and calcite	Batch: 23-80 $\mu\text{m}$ Continuous: 20-25 $\mu\text{m}$
<b>Martí et al., 2010</b>	Rejected liquors of different strategies of the sludge treatment line	Stirred tank reactor (continuous mode for the liquid phase, batchwise mode for the solid phase)	2.5 h (reaction zone)	70-90%	No	Struvite and calcium phosphates	n.d.
<b>Soare et al., 2012</b>	Synthetic saturated solution	Air-lift crystallizer (batch tests)	n.d.	n.d.	Yes (110 $\mu\text{m}$ of average seed)	n.d.	400-600 $\mu\text{m}$
<b>Stumpf et al., 2008</b>	WWTP's digested sludge	Batch tests and Air-lift pilot reactor	n.d.	Batch: 85% Air-lift: 58-90%	No	85-90% of the P was recovered as struvite	90-150 $\mu\text{m}$
<b>Ueno and Fujii, 2001</b>	Dewatered filtrate from anaerobic digestion	FBR	10 d	90%	Yes	Struvite and magnesium phosphates	500-1000 $\mu\text{m}$

## 7.4 Influence of suspended solids present in the feedstock matrix on the quality of the product recovered

The high solid content in the manure has been identified as one of the main challenges for struvite recovery from digested manure, and many authors stated a threshold concentration of  $1000 \text{ mg TSS}\cdot\text{L}^{-1}$  (Schuiling and Andrade, 1999; Barnes et al., 2007; Desmidt et al., 2013; Liu et al., 2013). In this context, the role of suspended solids in struvite nucleation and growth were studied in Chapter 5, and the quality of the product recovered was evaluated.

Solutions of 0% (control), 20% and 50% digestate ( $910 \pm 23 \text{ mg TSS}\cdot\text{L}^{-1}$  and  $2753 \pm 91 \text{ mg TSS}\cdot\text{L}^{-1}$ , respectively) were used to study the effect of solids on struvite formation. In all tests, high P-recovery efficiencies were achieved (higher than 90%), confirming the efficiency of the system for P-recovery was not affected by the digestate matrix. XRD analysis confirmed that struvite was the only crystal in the product recovered. Moreover, the product redissolution showed that struvite was the main compound in the product recovered in all the solutions tested, being the only compound when using the 20-50% digestate influent; whereas in the control solution, there was also the presence of  $\text{Mg}_3(\text{PO}_4)_2$ . However, there was a fraction of the product not identified (24-28%, respectively), and mainly related to the suspended solids in the influent used. Many researchers have established that the solids and the organic matter present in the struvite recovered was a restriction for struvite application as a fertilizer (Uysal et al., 2010; Münch and Barr, 2001; Liu et al., 2011; Rahman et al., 2014). On the contrary, Palm et al., 1997 highlighted the importance of the presence of organic matter in the fertilizer applied, as it could contribute positively to its fertilizing effects, and contribute to soil amendment. Thus, the product recovered would be of interest in poor soils, as it would supply nutrients and stabilized organic matter, due to the use of digested manure.



The average particle size of the product recovered was monitored over time, and allowed to determine that bigger particles were formed in synthetic tests ( $204 \pm 19 \mu\text{m}$ ) rather than with digestate tests ( $99 \pm 6 \mu\text{m}$  -  $133 \pm 8 \mu\text{m}$ ). Desmidt et al., 2013 suggested that the increase of nucleation sites at high VSS concentrations favored heterogeneous nucleation instead of crystal growth, having a competition between these phases. This phenomenon was observed in the microscope images (Figure 5. 5 in Chapter 5), as the presence of small nuclei indicated that nucleation perpetuated in time. This is also in agreement with Ping et al., 2016, who proved that the increase of total suspended particles (in the range of  $116\text{-}194 \text{ mg}\cdot\text{L}^{-1}$ ) reduced struvite particles' size by half, and established that concentrations of TSS higher than  $153 \text{ mg}\cdot\text{L}^{-1}$  were strongly negative to the crystallizer operation and pellet growth. In the present work, smaller particles were also recovered when the concentration of solids in the influent increased, although our results further support the viability of struvite recovery at high solids' concentration in the influent ( $910\text{-}2753 \text{ mg TSS}\cdot\text{L}^{-1}$ ).

In addition, solid particles favored the agglomeration of already formed crystals into a crystal net, acting as links between formed struvite crystals, thus, having a larger crystalline structure. These results are not in agreement with Capdevielle et al., 2016, and Desmidt et al., 2013. Capdevielle et al., 2016 observed a few or no agglomeration of crystals in biologically treated swine wastewater (around  $3500 \text{ mg VSS L}^{-1}$ ), and stated that the viscosity induced by the colloidal particles, which also slowed down the reaction kinetics, did not allow the agglomeration of particles; and Desmidt et al., 2013 stated that struvite crystals could only agglomerate at low sludge concentrations (around  $1000 \text{ mg VSS}\cdot\text{L}^{-1}$ ) and not at higher (around  $6000 \text{ mg VSS L}^{-1}$ ). Our results showed that the agglomeration of struvite crystals was possible at higher VSS concentration in the influent used.

The results obtained proved the struvite recovery from digested manure even at high solids concentration ( $2753 \pm 778 \text{ mg TSS L}^{-1}$ ). This demonstrated that solid particles not only did not inhibit struvite formation, but acted as nuclei enhancing heterogeneous nucleation.

## 7.5 Potassium: the third essential macronutrient

Potassium struvite contains the most limited macronutrient in soils (potassium) instead of nitrogen, and is considered an efficient fertilizer (Fernández-Lozano et al., 1999; Xu et al., 2015, 2011). Despite its potential use, little is known, and mainly tested in synthetic urine (Wilsenach et al., 2007; Xu et al., 2015, 2012, 2011) and real urine (Sun et al., 2010).

This PhD thesis aimed to establish a methodology for K-struvite recovery from manure (Chapter 6). The theoretical operational conditions were firstly determined by the freeware Visual Minteq software. The theoretical approach showed that higher temperatures favored potassium struvite crystallization. This represents a technical/economic advantage because the supernatant from the AD can already reach the average temperature of  $38^{\circ}\text{C}$ . Opposite to struvite formation, as Le Corre et al., 2009 stated that high temperatures difficult ammonium struvite formation and affect the size and shape of struvite crystals. According to the theoretical approach from Minteq software, K-struvite would not be the only product formed at  $38^{\circ}\text{C}$ , but also  $\text{Mg}_3(\text{PO}_4)_2$  and  $\text{Mg}(\text{OH})_2$ . The theoretical maximum recovery of K-struvite could be between pH 10 and 11. The experimental tests carried out with a 10% manure solution in a range of pH from 9 to 12, showed that higher pHs favored the formation of magnesium hydroxide versus the formation of K-struvite, and the highest percentage of  $\text{PO}_4^{3-}$  and  $\text{K}^+$  recovered was at pH between 9.8-10.3 (pH around 10). These results were in agreement with Xu et al., 2011, which determined that pH 10-

11 was the optimal for  $\text{PO}_4^{3-}$  and  $\text{K}^+$  removal in synthetic urine. Having established pH around 10 as the optimal for K-struvite recovery at 38°C, the influence of manure's matrix on nutrient recovery performance was tested using a 0% (control), 10%, 50% and 100% of ADox manure solution. The results regarding the recovery efficiencies and the redissolution of the product formed, showed that the  $\text{PO}_4^{3-}$  was recovered as K-struvite in the 50-100% ADox manure solution tests, whereas co-precipitation of K-struvite and  $\text{Mg}_3(\text{PO}_4)_2$  was detected in the 0-10% tests. Despite the differences in the products recovered, in all tests magnesium was also recovered as  $\text{Mg}(\text{OH})_2$ , as  $\text{Mg}^{2+}$  was overdosed to achieve a Mg/P molar ratio in the solution used around 2. However, the P-recovery efficiency decreased slightly with the increase of solids, indicating that the solid content in the solutions used could have an effect on the efficiency of the system, reducing the amount of product formed but recovering all the phosphate as K-struvite. Low recovery efficiencies were also observed by Zeng and Li, 2006, and related this to the complex matrix and the high suspended solids content.

Not only was the product recovered affected by the percentage of solids in the solution used, but also the morphology of the crystals recovered. Low percentage of manure induced the presence of individual needle-like crystals of 50-100  $\mu\text{m}$ , which is the typical form of K-struvite crystals, as stated by Graeser et al., 2008 and Shih and Yan, 2016. Interestingly, higher percentages of manure induced the aggregation of the needle-like crystals, resulting in a star/asterisk form, and crystal size was slightly increased to 100-200  $\mu\text{m}$ . Therefore, the results showed the same tendency of solids acting as linking bonds between crystals. The evaluation of the quality of the product recovered was of great interest. However, further reviews on the legislation are needed in order to contribute to a potential market for fertilizers recovered from waste streams, which would be in accordance to the new European policies that promote nutrient recovery.



## Chapter Eight

# Conclusions

---

Swine manure represents a “mining” opportunity for nutrient recovery. Struvite and K-struvite can be recovered from manure, and applied into the soil as excellent slow-release fertilizers.

This PhD thesis brings innovation and insights on the recovery of essential macronutrients (potassium, phosphorus and nitrogen) from swine manure.

The main conclusions could be summarized as follows:

- The particle size of struvite could be controlled by the up-flow velocity applied in the riser of the crystallizer, without affecting the system performance. The up-flow velocity in the riser was directly correlated with the particle size of the struvite recovered, as the average diameter of the crystals increased from 112.6 to 242.6  $\mu\text{m}$  (46%) by increasing the up-flow velocity from 13.3 to 26.3  $\text{m}\cdot\text{h}^{-1}$  (air-flow rate from 1 to 10  $\text{L}\cdot\text{min}^{-1}$ ).
- The up-flow velocity could be easily modified with the air-flow rate applied to the crystallizer. The up-flow velocity was proven as a useful and manageable tool for controlling particle size to customers’ requirements and achieve the desired size of particles for its agronomic purpose.
- The viability of controlling struvite particles’ size by the up-flow velocity, without using other methodologies to increase particle size other than the hydrodynamics of the designed crystallizer is proven.
- Ammonium struvite was recovered from swine manure, even at high solid concentrations in the influent. The increase of solid concentration from synthetic to 50% digestate solution led to the recovery of smaller crystals (from 204  $\mu\text{m}$  to 133  $\mu\text{m}$ ), as solid particles acted as nuclei for

heterogeneous nucleation, even at high TSS concentration in the influent (2753 mg TSS·L<sup>-1</sup>).

Not only evidences of heterogeneous nucleation were presented, but also a demonstration that solid particles acted as linking bonds between crystals favoring its aggregation and agglomeration.

- This PhD thesis represents the first proof-of-concept of K-struvite recovery from manure, and allowed to define temperature and pH as key operational conditions for its recovery. The results obtained so far opened the door to develop a sustainable technology for K-struvite recovery from digested manure after a S/L separation and a N removal through Anammox process to diminish the co-precipitation of struvite.

Therefore, a step forward to nutrient recovery from a complex waste stream was achieved. An evaluation of the quality of the product recovered was carried out. The results obtained exposed the need for further reviews on the legislation, which should distinguish between the future application of the fertilizer. For example, the limits of the emerging pollutants (veterinary drugs and heavy metals) should be specific for the type of plant to be fertilized (crops, ornamentals, vegetables, flower boards, garden grass, amongst others) and the location of these plants (soil and environmental conditions). The revision of the EU legislation must be in accordance to contribute to a potential market for fertilizers recovered from waste streams, which would be in accordance to the new European policies promoting nutrient recovery.





# Chapter Nine

## References

---

- Ahmed, S., Klassen, T.N., Keyes, S., Daly, M., Jones, D.L., Mavrogordato, M., Sinclair, I., Roose, T., 2016. Imaging the interaction of roots and phosphate fertiliser granules using 4D X-ray tomography. *Plant Soil* 401, 125–134. doi:10.1007/s11104-015-2425-5
- Ali, M.I., Schneider, P.A., 2008. An approach of estimating struvite growth kinetic incorporating thermodynamic and solution chemistry, kinetic and process description. *Chem. Eng. Sci.* 63, 3514–3525. doi:10.1016/j.ces.2008.04.023
- American Public Health Association, 2005. *Standard Methods for the Examination of Water and Wastewater*, 19th ed. Washington, DC, USA.
- APHA, 2005. *Standard Methods for the Examination of Water and Wastewater*, 19th ed. American Public Health Association, Washington, DC, USA.
- Bao, X.-D., Ye, Z.-L., Ma, J.-H., Chen, S.-H., Lin, L.-F., Yan, Y.-J., 2011. Effect of pH on precipitate composition during phosphorus recovery as struvite from swine wastewater. *Environ. Sci.* 32, 2598–2603.
- Barat, R., Bouzas, A., Martí, N., Ferrer, J., Seco, A., 2009. Precipitation assessment in wastewater treatment plants operated for biological nutrient removal : A case study in Murcia , Spain. *J. Environ. Manage.* 90, 850–857. doi:10.1016/j.jenvman.2008.02.001
- Barnes, D., Li, X., Chen, J., 2007. Determination of suitable pretreatment method for old-intermediate landfill leachate. *Environ. Technol.* 28, 195–203. doi:10.1080/09593332808618782
- Bateman, A., van der Horst, D., Boardman, D., Kansal, A., Carliell-Marquet, C., 2011. Closing the phosphorus loop in England: The spatio-temporal balance of phosphorus capture from manure versus crop demand for fertiliser. *Resour. Conserv. Recycl.* 55, 1146–1153. doi:10.1016/j.resconrec.2011.07.004
- Beegle, D.B., 1985. Comparing fertilizer materials. Penn State Extension, Agron. Facts 6.
- Bergmans, B., 2011. Struvite recovery from digested sludge. Delft University of Technology.
- Bhuiyan, M.I.H., Mavinic, D.S., Beckie, R.D., 2008. Nucleation and growth kinetics of struvite in a fluidized bed reactor. *J. Cryst. Growth* 310, 1187–1194. doi:10.1016/j.jcrysgro.2007.12.054

- Bouropoulos, N.C., Koutsoukos, P.G., 2000. Spontaneous precipitation of struvite from aqueous solutions. *J. Cryst. Growth* 213, 381–388.
- Capdevielle, A., Sýkorová, E., Béline, F., Daumer, M.-L., 2016. Effects of organic matter on crystallization of struvite in biologically treated swine wastewater. *Environ. Technol.* 37, 880–892. doi:10.1080/09593330.2015.1088580
- Capdevielle, A., Sýkorová, E., Biscans, B., Béline, F., Daumer, M.-L., 2013. Optimization of struvite precipitation in synthetic biologically treated swine wastewater - Determination of the optimal process parameters. *J. Hazard. Mater.* 244–245, 357–369. doi:10.1016/j.jhazmat.2012.11.054
- Cerrillo, M., Palatsi, J., Comas, J., Vicens, J., Bonmatí, A., 2015. Struvite precipitation as a technology to be integrated in a manure anaerobic digestion treatment plant - removal efficiency, crystal characterization and agricultural assessment. *J. Chem. Technol. Biotechnol.* 90, 1135–1143. doi:10.1002/jctb.4459
- Chisti, Y., Moo-Young, M., 1988. Prediction of liquid circulation velocity in airlift reactors with biological media. *J. Chem. Technol. Biotechnol.* 42, 211–219. doi:10.1002/jctb.280420305
- Cordell, D., Drangert, J.-O., White, S., 2009. The story of phosphorus: global food security and food for thought. *Glob. Environ. Chang.* 19, 292–305. doi:10.1016/j.gloenvcha.2008.10.009
- Crutchik, D., 2015. Strategies for phosphorus recovery from wastewater by struvite crystallization. Universidade de Santiago de Compostela.
- Crutchik, D., Garrido, J.M., 2011. Struvite crystallization versus amorphous magnesium and calcium phosphate precipitation during the treatment of a saline industrial wastewater. *Water Sci. Technol.* 64, 2460–2467. doi:10.2166/wst.2011.836
- Davies, C.W., 1962. *Ion Association*. Washington, D. C. doi:10.1126/science.143.3601.37
- De-Bashan, L.E., Bashan, Y., 2004. Recent advances in removing phosphorus from wastewater and its future use as fertilizer (1997-2003). *Water Res.* 38, 4222–46. doi:10.1016/j.watres.2004.07.014
- Desmidt, E., Ghyselbrecht, K., Monballiu, A., Rabaey, K., Verstraete, W., Meesschaert, B.D., 2013. Factors influencing urease driven struvite precipitation. *Sep. Purif. Technol.* 110, 150–157. doi:10.1016/j.seppur.2013.03.010

- Doyle, J.D., Parsons, S.A., 2002. Struvite formation, control and recovery. *Water Res.* 36, 3925–3940.
- El Diwani, G., El Rafie, S., El Ibiari, N.N., El-Aila, H.I., 2007. Recovery of ammonia nitrogen from industrial wastewater treatment as struvite slow releasing fertilizer. *Desalination* 214, 200–214. doi:10.1016/j.desal.2006.08.019
- ESPP, 2017. SCOPE Newsletter 124. *Scope Newsl.* 29.
- ESPP, 2016. SCOPE Newsletter 118. *Scope Newsl.* 28.
- ESPP, 2015. SCOPE Newsletter 111. *Scope Newsl.* 22.
- ESPP, 2014. *Scope Newsletter* 101. *Scope Newsl.* 1–22.
- Etter, B., Tilley, E., Khadka, R., Udert, K.M., 2011. Low-cost struvite production using source-separated urine in Nepal. *Water Res.* 45, 852–862. doi:10.1016/j.watres.2010.10.007
- European Commission, 2016. Circular Economy Package proposal for a Regulation of the European Parliament and of the Council (COM(2016) 157 final) laying down rules on the making available on the market of CE marked fertilising products and amending Regulations (EC) N°1069/2009 and .
- European Commission, 2015. Closing the loop - An EU action plan for the Circular Economy. Commun. from Comm. to Eur. Parliam. Counc. Eur. Econ. Soc. Comm. Comm. Reg. COM(2015) 614 Final. doi:10.1017/CBO9781107415324.004
- Fattah, K.P., 2004. Pilot scale struvite recovery potential from centrate at Lulu Island Wastewater Treatment Plant. Univ. of British Columbia, Vancouver, Canada.
- Fattah, K.P., Mavinic, D.S., Koch, F.A., 2012. Influence of process parameters on the characteristics of struvite pellets. *J. Environ. Eng.* 138, 1200–1209. doi:10.1061/(ASCE)EE.1943-7870.0000576.
- Fernández-Lozano, J.A., Colmenares, A.R., Rosas, D., 1999. A novel process for the production of multinutrient phosphatic base fertilizers from seawater bittern and phosphoric acid. *Interciencia* 24, 317–320.
- Foged, H.L., Flotats, X., Bonmatí, A., Palatsi, J., Magri, A., Schelde, K.M., 2001. Inventory of manure processing activities in Europe.

- Gabarró, J., González-Cárcamo, P., Rusalleda, M., Ganigué, R., Gich, F., Balaguer, M.D., Colprim, J., 2014. Anoxic phases are the main N<sub>2</sub>O contributor in partial nitrification reactors treating high nitrogen loads with alternate aeration. *Bioresour. Technol.* 163, 92–99. doi:10.1016/j.biortech.2014.04.019
- Gaterell, M.R., Gay, R., Wilson, R., Gochin, R.J., Lester, J.N., 2000. An economic and environmental evaluation of the opportunities for substituting phosphorus recovered from wastewater treatment works in existing UK fertiliser markets. *Environ. Technol.* 21, 1067–1084.
- Graeser, S., Postl, W., Bojar, H.-P., Berlepsch, P., Armbruster, T., Raber, T., Ettinger, K., Walter, F., 2008. Struvite-(K), KMgPO<sub>4</sub>·6H<sub>2</sub>O, the potassium equivalent of struvite – a new mineral. *Eur. J. Mineral.* 20, 629–633. doi:10.1127/0935-1221/2008/0020-1810
- Hanhoun, M., Montastruc, L., Azzaro-Pantel, C., Biscans, B., Frèche, M., Pibouleau, L., 2011. Temperature impact assessment on struvite solubility product: A thermodynamic modeling approach. *Chem. Eng. J.* 167, 50–58. doi:10.1016/j.cej.2010.12.001
- Harris, W.G., Wilkie, A.C., Cao, X., Sirengo, R., 2008. Bench-scale recovery of phosphorus from flushed dairy manure wastewater. *Bioresour. Technol.* 99, 3036–3043. doi:10.1016/j.biortech.2007.06.065
- Hauber, R.J., Boydston, G.D., Frailey, N., Lamberet, S., Pattarkine, G. V., Cherian, I.K., Centurione, S., Ghosh, A., 2017. Struvite-K and syngenite composition for use in building materials. US patent n° 20170008804 A1.
- Huchzermeier, M.P., Tao, W., 2012. Overcoming challenges to struvite recovery from anaerobically digested dairy manure. *Water Environ. Res.* 84, 34–41. doi:10.2175/106143011X13183708018887
- Hwang, H.-J., Choi, E., 1998. Nutrient control with other sludges in anaerobic digestion of BPR sludge. *Water Sci. Technol.* 38, 295–302. doi:10.1016/S0273
- Jin, Y., Hu, Z., Wen, Z., 2009. Enhancing anaerobic digestibility and phosphorus recovery of dairy manure through microwave-based thermochemical pretreatment. *Water Res.* 43, 3493–3502. doi:10.1016/j.watres.2009.05.017

- Johnston, A.E., Richards, I.R., 2003. Effectiveness of different precipitated phosphates as phosphorus sources for plants. *Soil Use Manag.* 19, 45–49. doi:10.1079/SUM2002162
- Jones, A.G., 2002. *Crystallization process systems*. Butterworth/Heinemann, Oxford, Great Britain. doi:10.1016/B978-075065520-0/50007-9
- Kabdaşlı, I., Parsons, S.A., Tünay, O., 2006. Effect of major ions on induction time of struvite precipitation. *Croat. Chem. Acta* 79, 243–251.
- Kim, D., Ryu, H.-D., Kim, M.-S., Kim, J., Lee, S.-I., 2007. Enhancing struvite precipitation potential for ammonia nitrogen removal in municipal landfill leachate. *J. Hazard. Mater.* 146, 81–85. doi:10.1016/j.jhazmat.2006.11.054
- Kofina, A.N., Koutsoukos, P.G., 2005. Spontaneous precipitation of struvite from synthetic wastewater solutions. *Cryst. Growth Des.* 5, 489–496. doi:10.1021/cg049803e
- Korchef, A., Saidou, H., Ben Amor, M., 2011. Phosphate recovery through struvite precipitation by CO<sub>2</sub> removal: Effect of magnesium, phosphate and ammonium concentrations. *J. Hazard. Mater.* 186, 602–613. doi:10.1016/j.jhazmat.2010.11.045
- Le Corre, K.S., Valsami-Jones, E., Hobbs, P., Parsons, S.A., 2009. Phosphorus recovery from wastewater by struvite crystallization: A review. *Crit. Rev. Environ. Sci. Technol.* 39, 433–477. doi:10.1504/IJSTL.2015.069123
- Le Corre, K.S., Valsami-Jones, E., Hobbs, P., Parsons, S.A., 2005. Impact of calcium on struvite crystal size, shape and purity. *J. Cryst. Growth* 283, 514–522.
- Liu, Y., Kumar, S., Kwag, J.-H., Kim, J., Kim, J., Ra, C., 2011a. Recycle of electrolytically dissolved struvite as an alternative to enhance phosphate and nitrogen recovery from swine wastewater. *J. Hazard. Mater.* 195, 175–181. doi:10.1016/j.jhazmat.2011.08.022
- Liu, Y., Kumar, S., Kwag, J.-H., Ra, C., 2013. Magnesium ammonium phosphate formation, recovery and its application as valuable resources: a review. *J. Chem. Technol. Biotechnol.* 88, 181–189. doi:10.1002/jctb.3936
- Liu, Y., Kwag, J.-H., Kim, J.-H., Ra, C., 2011b. Recovery of nitrogen and phosphorus by struvite crystallization from swine wastewater. *Desalination* 277, 364–369. doi:10.1016/j.desal.2011.04.056

- Liu, Y., Rahman, M.M., Kwag, J.-H., Kim, J.-H., Ra, C., 2011c. Eco-friendly production of maize using struvite recovered from swine wastewater as a sustainable fertilizer source. *Asian-Australasian J. Anim. Sci.* 24, 1699–1705. doi:10.5713/ajas.2011.11107
- Liu, Z., Zhao, Q., Lee, D.-J., Yang, N., 2008. Enhancing phosphorus recovery by a new internal recycle seeding MAP reactor. *Bioresour. Technol.* 99, 6488–6493. doi:10.1016/j.biortech.2007.11.039
- Lu, Q., He, Z.L., Stoffella, P.J., 2012. Land application of biosolids in the USA: A review. *Appl. Environ. Soil Sci.* 2012. doi:10.1155/2012/201462
- Manning, D.A.C., 2015. How will minerals feed the world in 2050? *Proc. Geol. Assoc.* 126, 14–17. doi:10.1016/j.pgeola.2014.12.005
- Martí, N., Bouzas, A., Seco, A., Ferrer, J., 2008. Struvite precipitation assessment in anaerobic digestion processes. *Chem. Eng. J.* 141, 67–74. doi:10.1016/j.cej.2007.10.023
- Martí, N., Pastor, L., Bouzas, A., Ferrer, J., Seco, A., 2010. Phosphorus recovery by struvite crystallization in WWTPs: influence of the sludge treatment line operation. *Water Res.* 44, 2371–2379. doi:10.1016/j.watres.2009.12.043
- Mehta, C.M., Batstone, D.J., 2013. Nucleation and growth kinetics of struvite crystallization. *Water Res.* 47, 2890–2900. doi:10.1016/j.watres.2013.03.007
- Menció, A., Boy, M., Mas-Pla, J., 2011. Analysis of vulnerability factors that control nitrate occurrence in natural springs (Osona Region, NE Spain). *Sci. Total Environ.* 409, 3049–3058. doi:10.1016/j.scitotenv.2011.04.048
- Merchuk, J.C., Gluz, M., 1999. Airlift reactors, in: *Encyclopedia of Bioprocess Technology*. John Wiley & Sons, New York, pp. 320–353.
- Moerman, W., Carballa, M., Vandekerckhove, A., Derycke, D., Verstraete, W., 2009. Phosphate removal in agro-industry: Pilot- and full-scale operational considerations of struvite crystallization. *Water Res.* 43, 1887–1892.
- Morales, N., Boehler, M.A., Buettner, S., Liebi, C., Siegrist, H., 2013. Recovery of N and P from urine by struvite precipitation followed by combined stripping with digester sludge liquid at full scale. *Water* 5, 1262–1278. doi:10.3390/w5031262

- Morse, G., Brett, S., Guy, J., Lester, J., 1998. Review: Phosphorus removal and recovery technologies. *Sci. Total Environ.* 212, 69–81. doi:10.1016/S0048-9697(97)00332-X
- Münch, E. V., Barr, K., 2001. Controlled struvite crystallisation for removing phosphorus from anaerobic digester sidestreams. *Water Res.* 35, 151–159.
- Münch, E. V., Benesovsky-Scott, A., Josey, J., Barr, K., 2001. Making a business from struvite crystallisation for wastewater treatment: Turning waste into gold, in: 2nd Int. Conf. on Recovery of Phosphates from Sewage and Animal Wastes. Holland, 12-13 March 2001.
- Myerson, S.A., 1993. Handbook of crystallization, 1st editio. ed. Butterworth-Heinemann Series in Chemical Engineering, Boston (USA).
- Nelson, N.O., Mikkelsen, R.L., Hesterberg, D.L., 2003. Struvite precipitation in anaerobic swine lagoon liquid: effect of pH and Mg:P ratio and determination of rate constant. *Bioresour. Technol.* 89, 229–236. doi:10.1016/S0960-8524(03)00076-2
- Ohlinger, K.N., Young, T.M., Schroeder, E.D., 1999. Kinetics effects on preferential struvite accumulation in wastewater. *J. Environ. Eng.* 125, 730–737.
- Ohlinger, K.N., Young, T.M., Schroeder, E.D., 1998. Predicting struvite formation in digestion. *Water Res.* 32, 3607–3614.
- Orzi, V., Scaglia, B., Lonati, S., Riva, C., Boccasile, G., Alborali, G.L., Adani, F., 2015. The role of biological processes in reducing both odor impact and pathogen content during mesophilic anaerobic digestion. *Sci. Total Environ.* 526, 116–126. doi:10.1016/j.scitotenv.2015.04.038
- Palm, C.A., Myers, R.J.K., Nandwa, S.M., 1997. Combined use of organic and inorganic nutrient sources for soil fertility maintenance and replenishment, in: Buresh, R.J., Sanchez, P.A., Calhoun, F. (Eds.), *Replenishing Soil Fertility in Africa*, SSSA Spec., SSSA Special Publication SV - 51. Soil Science Society of America and American Society of Agronomy, pp. 193–217. doi:10.2136/sssaspecpub51.c8
- Pastor, L., Mangin, D., Barat, R., Seco, A., 2008. A pilot-scale study of struvite precipitation in a stirred tank reactor: conditions influencing the process. *Bioresour. Technol.* 99, 6285–91. doi:10.1016/j.biortech.2007.12.003



- Ping, Q., Li, Y., Wu, X., Yang, L., Wang, L., 2016. Characterization of morphology and component of struvite pellets crystallized from sludge dewatering liquor: Effects of total suspended solid and phosphate concentrations. *J. Hazard. Mater.* 310, 261–269. doi:10.1016/j.jhazmat.2016.02.047
- Pintucci, C., Carballa, M., Varga, S., Sarli, J., Peng, L., Bousek, J., Pedizzi, C., Rusalleda, M., Tarragó, E., Prat, D., Colica, G., Picavet, M., Colsen, J., Benito, O., Balaguer, M.D., Puig, S., Lema, J.M., Colprim, J., Fuchs, W., Vlaeminck, S.E., 2016. The ManureEcoMine pilot installation: advanced integration of technologies for the management of organics and nutrients in livestock waste. *Water Sci. Technol.* 75, 1281–1293. doi:10.2166/wst.2016.559
- Rahman, M.M., Liu, Y., Kwag, J.-H., Ra, C., 2011. Recovery of struvite from animal wastewater and its nutrient leaching loss in soil. *J. Hazard. Mater.* 186, 2026–2030. doi:10.1016/j.jhazmat.2010.12.103
- Rahman, M.M., Salleh, M.A.M., Rashid, U., Ahsan, A., Hossain, M.M., Ra, C., 2014. Production of slow release crystal fertilizer from wastewaters through struvite crystallization - A review. *Arab. J. Chem.* 7, 139–155. doi:10.1016/j.arabjc.2013.10.007
- Riva, C., Orzi, V., Carozzi, M., Acutis, M., Boccasile, G., Lonati, S., Tambone, F., D'Imporzano, G., Adani, F., 2016. Short-term experiments in using digestate products as substitutes for mineral (N) fertilizer: Agronomic performance, odours, and ammonia emission impacts. *Sci. Total Environ.* 547, 206–214. doi:10.1016/j.scitotenv.2015.12.156
- Ronteltap, M., Maurer, M., Gujer, W., 2007. The behaviour of pharmaceuticals and heavy metals during struvite precipitation in urine. *Water Res.* 41, 1859–1868. doi:10.1016/j.watres.2007.01.026
- Ronteltap, M., Maurer, M., Hausherr, R., Gujer, W., 2010. Struvite precipitation from urine - Influencing factors on particle size. *Water Res.* 44, 2038–2046.
- Rusalleda, M., Puig, S., Mora, X., López, H., Ganigué, R., Balaguer, M.D., Colprim, J., 2010. The effect of urban landfill leachate characteristics on the coexistence of anammox bacteria and heterotrophic denitrifiers. *Water Sci. Technol.* 61, 1065–1071. doi:10.2166/wst.2010.610
- Ryu, H.-D., Lim, C.-S., Kang, M.-K., Lee, S.-I., 2012. Evaluation of struvite obtained from semiconductor wastewater as a fertilizer in cultivating Chinese cabbage. *J. Hazard. Mater.* 221–222, 248–255. doi:10.1016/j.jhazmat.2012.04.038

- Schuiling, R.D., Andrade, A., 1999. Recovery of struvite from calf manure. *Environ. Technol.* 20, 765–768.
- SCOPE Newsletter, 2001. The phosphate industry's editorial. 41.
- Shih, K., Yan, H., 2016. The crystallization of struvite and its analog (K-Struvite) from waste streams for nutrient recycling, in: *Environmental Materials and Waste: Resource Recovery and Pollution Prevention*. pp. 665–686. doi:10.1016/B9780128038376.000263
- Shikazono, N., 2003. Geochemical and tectonic evolution of Arc-Backarc hydrothermal systems: Implications for the origin of Kuroko and epithermal vein-type mineralizations and the global geochemical cycle. Elsevier Science B. V., Amsterdam.
- Shu, L., Schneider, P., Jegatheesan, V., Johnson, J., 2006. An economic evaluation of phosphorus recovery as struvite from digester supernatant. *Bioresour. Technol.* 97, 2211–2216.
- Singh, D., Mandalika, V.R., Parulekar, S.J., Wagh, A.S., 2006. Magnesium potassium phosphate ceramic for <sup>99</sup>Tc immobilization. *J. Nucl. Mater.* 348, 272–282. doi:10.1016/j.jnucmat.2005.09.026
- Soare, A., Lakerveld, R., van Royen, J., Zocchi, G., Stankiewicz, A.I., Kramer, H.J.M., 2012. Minimization of attrition and breakage in an airlift crystallizer. *Ind. Eng. Chem. Res.* 51, 10895–10909. doi:10.1021/ie300432w
- Song, Y.-H., Qiu, G.-L., Yuan, P., Cui, X.-Y., Peng, J.-F., Zeng, P., Duan, L., Xiang, L.-C., Qian, F., 2011. Nutrients removal and recovery from anaerobically digested swine wastewater by struvite crystallization without chemical additions. *J. Hazard. Mater.* 190, 140–149. doi:10.1016/j.jhazmat.2011.03.015
- Song, Y.-H., Qiu, G.-L., Yuan, P., Cui, X.-Y., Peng, J.-F., Zeng, P., Duan, L., Xiang, L.-C., Qian, F., 2011. Nutrients removal and recovery from anaerobically digested swine wastewater by struvite crystallization without chemical additions. *J. Hazard. Mater.* 190, 140–9. doi:10.1016/j.jhazmat.2011.03.015
- Steen, I., 1998. Phosphorus availability in the 21st century: Management of a non-renewable resource. *Phosphorus & Potassium* 217, 25–31.
- Stratful, I., Scrimshaw, M.D., Lester, J.N., 2004. Removal of struvite to prevent problems associated with its accumulation in wastewater treatment. *Water Environ. Res.* 76, 437–443.

- Stratful, I., Scrimshaw, M.D., Lester, J.N., 2001. Conditions influencing the precipitation of magnesium ammonium phosphate. *Water Res.* 35, 4191–4199.
- Stumpf, D., Zhu, H., Heinzmann, B., Kraume, M., 2008. Phosphorus recovery in aerated systems by MAP precipitation: Optimizing operational conditions. *Water Sci. Technol.* 58, 1977–1983. doi:10.2166/wst.2008.549
- Sun, W.-D., Wang, J.-Y., Zhang, K.-C., Wang, X.-L., 2010. Study on precipitation of struvite and struvite-K crystal in goats during onset of urolithiasis. *Res. Vet. Sci.* 88, 461–466. doi:10.1016/j.rvsc.2009.11.010
- Sutton, M.A., Bleeker, A., Howard, C.M., Erisman, J.W., Abrol, Y.P., Bekunda, M., Datta, A., Davidson, E., de Vries, W., Oenema, O., Zhang, F.S., 2012. Our Nutrient World, in: *Our Nutrient World. The Challenge to Produce More Food & Energy with Less Pollution. Key Messages for Rio+20.* Published by the Centre for Ecology & Hydrology on behalf of the Global Partnership on Nutrient Management (GPNM) and the International Nitrogen Initiative (INI).
- Suzuki, K., Tanaka, Y., Kuroda, K., Hanajima, D., Fukumoto, Y., 2005. Recovery of phosphorous from swine wastewater through crystallization. *Bioresour. Technol.* 96, 1544–1550. doi:10.1016/j.biortech.2004.12.017
- Suzuki, K., Tanaka, Y., Kuroda, K., Hanajima, D., Fukumoto, Y., Yasuda, T., Waki, M., 2007. Removal and recovery of phosphorous from swine wastewater by demonstration crystallization reactor and struvite accumulation device. *Bioresour. Technol.* 98, 1573–1578. doi:10.1016/j.biortech.2006.06.008
- Suzuki, K., Tanaka, Y., Osada, T., Waki, M., 2002. Removal of phosphate, magnesium and calcium from swine wastewater through crystallization enhanced by aeration. *Water Res.* 36, 2991–2998.
- Tarragó, E., Puig, S., Rusalleda, M., Balaguer, M.D., Colprim, J., 2016. Controlling struvite particles' size using the up-flow velocity. *Chem. Eng. J.* 302, 819–827. doi:http://dx.doi.org/10.1016/j.cej.2016.06.036
- Tünay, O., Kabdasi, I., Orhon, D., Kolçak, S., 1997. Ammonia removal by magnesium ammonium phosphate precipitation in industrial wastewaters. *Water Sci. Technol.* 36, 225–228.

- Ueno, Y., Fujii, M., 2001. Three years experience of operating and selling recovered struvite from full-scale plant. *Environ. Technol.* 22, 1373–1381.
- Uludag-Demirer, S., Demirer, G.N., Chen, S., 2005. Ammonia removal from anaerobically digested dairy manure by struvite precipitation. *Process Biochem.* 40, 3667–3674. doi:10.1016/j.procbio.2005.02.028
- UN Industrial Development Organization, 1998. *Fertilizer Manual*. Springer Science & Business Media.
- Uysal, A., Yilmazel, Y.D., Demirer, G.N., 2010. The determination of fertilizer quality of the formed struvite from effluent of a sewage sludge anaerobic digester. *J. Hazard. Mater.* 181, 248–254. doi:10.1016/j.jhazmat.2010.05.004
- van Dijk, K., Oenema, O., Lesschen, J.P., 2014. Present and future phosphorus use in Europe: food system scenario analyses.
- Wang, J., Burken, J.G., Zhang, X., 2006. Effect of seeding materials and mixing strength on struvite precipitation. *Water Environ. Res.* 78, 125–132. doi:10.2175/106143005X89580
- Wiesmann, U., Choi, I.S., Dombrowski, E.-M., 2007. *Fundamentals of biological wastewater treatment*. WILEY-VCH Verlag GmbH & Co. KGaA, Weinheim. doi:10.1002/9783527609604
- Wilsenach, J.A., Schuurbiers, C.A.H., van Loosdrecht, M.C.M., 2007. Phosphate and potassium recovery from source separated urine through struvite precipitation. *Water Res.* 41, 458–466. doi:10.1016/j.watres.2006.10.014
- Xu, K., Li, J., Zheng, M., Zhang, C., Xie, T., Wang, C., 2015. The precipitation of magnesium potassium phosphate hexahydrate for P and K recovery from synthetic urine. *Water Res.* 80, 71–79.
- Xu, K., Wang, C., Liu, H., Qian, Y., 2011. Simultaneous removal of phosphorus and potassium from synthetic urine through the precipitation of magnesium potassium phosphate hexahydrate. *Chemosphere* 84, 207–212. doi:10.1016/j.chemosphere.2011.04.057
- Xu, K., Wang, C., Wang, X., Qian, Y., 2012. Laboratory experiments on simultaneous removal of K and P from synthetic and real urine for nutrient recycle by crystallization of magnesium-potassium-phosphate-hexahydrate in a draft tube and baffle reactor. *Chemosphere* 88, 219–223. doi:10.1016/j.chemosphere.2012.02.061

- Yen, T.F., 2007. Chemical processes for environmental engineering. World Scientific Publishing Co., Inc., Hackensack, New Jersey, USA, p. 568. doi:10.1080/15567030701791790
- Yetilmezsoy, K., Sapci-Zengin, Z., 2009. Recovery of ammonium nitrogen from the effluent of UASB treating poultry manure wastewater by MAP precipitation as a slow release fertilizer. *J. Hazard. Mater.* 166, 260–269. doi:10.1016/j.jhazmat.2008.11.025
- Zeng, L., Li, X., 2006. Nutrient removal from anaerobically digested cattle manure by struvite precipitation. *J. Environ. Eng. Sci.* 5, 285–294. doi:10.1139/S05
- Zhang, T., Bowers, K.E., Harrison, J.H., Chen, S., 2010. Releasing phosphorus from calcium for struvite fertilizer production. *Water Environ. Res.* 82, 34–42.



